Carbon Nanotubes in RNA capture – characterization and application in biotechnological processes

Ana Margarida Ferreira Videira

Dissertação para obtenção do Grau de Mestre em
Biotecnologia
(2º ciclo de estudos)

Orientador: Profª. Doutora Fani Pereira de Sousa
Co-orientador: Profª. Doutora Cláudia Gomes Silva

outubro de 2022

Declaração de Integridade

Eu, Ana Margarida Ferreira Videira, que abaixo assino, estudante com o número de inscrição 11122 de Biotecnologia da Faculdade de Ciências, declaro ter desenvolvido o presente trabalho e elaborado o presente texto em total consonância com o **Código de Integridades da Universidade da Beira Interior**.

Mais concretamente afirmo não ter incorrido em qualquer das variedades de Fraude Académica, e que aqui declaro conhecer, que em particular atendi à exigida referenciação de frases, extratos, imagens e outras formas de trabalho intelectual, e assumindo assim na íntegra as responsabilidades da autoria.

Universidade da Beira Interior, Covilhã 10 /10 /2022

Ana Margarida Ferreira Videira

Agradecimentos

Esta Dissertação de Mestrado representa o final de uma etapa de aprendizagem importante do meu percurso académico e o início de uma vida profissional. Não posso, no entanto, esquecer todos aqueles que ao longo desta caminhada me acompanharam e me apoiaram incondicionalmente e que, sem eles, não seria possível a concretização deste trabalho.

Especialmente à minha orientadora, Professora Fani Sousa, agradeço por me ter aceitado e integrado no seu grupo de investigação, acreditando em mim e nas minhas capacidades. Agradeço ainda toda a confiança transmitida nos momentos em que pensei que nada estava a correr bem. Este apoio foi fundamental para acreditar no meu trabalho, não permitindo que o desalento se instalasse. Nada disto seria possível sem o seu profissionalismo, apoio, dedicação e conhecimento científico que, sem dúvida, me ajudaram a crescer tanto a nível pessoal como profissional, tornando-me uma pessoa mais madura e mais competente.

Agradeço, de igual forma, à Professora Cláudia Silva e à Doutora Maria José Sampaio, da Faculdade de Engenharia da Universidade do Porto (FEUP), por terem disponibilizado os materiais de carbono utilizados neste trabalho e pela colaboração na realização do mesmo, destacando a sua preciosa ajuda na análise de dados.

Quero agradecer também aos meus colegas de laboratório pela paciência, pela partilha de conhecimento e pelos momentos de entreajuda que foram valiosos para a concretização deste trabalho. Em especial, ao Pedro Ferreira pelo apoio incansável, estando sempre disponível para me ajudar em qualquer dificuldade no laboratório. Com ele aprendi muito e sem ele parte deste trabalho não seria possível, e à Ana Ferro pela amizade e pelas palavras na hora certa, estando sempre presente nos bons e maus momentos, o meu sincero obrigada.

Aos meus amigos e também eles companheiros de laboratório, Sérgio Nunes e Bruno Rodrigues, quero deixar um agradecimento muito especial pois sem vocês tudo isto seria mais difícil. Obrigada por todos os momentos passados, por ouvirem as minhas preocupações e dúvidas, mas também as minhas vitórias ao longo deste percurso. Podem contar comigo para tudo!

Aos meus amigos que nunca estiveram ausentes, desde os de longa data até aos mais recentes, obrigada pelo carinho e companheirismo. Este trabalho reflete uma longa viagem, pautada por inúmeros desafios dos quais resultaram muitas alegrias, mas também algumas incertezas perante os percalços que foram surgindo. E é por isso mesmo que deixo o meu especial agradecimento à minha amiga Priscilla Cravo que me ouviu, aconselhou, ajudou e principalmente me incentivou sempre. Trilhar este caminho tornou-se mais fácil com o teu apoio e força. Sou muito grata pela nossa amizade!

E, finalmente, agradeço à minha família pelo incentivo recebido ao longo destes anos. Ao meu irmão e à minha prima Carolina, um enorme obrigada pelo apoio, motivação e presença em todas as minhas conquistas. Aos meus pais, agradeço tudo o que fizeram por mim ao longo desta viagem de 5 anos. Obrigada por todos os ensinamentos de vida, por estarem presentes em todas as etapas da minha vida e por me ajudarem a percorrer esta longa caminhada. A vocês, dedico este trabalho!

Este trabalho foi apoiado pelo projeto PTDC/BII-BBF/29496/2017 financiado pelo FEDER através do COMPETE2020-POCI e por fundos nacionais, através da FCT/MCTES. O trabalho decorreu ainda no âmbito dos projetos UIDB/00709/2020, UIDP/00709/2020, UIDB/50020/2020 e UIDP/50020/2020, e LA/P/0045/2020 (ALiCE) financiados por fundos nacionais, através da FCT/MCTES (PIDDAC).

Cofinanciado por:

COMPETE 2020
PROGRAMA OPERACIONAL COMPETITIVIDADE E INTERNACIONALIZAÇÃO

PORTUGAL 2020

UNIÃO EUROPEIA
Fundo Europeu de Desenvolvimento Regional

FCT
Fundação para a Ciência e a Tecnologia
MINISTÉRIO DA EDUCAÇÃO E CIÊNCIA

Resumo alargado

Nos últimos anos, a investigação tem conduzido a progressos notáveis no desenvolvimento de terapias baseadas em ácidos nucleicos. Apesar destas abordagens terem como ponto de partida o DNA, investigações recentes têm avaliado o potencial terapêutico do RNA. A compreensão das funções do RNA e do seu papel preponderante em várias doenças, destacou o seu potencial de aplicação como biomolécula terapêutica. Neste contexto, o recente desenvolvimento de vacinas eficazes baseadas em mRNA em resposta à pandemia da COVID-19 despertou ainda mais o interesse da investigação em terapias baseadas em RNA. No entanto, os processos efetivos de produção ainda enfrentam inúmeros desafios. Um dos processos mais cruciais é a recuperação e purificação do RNA, uma vez que associado ao processo de produção várias biomoléculas consideradas impurezas estão presentes, e são difíceis de eliminar pois partilham várias características com o RNA. Além disso, a presença destas impurezas no produto final pode representar problemas de imunogenicidade quando se considera a etapa final de entrega e administração terapêutica, tornando o seu processo de remoção obrigatório. Contudo, os métodos atualmente disponíveis e utilizados para o isolamento de RNA são limitados, demorados, pouco eficientes e muitas vezes requerem o uso de reagentes tóxicos, o que, para além de causar um enorme impacto a nível ambiental, pode comprometer a pureza, integridade e atividade biológica do RNA, parâmetros considerados imprescindíveis na recuperação do produto a ser aplicado biologicamente. Para responder a este problema, a utilização de materiais à base de carbono como candidatos a adsorventes para a captura de ácidos nucleicos surge como uma opção muito promissora devido às suas excelentes propriedades mecânicas, químicas e térmicas. Dentro destes materiais de carbono, os nanotubos de carbono (CNTs), destacam-se consideravelmente devido principalmente à excelente capacidade de adsorção de várias biomoléculas, o que tem potenciado a sua aplicação em diversas aplicações biológicas. Adicionalmente, os CNTs já demonstraram ser capazes de adsorver RNA. Porém, a forte interação CNT-RNA torna a dessorção de RNA um passo bastante crítico.

Deste modo, neste estudo, é descrito um método eficaz, simples e economicamente mais rentável para a captura e recuperação de RNA a partir de um extrato complexo de *Escherichia coli* usando CNTs, comparando a eficiência do processo com outros materiais de carbono com diferentes estruturas e modificações de superfície. A amostra de lisado celular, além de conter a biomolécula de interesse, o RNA, contém proteínas, bem como outros ácidos nucleicos contaminantes, como RNA e DNA genómico (gDNA). Os ensaios realizados no presente trabalho podem ser divididos em 2 partes: (1) realização de ensaios de adsorção de RNA usando CNTs de parede múltipla (*multi-walled carbon nanotubes,* MWCNTs) e avaliação de diferentes estratégias de regeneração dos MWCNTs para serem aplicados em novos ciclos, uma vez comprovada a incapacidade de dessorção de RNA deste material, em condições favoráveis à manutenção da sua integridade e estabilidade; (2) realização de ensaios de *screening* de adsorção e dessorção de RNA utilizando CNTs e outros materiais de carbono; estudo da reutilização dos materiais; avaliação do potencial de seletividade entre RNA e pDNA a partir de misturas de ácidos nucleicos e de amostras complexas de lisado, com posterior caraterização da pureza relativa e integridade do RNA recuperado.

Os resultados obtidos da primeira parte do trabalho demonstraram o enorme potencial dos MWCNTs em adsorver RNA, exibindo uma capacidade máxima de adsorção de aproximadamente 175 mg/g. Quanto à capacidade de reutilizar este material, foram aplicadas estratégias de regeneração química, ultrassónica e térmica, sendo que, quando aplicada a regeneração química seguida de novo ensaio de adsorção de RNA, foi obtida a melhor percentagem de adsorção (73%) comparativamente às restantes estratégias mencionadas. Através da análise FTIR dos MWCNTs, demonstrou-se que o material foi capaz de recuperar as propriedades iniciais de superfície após terem sido aplicadas as estratégias de regeneração química e térmica. Relativamente aos resultados dos ensaios referentes à segunda parte do trabalho, foram realizados ensaios de *screening* de adsorção e dessorção de RNA a partir de diferentes materiais de carbono. Entre eles, os CNTs dopados com N e oxidados com HNO_3 e as fibras de carbono oxidadas com HNO_3, apesar de apresentarem capacidades de adsorção de RNA mais baixas, de 42% e 55% respetivamente, quando comparadas com MWCNTs e outros CNTs sem qualquer modificação de superfície, demonstraram ser capazes de dessorver o RNA capturado, obtendo percentagens de dessorção do RNA de 81% e 72%, respetivamente. Além disso, demonstrou-se a possibilidade de reutilização e reaproveitamento dos materiais pois estes foram capazes de manter a capacidade de adsorção de RNA ao longo de vários ciclos. Os resultados obtidos revelaram também a capacidade dos materiais em capturar com alguma seletividade o RNA de amostras complexas e, posteriormente, recuperá-lo sem a presença de DNA, ao longo de 3 ciclos. De notar que os CNTs dopados com N e oxidados com HNO_3 apresentaram uma maior seletividade em comparação com as fibras de carbono oxidadas com HNO_3. Os resultados evidenciaram também que os materiais foram capazes de capturar totalmente a quantidade de proteínas presente na amostra de lisado, sendo que no caso dos CNTs dopados com N e oxidados com HNO_3 foi apenas necessário 1 ciclo de extração para capturar a totalidade de proteínas presente. A par disso, a recuperação final de RNA não foi comprometida, dado que as frações representativas de RNA dessorvido não continham a presença de proteína, possibilitando a clarificação rápida e simples do RNA. Por último, os resultados relativos aos espetros de dicroísmo circular garantiram a manutenção da integridade e estabilidade do RNA recuperado de ambos os materiais.

Assim, globalmente, os resultados obtidos neste trabalho demonstram o potencial dos materiais de carbono em capturar e recuperar o RNA, permitindo o desenvolvimento de um método simples, rápido e amigo do ambiente para a captura e pré-purificação eficiente de RNA.

Palavras-chave

Biofármacos; Materiais à base de carbono; Nanotubos de carbono; Adsorventes; Separação de ácidos nucleicos; RNA.

Abstract

In recent years, research has led to remarkable progress in the development of nucleic acid-based therapies. While these approaches had DNA as their starting point, recent investigations have evaluated the therapeutic potential of RNA. Understanding the cellular functions of RNA and its crucial role in various diseases has highlighted its potential application as a therapeutic biomolecule. In this context, the recent development of effective mRNA-based vaccines in response to the COVID-19 pandemic has further aroused research interest in RNA-based therapies. However, effective production processes still face numerous challenges. One of the most critical processes is RNA recovery and purification, since associated with the production process several biomolecules that are considered impurities are present and are difficult to eliminate as they share several characteristics with the RNA. Furthermore, the presence of these impurities in the final product may pose immunogenicity problems when considering the final stage of therapeutic delivery and administration, making their removal process mandatory. However, the methods currently available for RNA isolation are limited, time-consuming, not very efficient, and often require the use of toxic reagents, which, in addition to causing an enormous environmental impact, can compromise the purity, integrity, and biological activity of RNA, essential parameters to consider in the recovery of one product to be biologically applied. To address this problem, the use of carbon-based materials as candidate adsorbents for nucleic acids capture, emerges as a very promising option due to their excellent mechanical, chemical, and thermal properties. Within these carbon materials, carbon nanotubes (CNTs) stand out considerably, mainly due to their excellent adsorption capacity of several biomolecules, which has potentiated their application. Additionally, CNTs have already been shown to be able to adsorb RNA. However, the strong CNT-RNA interaction makes RNA desorption a very critical step.

Thus, in this study, an efficient, simple, and cost-effective method for RNA capture and recovery from a complex extract of *Escherichia coli* using CNTs is described, comparing the process efficiency with other carbon materials with different structures and surface modifications. The cell lysate sample, in addition to containing the biomolecule of interest, RNA, also contains proteins as well as other contaminating nucleic acids such as RNA and genomic DNA (gDNA). The assays performed in the present work can be divided into 2 parts: (1) performing RNA adsorption assays using *multi-walled carbon nanotubes* (MWCNTs) and evaluating different regeneration strategies of the MWCNTs to be applied in new cycles, once the RNA desorption inability of this material is proven,

under conditions favorable to maintain its integrity and stability; (2) performing RNA adsorption and desorption screening assays using CNTs and other carbon materials; studying the reuse of the materials; evaluating the potential selectivity between RNA and pDNA from mixtures of nucleic acids and complex lysate samples, with a subsequent characterization of the relative purity and integrity of the recovered RNA.

The results obtained from the first part of the work demonstrated the great potential of MWCNTs to adsorb RNA, exhibiting a maximum adsorption capacity of approximately 175 mg/g. Regarding the ability to reuse this material, chemical, ultrasonic, and thermal regeneration strategies were applied. When chemical regeneration was applied followed by a new RNA adsorption experiment, 73% of RNA adsorption was obtained, which was the highest value, when compared to the other strategies. Through FTIR analysis of the MWCNTs it was demonstrated that the material was able to recover the initial surface properties after the chemical and thermal regeneration strategies. Regarding the second part of the work, RNA adsorption and desorption screening experiments were performed with different carbon materials. N-doped CNTs oxidized with HNO_3 and carbon fibers oxidized with HNO_3 showed lower RNA adsorption capacities (42% and 55% respectively) than MWCNTs and other CNTs without any surface modification. However, these materials allowed effective desorption of captured RNA, with desorption percentages of 81% and 72%, respectively, which was a great advantage over other materials. In addition, it was demonstrated the possibility of reusing the materials, as they were able to maintain the RNA adsorption capacity over several cycles. The results obtained also revealed the capacity of the materials to capture RNA from complex samples with some selectivity, being subsequently recovered without DNA, over 3 consecutive cycles. Of note, N-doped CNTs oxidized with HNO_3 showed higher selectivity compared to carbon fibers oxidized with HNO_3. The results also showed that the materials were able to fully capture the amount of protein present in the lysate sample, and in the case of N-doped CNTs oxidized with HNO_3, only 1 extraction cycle was required. In addition, the final RNA recovery was not compromised since the representative fractions of desorbed RNA did not contain proteins. Moreover, circular dichroism spectra showed that RNA maintained its integrity and stability when recovered from both materials.

Thus, overall, the results obtained in this work demonstrate the potential of carbon materials to capture and recover RNA, enabling the development of a simple, rapid, and environmentally friendly method for efficient RNA capture and pre-purification.

Keywords

Biopharmaceuticals; Carbon-based materials; Carbon nanotubes; Adsorbents; Nucleic acids separation; RNA.

Table of Contents

List of Figures

List of Tables

List of Acronyms

0D	Zero-dimensional
1D	One-Dimensional
2D	Two-Dimensional
3D	Three-Dimensional
AFM	Atomic force microscopy
ATPS	Aqueous two-phase systems
CNT	Carbon nanotube
CVD	Chemical vapor deposition
DC	Direct current
DOX	Doxorubicin
d-SPE	Dispersive solid-phase extraction
DTG	Derivative thermogravimetry
E. coli	*Escherichia coli*
FDA	Food and Drug Administration
FTIR	Fourier-transform infrared spectroscopy
GCN-T	Graphite-like carbon nitride
gDNA	Genomic DNA
GO	Graphene oxide
HRTEM	High-resolution transmission electron microscopic imaging
IR	Infrared
IUPAC	International Union of Pure and Applied Chemistry
LLE	Liquid-liquid extraction
mAbs	Monoclonal antibodies
MEPS	Microextraction by packed sorbent
mRNA	Message RNA
MSPD	Matrix solid-phase dispersion
MWCNTs	Multi-walled carbon nanotubes
ND	Nanodiamond
NIR	Near-infrared
NNI	National Nanotechnology Initiative
pDNA	Plasmid DNA
PEG	Polyethylene glycol
RNAi	RNA interference
SBSE	Stir-bar sorptive extraction
SDBS	Sodium dodecylbenzene sulfonate
SDS	Sodium dodecyl sulfate
SEM	Scanning electron microscopy
siRNA	Short-interfering RNA
SM	Small molecule
SPDE	Dynamic solid-phase extraction
SPE	Solid phase extraction
SPME	Solid-phase microextraction
SWCNTs	Single-walled carbon nanotubes
TEM	Transmission electron microscopy
TGA	Thermal gravimetric analysis
tRNA	Transfer RNA
UV	Ultraviolet

List of Scientific Communications

- **Oral Presentation - Award for "Pitch Presentation"**

Ana Videira, Pedro Ferreira, Cláudia G. Silva, Fani Sousa. Carbon Nanotubes in RNA capture – characterization and application in biotechnological processes. VI Ciclo de Conferências em Biotecnologia. 12-13 May 2022, Covilhã, Portugal.

- **Oral Presentation**

Ana Videira, Pedro Ferreira, Cláudia G. Silva, Fani Sousa. Carbon Nanotubes in RNA capture. XVII International CICS-UBI Symposium. 20-21 July 2022, Covilhã, Portugal.

CHAPTER 1

Introduction

1.1- Carbon-based materials

Some chemical elements can be organized in different molecular structures composed of the same type of atoms, a characteristic known as allotropy. Carbon has been always considered an excellent friend of humans due to its involvement in countless structures, mechanisms and applications. Recent research in this field is giving new life to this ancient material [1]. Carbon is one of the most abundant elements in the environment and the human body, possessing a special ability to bind to different types of elements, often with fundamentally different properties. The different chemical and physical properties of these materials are determined by the structural geometry of the atoms and the type of chemical bonds present in the molecules [2]. Until the 1980s, only three natural carbon allotropes were effectively known, which were the amorphous carbon, graphite, and diamond. However, due to carbon's ability to hybridize in sp, sp^2, and sp^3 configurations, new carbon-based materials have been studied and characterized and have gained attention due to their significant role in the development of materials science [1]. The increasing popularity of carbon materials is due to a unique combination of physical and chemical properties, such as remarkable electrical conductivity, good thermal and mechanical properties, chemical stability, high surface area, low cost, and highly developed and adjustable porosity [3]. In addition, they are materials that can be arranged in a variety of structures and textures, their surface can be easily modified, and are also compatible with other materials, making them ideal materials for composites [3].

1.1.1- Carbon-based nanomaterials

Nanotechnology has gained considerable prominence, especially in the last 4 decades, increasing the application of nanomaterials on different situations [4]. According to the National Nanotechnology Initiative (NNI), the production and application of nanoscale-based materials are increasing significantly every year [5]. Due essentially to their high surface-to-volume ratio, nanomaterials can be applied in different areas, including industry, medicine, pharmacy, biology, agriculture and cosmetics [6]. Particularly, during the last decades of the 20th century, the list of known carbon allotropes expanded, following the discovery of novel forms of low-dimensional carbon, specifically carbon-based nanomaterials [2].

Carbon nanomaterials can be divided into 4 categories based on the number of dimensions: zero-dimensional (0D) materials like fullerenes and carbon dots; one-dimensional (1D) materials like carbon nanotubes (CNTs); two-dimensional (2D) layered materials like graphene; and three-dimensional (3D) structures like nanodiamonds (NDs) (Figure 1) [7].

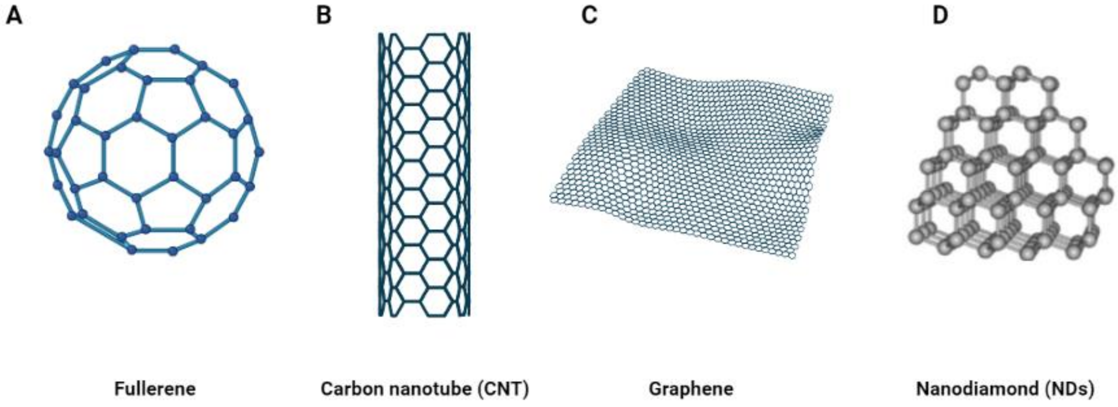

Figure 1- Structure of the main carbon-based nanomaterials with different dimensionalities.

These materials possess unique properties, thus opening up new perspectives and potential technological applications [8]. In 1985, the discovery of fullerenes, which is a molecule containing 60 or more carbon atoms in the shape of a soccer, was followed by the discovery of CNTs, which corresponds to a new form of fullerenes. The isolation and characterization of graphene in 2004 opened new research opportunities, consequently increasing the interest in carbon nanomaterials [9-11]. Figure 2 illustrates a timeline of discovery and awards for work related to carbon nanomaterials.

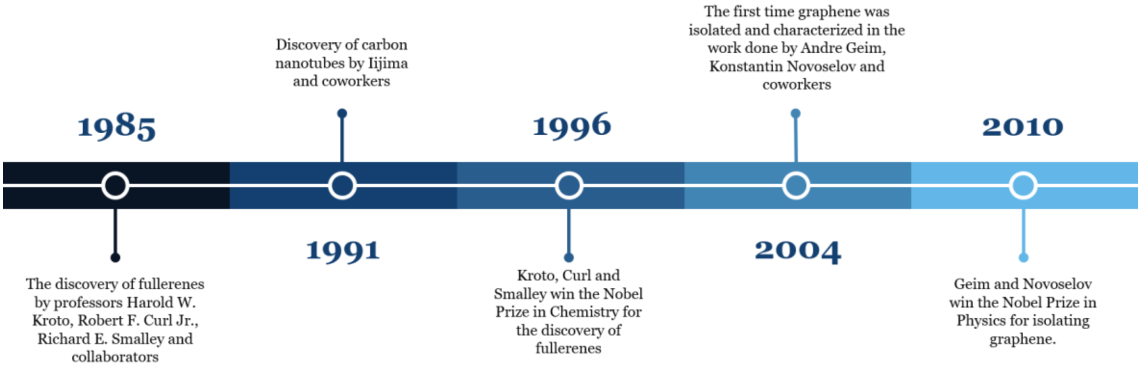

Figure 2- Main carbon-based nanomaterials (Adapted from [12]).

Low-dimensional carbon nanomaterials possess a variety of extremely good and promising physical, chemical, optical, magnetic, and electrical properties [12]. Table 1 shows some properties of the main carbon-based nanomaterials [13].

Table 1- General properties of the main carbon-based nanomaterials (Adapted from [13]).

Carbon Nanomaterials	Dimensions	Hybridization	Experimental Specific Surface Area (m^2/g)	Thermal Conductivity (W /m/K)	Electrical Conductivity (S/cm)	Tenacity	Hardness
Fullerene	0	Mostly sp^2	80–90	0.4	10^{-10}	Elastic	High
Carbon nanotube	1	Mostly sp^2	~1300	3500	Structure-dependent	Flexible, elastic	High
Graphene	2	sp^2	~1500	4840–5300	~2000	Flexible, elastic	Uppermost (for single layer)

1.1.1.1- Carbon-based nanomaterials for biomedical applications

The various possibilities to modify and tailor carbon nanomaterials are associated with their small size, approaching the size of many fundamental biomolecules, their large specific surface area, high electrical and thermal conductivity, unique optical properties, and superior mechanical properties, which have enabled the use of these materials for a wide range of applications [14]. These materials have gained enormous interest in the biomedical field [15].

In general, these materials have very small dimensions (1-100 nm) that are comparable to the dimensions of several biological molecules, namely DNA (2-3 nm in width) and different proteins (1-100 nm). These dimensions, combined with the possibility of functionalizing the surface of these materials with oxygen or nitrogen-based functional groups, favor cellular interaction, making them candidate materials for the delivery of drugs and biologics *in vivo* [16]. However, the stability of these materials in aqueous suspensions is still considered one of the main obstacles and challenges for their practical use in therapeutic applications, and further studies are needed to address this problem [17]. Nevertheless, the high surface area coupled with good optical properties make carbon-based nanomaterials ideal platforms for theragnostic applications due essentially to the high absorption in the near-infrared (NIR) zone, which allows their use in photoacoustic imaging and phototherapy [18].

In particular, since their discovery, CNTs immediately received a spotlight from the scientific community, as demonstrated in several ongoing studies [19, 20]. In this regard, CNTs can be used as components of sensing equipment [21, 22], in drug delivery systems for the treatment of various cancer-related diseases [23, 24] and in tissue engineering [25, 26]. For these reasons, in the next topics of this work, a more detailed description of this type of carbon nanomaterial is presented.

1.2- Carbon nanotubes (CNTs)

In 1991, the Japanese scientist Sumio Iijima reported on a structural allotropic form of carbon, obtained by synthesizing nanoscale fibers using the arc discharge technique [10]. Using high-resolution transmission electron microscopic imaging (HRTEM), Iijima observed CNTs for the first time. From then on, CNTs became considered a first-class subject in academic research as well as in various industrial areas [10]. Morphologically, CNTs consist exclusively of carbon atoms arranged in a series of benzene rings condensed and rolled into a tubular structure. Their internal structure is hollow, and the surface is composed of single or multiple layers of graphene sheets. The chemical bonding in nanotubes is entirely composed of sp^2 bonds, which are stronger than the sp^3 bonds found in diamonds and provide CNTs with high mechanical strength. The sp^2 covalent bonds between carbon atoms give them excellent strength properties because these bonds help increase the materials' tensile strength and modulus of elasticity [27].

The specific characteristics responsible for the high interest on CNTs are their length and diameter. CNTs have a length up to the micron scale and a diameter in the nanometer range (~ 1 nm), which results in a large aspect ratio [28]. This length-to-diameter ratio ($> 10^4$) can reach values greater than 100 000 000:1, far greater than any other known material [29, 30]. Due to the unique hexagonal structure, they can aggregate different attractive properties at mechanical, electrical and also molecular levels [28, 31].

1.2.1- Classification of CNTs

CNTs can have different classifications taking into consideration the number of graphene sheets that form the tubular structure, chirality, and conductivity [34, 38, 41]. The following sections briefly presents the different classifications of CNTs.

1.2.1.1- Classification by layers

In structural terms, and as represented in Figure 3, CNTs can be divided into 2 types [32]:

- **SWCNTs** - Single-walled carbon nanotubes
- **MWCNTs** - Multi-walled carbon nanotubes

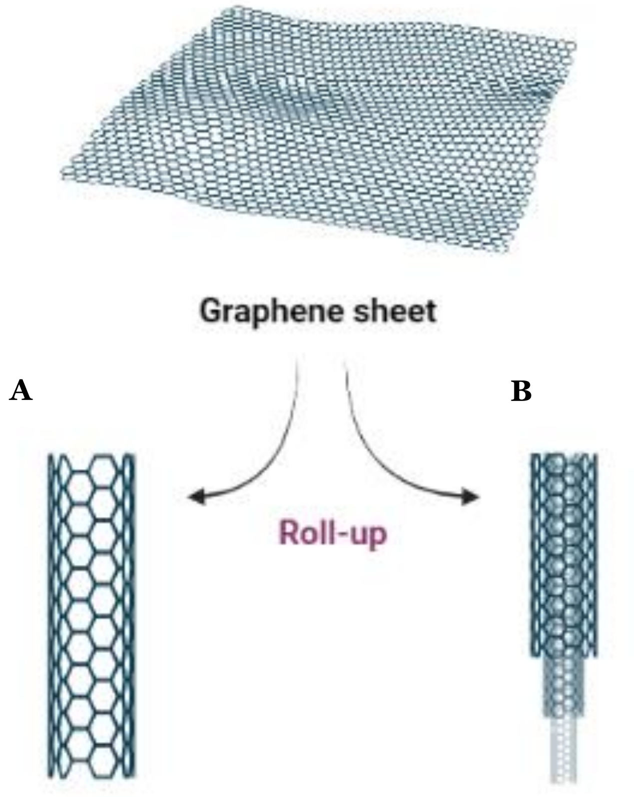

Figure 3- Structure of carbon nanotubes, according to the number of graphene layers. A: SWCNTs; B: MWCNTs.

SWCNTs consists of a single cylindrical layer of carbon atoms with a diameter in the range of 0.4-2 nm, depending on the temperature at which they are synthesized [33]. On the other hand, MWCNTs consist of multiple layers of graphene wound onto themselves, forming several coaxial cylinders, each made of a single sheet of graphene around a hollow core (Figure 3). The outer diameter of MWCNTs ranges from 2-100 nm, while the inner diameter is in the 1-3 nm range, and their length is from one to several micrometers. Due to the multilayer pattern of MWCNTs, the outer walls are not only able to protect the inner CNTs from chemical interactions with external solutions, but also provide high tensile strength properties [34]. A comparison between SWCNT and MWCNT is presented in Table 2

Table 2- Comparison between SWCNT and MWCNT (Adapted from [34]).

SWCNT	MWCNT
A single layer of graphene	Multiple layers of graphene
Expensive	Expensive
Catalyst is required for synthesis	Can be produced without catalyst
Bulk synthesis is difficult as it requires proper control of overgrowth and atmospheric condition	Bulk synthesis is easy
Low purity	High purity
A chance of defect is higher during functionalization	A chance of defect is less but once occurred it's difficult in body
Less accumulation in body	More accumulation in body
More defection during the functionalization	Less defection, but hard to improve

1.2.1.2- Classification by chirality

The structure of SWCNTs is determined by the way they roll onto themselves in the hexagonal graphene network [35]. The orientation of the hexagonal network and the longitudinal axis of a CNT determines a very important structural property of the tubular structure: the chirality. Chirality is defined as the method by which atoms bond, giving rise to differently shaped bond ends, i.e., it is determined by the orientation of the graphene sheet and can be defined in terms of the unit cell and using the chiral vector C_h, as defined in equation (1) [36]:

$$C_{h=na_1+ma_2} \tag{1}$$

where n and m represent the number of steps along the unit vectors a_1 and a_2 in the hexagonal graphene sheet, shown in Figure 4. These structural parameters show the extent of torsion of a nanotube. If $m = 0$, the nanotubes are named ZigZag, for example (1, 0), (2, 0), (5, 0); if $n = m$, the nanotubes are named Armchair, for example (1, 1), (2, 2), (3, 3) and if $n \neq m$, the nanotubes are named chiral nanotubes, for example (4, 2), (3, 2), (4, 1). The degree of symmetry is more pronounced in the Armchair and ZigZag (achiral) configuration [34].

The chirality can also be specified by the angle Θ that represents the orientation angle or the chiral angle formed by the rolling direction of the nanotube and the direction of the common edge of 2 adjacent hexagons. The optional rolling directions are performed at angles Θ = 0° and Θ = 30°, corresponding to the chiralities (n, 0) and (n, n), respectively. This property has significant implications for the properties of CNTs, in particular to the electrical properties [37].

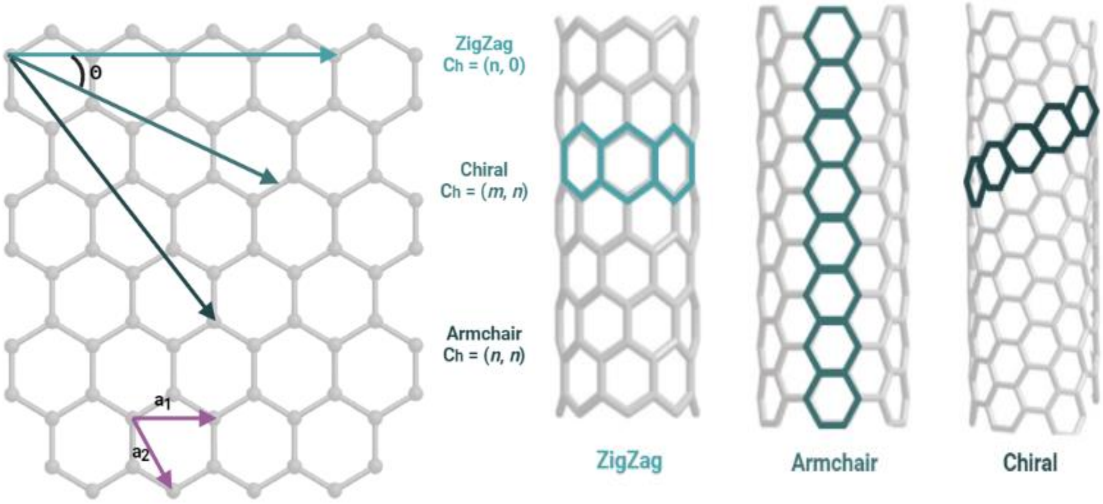

Figure 4- Schematic diagram showing Zigzag, Armchair and Chiral CNTs.

1.2.1.3- Classification by conductivity

Depending on the diameter and chirality (which describes how the graphene sheet is wound), CNTs can be classified as either metallic or semiconducting [38]. Therefore, when $n - m$ is a multiple of 3, the nanotube is highly conductive and known as metallic. Otherwise, the nanotube is semimetallic or semiconductor. All CNTs with the Armchair configuration are considered metallic, while CNTs with the ZigZag and Chiral configurations can be either metallic or semiconducting [39]. Due to the conductive or semiconducting nature, most of the studies using the potential of CNTs in the electric field are directed towards the development of solar cells [40]. To further realize the electrical potential of CNTs, in the future they could be used in the development of lightweight and strong high-conductivity cables for electrical power transmission, making the dream of the space elevator a reality [41].

1.2.2- Properties of CNTs

Currently, CNTs are considered one of the materials with the highest hardness and strength, being these properties a consequence of their structural arrangement and the presence of covalent C - C bonds. The chemical bonding in CNTs is entirely based on sp^2 bonds and these tend to align in bundles where the tubes are held together by van der Waals forces, further increasing the strength of this material [42]. CNTs are characterized by having high strength and stiffness in the axial direction and extraordinary flexibility in the transversal direction. The highest tensile strength or tensile stress measured for a CNT was 63 GPa, which is about 50 times higher than steel. On the other hand, elasticity is another remarkable property of CNTs [43]. They are characterized as quite flexible materials that do not suffer damage when they are bent or even subjected to high pressures. When MWCNTs are subjected to high stresses, only the last layer tends to suffer some rupture. However, the existence of imperfections in its structure causes the strength value to drop. Still, its value is considerably higher than that of other materials [44]. The modulus of elasticity in CNTs reaches values on the order of 1 TPa which is about 5 times higher than that of steel [45].

CNTs are also very good thermal conductors along the tube axis direction. Thermal conductivity measurements confirmed values of around 3000 W/mK for MWCNTs and above 2000 W/mK for SWCNTs. Both values are much higher than copper, a metal well known for its good thermal conductivity, of about 385 W/mK [46, 47]. These extremely high thermal conductivity values contribute to effective heat removal, which is also facilitated by the extremely high surface area of CNTs [48]. Considering that each carbon atom is covalently bonded to 3 neighboring carbons through sp^2 molecular orbitals, the fourth valence electron remains free in each unit, and these free electrons are delocalized over all atoms, thus contributing to the electrical nature of CNTs. So, they can be considered conductors or semiconductors, depending on the type of chirality [49], as previously stated. Metallic CNTs can conduct electricity extremely well, because the conductivity can be 8 times higher than that of copper, and can also carry a higher current density, when compared to any other known metallic wire [42]. SWCNTs and MWCNTs have structural differences, and there are also differences in their physical properties. Table 3 shows a comparison between some of the main properties reported by different researchers.

Table 3- Comparison between the main physical properties of SWCNTs and MWCNTs.

Properties	SWCNTs	MWCNTs	References
Diameter range (nm)	0.4 -2	Inner tubes: 1-3	[33]
		Outer tubes: 2-100	[50]
Tensile Strength (GPa)	13-52	11-63	[51]
Young's Modulus (GPa)	1054	1200	[52]
Thermal conductivity (W/m/K)	3500	3000	[53]
Electrical properties	Semiconductor or metallic	Semiconductor	[54]
Current Density (A/cm^2)	10^7 –10^8	10^9	[55, 56]
Electrical Conductivity (S/cm)	10^2-10^6	10^3-10^5	[57]

1.2.3- Methods for the Synthesis of CNTs

The high price of CNTs (e.g., about 50-100 €/g of SWCNTs) is a major concern for their large-scale synthesis [56]. In general, the chemical synthesis of CNTs is considered a difficult task, since their dimensions, arrangement and the number of graphene layers are parameters that must be controlled [58]. The 3 main methods used for the synthesis of SWCNTs and MWCNTs are the arc discharge method [10], laser ablation method [59] and chemical vapor deposition (CVD) method [59]. The arc discharge and laser ablation methods generally require high temperatures (1700 °C) during the synthesis. Thus, these methods have been replaced by CVD, which can be conducted at lower temperatures (<800 °C) [60]. The main synthesis strategies for CNTs are briefly described below.

The arc discharge method was the first method used, in 1991 by Iijima, to synthesize MWCNTs [10]. This technique produces good quality CNTs using an easy and simple procedure. The procedure involves establishing a direct current (DC) between a pair of graphite electrodes under an inert gas (helium or argon) at about 500 torrs. A DC of 50-100 A, driven by a potential difference of about 20 V, creates a high temperature discharge between the 2 electrodes. Obtaining this plasma discharge is the main factor for generating a favorable environment for nanotube growth. The high temperature arc (>4000 °C) leads to sublimation of the anode material, which is transferred to the cathode and the surrounding walls of the device. As the anode is consumed, it is moved toward the cathode to maintain discharge stability [61, 62]. MWCNTs are produced by arc discharge without requiring any metal catalyst, whereas mixed metal catalysts (Fe, Co, and Ni) are required for the production of SWCNTs [63]. Typically, CNTs synthesized by this technique exhibit a high degree of structural perfection. However, several variables such as chamber temperature, catalyst composition and concentration, and the presence of hydrogen influence their size and structure [64].

The synthesis of CNTs using the laser ablation method was first reported in 1995 by Guo and co-workers and achieved yields of over 70% by weight purity [51]. The laser ablation method involves vaporizing material from a solid target. A pulsed or continuous laser is used to vaporize a graphite target that holds the catalyst material in a quartz tube furnace at 1200 °C, while an inert gas (helium or argon) is mixed into the chamber to maintain the pressure at 500 torrs. Laser ablation is very similar to the arc discharge method in terms of principles and mechanism. Both methods use a metal-impregnated graphite target (anode) to produce SWCNTs, and both produce MWCNTs when pure graphite is used. The only difference comes from the fact that in the laser ablation method, the energy required is provided by a laser. CNTs prepared by the laser ablation method exhibit a high degree of structural perfection, probably due to the high temperatures involved during the synthesis. In addition, this method has the ability to produce CNTs with higher purity than the arc discharge process [34]. The main disadvantages of this method are the high power required and lower amounts of CNTs produced when compared to the arc discharge method. Several variables affect the quantity and quality of CNTs produced by laser ablation, such as the chemical composition of the target material, wavelength, laser power and the distance between the target and substrates [60].

CVD is currently the most intensively investigated method for the mass production of different types of CNTs, mainly due to its improved yield rate and simplicity compared to previously reported methods [34]. In this method, a hydrocarbon gas source, i.e., ethanol, acetylene or propylene is heated to 600-1000 °C in a tubular reactor, in which a transition metal catalyst (Fe, Co, Ni) is present to decompose the hydrocarbon. CNTs grow on the catalyst and can be collected when the system is cooled to room temperature. CVD allows for large-scale production, good alignment, and controlled growth of the nanotubes. In addition, it also allows better control of the growth parameters as growth occurs at a lower temperature and the fact that the metal catalyst is held on a substrate benefits the growth of nanotubes aligned in the desired direction relative to the substrate [34]. The disadvantage of this method is a higher defect density (amorphous carbon) of the CNTs obtained when compared to the other two methods. These defects negatively affect the electrical, thermal, and structural characteristics of CNTs [65]. Table 4 summarizes the main characteristics of each method described, as well as the advantages and disadvantages.

Table 4- Comparison between the main physical properties of SWCNTs and MWCNTs produced by 3 different methods.

Method	Arc Discharge Method	Laser Ablation	Chemical Vapor Deposition
Typical yield [66]	30-90%	Up to 70%	20-99%
Temperature	1700 °C	1200 °C	< 800 °C
Average diameter of the tubes [67]	1.3–1.4 nm	1.4 nm	1 nm
Process control	Difficult	Difficult	Easy
Energy Requirement	High	High	Moderate
Advantages	High degree of structural perfection	High degree of structural perfection and synthesis in room temperature production	Large scale production, good alignment, simple and high purity
Disadvantages	High Temperature and carbon impurities	Limited method to the lab scale	Higher defect density

1.2.4- Purification of CNTs

During the CNTs synthesis, several impurities, such as carbonaceous materials and metals present in the colloidal suspensions of CNTs, may be formed depending on the technique used [68]. For this reason, it becomes essential to evaluate and characterize this nanomaterial to prevent the possible toxic effects and also to improve the quality of the final material, aiming at its use in biomedical applications. In this regard, various spectroscopic methods, diffraction techniques and separation techniques have been applied to determine the physical and chemical nature of CNTs (Table 5) [69].

Table 5- Overview of the main techniques used for characterizing the properties of CNTs.

CNT properties	Characterization technique	References
Internal structure, diameter, number of layers, and intershell spacing	Atomic force microscopy (AFM) Transmission electron microscopy (TEM)	[70, 71]
Aggregation, diameter, and length	Scanning electron microscopy (SEM)	[71, 72]
Thermal stability and purity of CNTs	Thermal gravimetric analysis (TGA) and Derivative thermogravimetry (DTG)	[73]
Relative purity measurement, dispersion capacity, length and diameter distribution	UV-Vis spectroscopy	[73]
Impurities remaining after synthesis and functional group after surface modification	Infrared (IR) and Fourier-transform infrared spectroscopy (FTIR)	[70]

After the synthesis process it is necessary to remove the impurities generated to ensure the purity of the material, without the presence of unwanted composites. The purification methods of CNTs can be divided into 3 categories: chemical methods, physical methods and a combination of both [74]. The chemical method purifies CNT based on selective oxidation, in which carbon impurities are oxidized at a faster rate than CNTs and there is a dissolution of metal impurities using acids. This method can effectively remove amorphous carbon and metal particles that may form during synthesis. However, it is a method that influences the structure of CNTs due to the oxidation involved. On the other hand, the physical method separates CNTs from impurities based on differences in their physical size, aspect ratio, gravity and magnetic properties. Since it does not require the oxidation step, it does not expose CNTs to serious damage, although it is a more time-consuming, more complex and less effective method [74]. The chemical method encompasses liquid-phase oxidation and gas-phase oxidation techniques, while the physical method applies ultrasonication, filtration, and chromatography techniques [75]. To achieve the desired CNTs with a considerable yield and purity level, combinations of chemical and physical purification methods have been investigated. According to the different needs, various types of multi-step purification methods are reported [74]. For example, graphite particles existing in CNTs synthesized by arc discharge method or laser ablation method are difficult to remove through chemical oxidation, so filtration is adopted in some purifications as a subsequent technique [76].

1.2.5- Dispersion of CNTs

Dispersion is a key parameter for improving the performance of materials [77]. Regarding carbon-based materials, these are very difficult materials to stabilize and disperse in aqueous solutions mainly due to substantial van der Waals attractions and specific hydrophobic interactions [78]. In the specific case of CNTs, dispersion in polymeric matrices and even in various solvents is a difficult process for 3 main reasons: CNTs tend to agglomerate with each other due to weaker intermolecular forces, more specifically through van der Waals forces, creating large bundles that are held tightly together [79]. Furthermore, due to their rigidity and chemical inertness, CNTs do not interact with other materials and, finally, due to their low density, CNTs tend to occupy a large volume in the matrix [77].

To obtain the desired dispersion, Foldvari and co-workers proposed 4 basic approaches: surfactant-assisted dispersion, solvent dispersion, sidewall functionalization, and biomolecular dispersion [80]. In particular, functionalization has been considered as the most effective method to prevent the agglomeration of CNTs and improve charge transfer across the interface of CNTs and polymer [81]. Furthermore, the functionalization of CNTs has shown significant evidence in decreasing cytotoxicity, improving biocompatibility and processability, and enabling the attachment of drug molecules, proteins, or genes to build delivery systems [80]. Thus, while the purification step is important in removing unwanted particles after synthesis of CNTs, functionalization is responsible for introducing a specific functional group into the side chains or ends of CNTs [82].

1.2.6- Functionalization of CNTs

Several researchers have been looking for novel alternatives to address such challenges in the aggregation or bundling of carbon materials, and the main approach used is their surface functionalization [83]. Functionalization means the introduction of functional groups along the side chains or ends of the CNTs [82]. This can be achieved by 2 main phenomena: covalent functionalization (chemical bonding) or by non-covalent functionalization (physical adsorption). In general, in covalent functionalization, chemical reactions are carried out that result in the formation of bonds with the sidewall surface of CNTs, while in non-covalent functionalization, the hydrophobic surface of CNTs is explored for possible interaction with the hydrophobic portion of amphiphilic molecules, for example surfactants and some biomolecules. For a better and correct understanding of these 2 functionalization methods, a more detailed explanation follows below [83].

Covalent functionalization of CNTs can be done in 2 ways: by directly adding functional groups or active species to the sidewalls of the CNTs or by attaching modified functional groups to the ends of the nanotubes. The oxidation process is often used as a preparation step to create chemically active sites for covalent bonds. Therefore, by using oxidizing agents, namely HNO_3, H_2SO_4/HNO_3 or $KMnO_4/H_2SO_4$, carboxyl groups (COOH) are formed on the surface of the CNTs. The COOH group has the ability to create ester and amide bonds that subsequently allow molecules to covalently dock [83, 84]. Cristopher and co-workers demonstrated that functional groups covalently attached to CNTs alter hydrogen bonding, then reduce van der Waals interactions between CNTs, facilitating their separation into individual tubes while promoting their solubility [85]. Similarly, these groups allow the immobilization of other biomolecules on the surface of CNTs. For example, through carbodiimide chemistry, some compounds can react with carboxylated CNTs to activate the COOH group that can react directly with primary amines present in various biomolecules. Thus, an amide bond is formed between the COOH group and the primary amine [86]. Although covalent functionalization allows a strong interaction between the biomolecule and CNTs, the modification of the surface of CNTs by covalent bonds can alter some of the intrinsic properties of CNTs, such as the change in hybridization from sp^2 to sp^3, resulting in decreased conductivity and mechanical strength. In addition, this method can lead to the destruction of the structure of CNTs, which includes their shortening [79]. In addition to the oxidation method, photochemical functionalization and electrochemical functionalization also emerged as other forms of covalent functionalization [34]. In an attempt to come up with a functionalization strategy that did not involve the use of strong acids or organic solvents, Polo-Luque and co-workers reported the use of ionic liquids for functionalization reactions and were able to maintain the original properties of each component [87].

Alternatively, non-covalent functionalization of CNTs is a non-destructive method as, unlike chemical functionalization, it offers the advantage of adsorbing the functional groups to the walls of CNTs without affecting their structural integrity and physical and chemical properties [83]. A comparison of the properties between CNTs without any functionalization, covalently functionalized CNTs, and non-covalently functionalized CNTs can be found in Table 6.

Table 6- Comparison of pristine, covalently and non-covalently modified CNTs (Adapted from [88]).

Properties	Pristine CNTs	Covalent CNTs	Non-covalent CNTs
Solubility	-	+++	+++
Electrical properties	+++	-	+++
Structural alterations or fluctuations	-	+++	-
Degradation capacity	-	+++	++
Drug loading capacity	-	++	+++
Toxicity	+++	-	-

+: Low; ++: Moderate; +++: High; –: None

Non-covalent functionalization can be achieved through various interactions: π-π interaction, where aromatic molecules or polymers are used, CH-π involving interactions of biomolecules and CNTs, or electrostatic interactions. Currently, functionalization of CNTs with high-affinity molecules such as surfactants, conjugated aromatic molecules, and polymers is used to increase the solubility of CNTs in solvents that can promote the adsorption of biomolecules to their surfaces [84]. Among polymers, polyethylene glycol (PEG) is the most widely used to anchor a variety of biomolecules. The advantage of PEGylation is to protect CNTs from opsonization which leads to higher circulation times, when used as delivery systems. Surfactants such as sodium dodecyl sulfate (SDS), sodium dodecylbenzene sulfonate (SDBS) and Triton X-100 adsorb onto the surface of CNTs through π-π interactions to improve their solubility and permeability across biological membranes. Although the improvement in solubility of CNTs can still be considered low (between 0.1 and 0.9 mg/mL), it is still accepted for biological use [88]. Using the non-covalent functionalization approach, several molecules have been successfully adsorbed onto CNTs, for example polysaccharides [89], DNA [90], short-interfering RNA (siRNA) [91] and proteins [92]. Figure 5 gives some examples of functionalization of CNTs by different methods.

Nucleic acids are ideal candidates to form complexes based on the π-π interactions between the aromatic bases and the surface of CNTs. Zhao and co-workers studied the adsorption of DNA to an SWCNT in an aqueous environment. The hydrophobic end groups of the DNA were attracted to the hydrophobic surface of the SWCNT, while the hydrophilic structure of the DNA did not bind to the SWCNT [93].

In the literature, some works include the covalent and non-covalent functionalization methods into a broader category called exohedral functionalization, where then CNTs can be functionalized with various compounds through their outer area [94]. When therapeutic agents are trapped in the inner area of CNTs, we call it endohedral functionalization: molecules, such as drugs, access the inner area of CNTs by capillarity and are retained through hydrophobic interactions, van der Waals forces and π-π interactions between the charged molecules and the walls of CNTs. CNTs-based drug vehicles must therefore be carefully designed to obtain systems where the molecule is well held within the CNT cavity and only released at the target site [95].

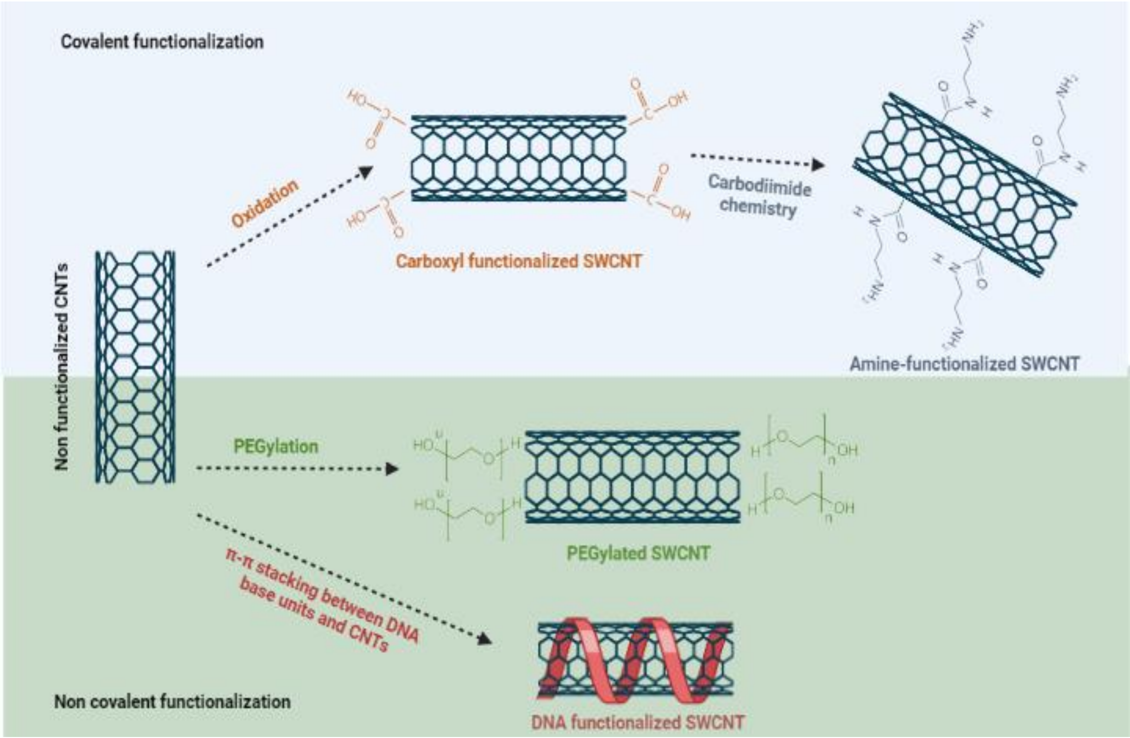

Figure 5- Overview of functionalization of CNTs by both covalent and non-covalent methods (Adapted from [97]).

1.2.7- Toxicity of CNTs

Although CNTs exhibit desirable biological properties in the body, there are still many concerns about their biosafety from both manufacturing and medical application perspectives. For this reason, several toxicity studies are needed to fully evaluate the *in vivo* impact of CNTs before widespread commercial biomedical application. This research topic has led to many inaccurate and incomplete toxicity studies, ranging from the use of animal models that do not mimic the actual routes of exposure to CNTs to studies that do not fully characterize the impurities, chemistry, loading, and dimensions of this type of nanomaterial [96]. Over the past years, numerous studies have been conducted on the toxic effects of CNTs both *in vivo* and *in vitro*, and it has been described that these nanomaterials exhibit different toxicity levels depending on their size, width, presence of metallic impurities, type of functionalization, presence of solubilizing agents and route of administration (dermal, intravenous injection or inhalation) [97].

The high surface area of nanomaterials is one of the main reasons for the toxicity mechanisms associated with them. Most researchers concluded that the reduction in size of nanomaterials contributes to an exponential increase in surface area, leading to increased surface reactivity (aggregation), which may consequently cause damage to the surrounding environment (biological factors). In particular, aggregation of CNTs can produce immune responses and cause their deposition in tissues [98]. An *in vivo* study conducted by Qu's team concluded that a high degree of MWCNT clumping resulted in increased accumulation of CNTs in vital organs such as the lungs and liver, subsequently initiating an inflammatory response [99].

Within this context, the functionalization of CNTs is described as one of the main parameters that contribute to a better solubility of CNTs and decreased cytotoxicity, directly affecting the quality of cellular uptake and cellular internalization mechanisms [100]. Yan and co-workers developed an active, pH-responsive targeting system to deliver doxorubicin (DOX) to tumor sites using folic acid functionalized MWCNTs. The results of this study proved that the functionalized CNTs were non-toxic to the cells, exhibiting cell viability of over 90% [101]. On the other hand, another study published in 2011 demonstrated that functionalization of SWCNTs with carboxylic acid induced higher toxicity compared to non-functionalized SWCNTs in HUVEC cell line. This result highlights the importance of the choice of functionalization type in inducing or reducing toxicity given the intended application [102].

1.2.8- Biomedical Applications of CNTs

CNTs have unique characteristics that enable their use for a variety of applications in biomedicine, namely their unique structure that gives rise to an extraordinary combination of mechanical and electrical properties. Although CNTs are hydrophobic by nature, they can be functionalized to specifically interact with cell surface receptors for cellular internalization. This approach allows for greater selectivity of CNTs to cells, thus reducing the amount of drugs required in the treatment of various diseases. In addition, this strategy may help minimize systemic toxicity and inflammation [103]. For example, Khazaei and co-workers found that covalent functionalization of SWCNTs with amide and ester bonds facilitates slow drug delivery for longer periods by improving solubility in aqueous and organic media [104].

In general, CNTs play very promising roles in biomedicine, specifically in drug delivery systems, gene delivery and gene therapy, biomedical imaging, diagnostics, biosensors, and tissue engineering [100]. Table 7 summarizes some of the most attractive features of CNTs in various biomedical applications.

Table 7- Summary of CNTs biomedical applications (Adapted from [105], [100]).

	Applications	Examples		Applications	Examples
	Diagnosis and Imaging			**Therapy applications**	
Biosensing	CNTs present special mechanical and electrical properties that make them candidate materials for the fabrication of optical and electrochemical biosensors	• NIR fluorescence biosensors (e.g., sensing of β-D-glucose) • Electrochemical biosensors (e.g., DNA, viruses, antigens)	**Photo-thermal therapy**	CNTs can convert near infrared radiation (NIR) into heat	Irradiation of tumors with a NIR light laser until thermal ablation is achieved
Biomedical imaging	Characteristics such as high photostability make CNTs suitable for bioimaging applications	•Photoacoustic imaging in mice •Raman imaging (targeted in vivo and multicolor imaging)	**Tissue engineering**	Good materials for tissue engineering due to their biocompatibility, stiffness, stimulation of cell adhesion and proliferation, and ability to form strong 3D architectures	•CNTs as scaffolds in bone regeneration •CNTs for neural applications
			Drug / gene delivery	CNTs have been considered transporters for drug/gene delivery due to their high surface area, multifunctional surface chemistry, lack of immunogenicity, and good ability to easily penetrate cell membranes.	•Covalently conjugated to CNTs (e.g., Pt (IV) pro-drug, paclitaxel) •Non-covalently conjugated to CNTs (e.g., doxorubicin) •Plasmid DNA and siRNA •Proteins covalently or noncovalently conjugated to CNTs

1.3- Biopharmaceuticals

Biopharmaceuticals are products of biological origin, such as proteins, nucleic acids, blood products, somatic cells or derivatives produced or extracted from living sources (microorganisms, cells, plants or animals). The main classes of biopharmaceuticals constitute enzymes, vaccines, monoclonal antibodies (mAbs), cytokines, hormones, recombinant blood products, hematopoietic growth factors, nucleic acids (DNA and RNA), and gene- and cell-based therapies [106, 107]. Currently, recombinant therapeutic proteins and antibodies are considered the most abundant types of biopharmaceutical products on the market [108]. The success of therapies using biopharmaceuticals is related to the development of recombinant DNA technology in the late 1970s, which allowed large-scale production of human proteins, promoting numerous clinical investigations using new therapeutic approaches [109]. In 1982, recombinant human insulin was the first biopharmaceutical approved for clinical use by Food and Drug Administration (FDA), becoming the first biotechnological therapy for the treatment of diabetes [110]. The approval of this biopharmaceutical obtained from the bacterium *Escherichia coli* has boosted the discovery of other biopharmaceuticals, offering a radical change in the pharmaceutical industry, modernizing the treatment of numerous diseases such as cancer, hematological problems, diabetes and immune diseases, thus providing better patient care and valuable targeted therapies. Thanks to the unique and promising characteristics of biopharmaceuticals, several researchers have developed studies exploring their therapeutic potential, while searching for alternatives to solve their limitations [111].

In 2018, a total of 374 biopharmaceuticals were approved by the US and EU to treat various diseases [112]. Approximately 270 peptides are estimated to be currently tested in clinical trials and more than 500 are in preclinical development, numbers that give very good indications for a rapidly growing market [113]. The success of biopharmaceuticals is attributed to their targeted, specific, disease-modifying therapy. Although more complex and highly challenging to develop and manufacture, they outperform chemically synthesized molecules with fewer nonspecific side effects, shorter development and approval times, and a higher probability of success [112, 114]. In 2019, approximately 50% of approved biologics represented monoclonal antibodies and vaccines. Compared to small molecule (SM) drugs, biopharmaceuticals are considered less dangerous by the European Medicines Agency's Committee for Medicinal Products for Human Use because they are derived from a biological source [115]. The structural complexity and macromolecular nature of biopharmaceuticals contribute to their high specificity, but simultaneously also make them more challenging in terms of final formulation, distribution, and evaluation by regulatory agencies [112].

1.3.1- Biopharmaceuticals production - general process

Several fields must interact and work collaboratively in the development of the biopharmaceutical production process, starting with the identification studies of drug targets and receptor molecules, which are related to medical conditions of interest, to the implementation of appropriate strategies for the production of biological molecules and the experimental pharmacological and toxicological studies. After these steps, the most promising biomolecules are expressed recombinantly, and production yields and product characteristics are optimized [116]. A biopharmaceutical production process needs to meet the standards set by regulatory agencies to be integrated into the market. In addition, reproducibility and techno-economic feasibility are required, as well as specified quality of the therapeutic molecule [117].

A bioprocess can be divided into 2 main parts: the upstream and the downstream stages. Upstream processing comprises the transformation of the raw material into the product and is dependent on a large number of variables, namely: (1) the cell line used (host cell selection, vector construction technology, metabolic engineering, etc.); (2) the culture medium composition (essential nutrients and their concentrations, complex or chemically defined nutrients, etc.); (3) the operation strategy (batch, fed-batch, perfusion, continuous cultivation, etc.); (4) bioreactor design (type, mixing strategy, oxygen supply, shear stress, scale-up, automation, etc.); (5) process monitoring (pH, dissolved oxygen, temperature, nutrient concentrations, secondary metabolites, product concentrations, etc.); and (6) product analysis (detection of impurities, aggregates, endotoxins, lipopolysaccharides, viruses, etc.) [118]. Typically, biologics are produced by microorganisms (for example *E. coli* or yeast) or mammalian cells. There is, however, a clear trend towards using mammalian-based expression systems, since there are quite a few biomolecules that require post-translational modifications, particularly glycosylation [119].

On the other hand, the downstream process primarily aims to capture the target biomolecule and remove host cell-related impurities (e.g., host cell proteins, genomic DNA, host RNAs), process-related contaminants (e.g., buffers, leached binders, antifoams), and product-related impurities (e.g., aggregates, fragments). To accomplish a high purity degree, the downstream process usually comprises several steps and each of these purification steps is capable of removing one or more classes of impurities. Due to this complex task of purifying the target product, the downstream processing costs represent around 70-80% of the total production cost of a given biopharmaceutical. For this reason, efficient recovery and purification of biopharmaceuticals has been referred to as a critical part of the production process. With the increase in product yields observed over the years, there is currently more pressure on this process and much interest in its constant improvement [107, 120]. The type and number of unit operations ultimately depend on the final use of the product. For industrial enzymes, 80-90% purity is usually acceptable. For diagnostic proteins, the required purity should be at least 95%, whereas for therapeutic applications, purity higher than 99% is often required. Downstream processing is usually divided into 3 steps. The first step is an initial recovery where the main goal is to remove solids, release the product, and reduce volume. For this, techniques such as filtration, centrifugation, precipitation, or sedimentation are used [119]. This step is significantly affected by the location of the target product in its production phase. For products associated with cells, it is necessary to perform cell disruption, a process that is carried out on the dense cells obtained after clarification of the culture medium. Intracellular products make the process of purification of biomolecules more difficult compared to extracellular products, as they require cell disruption. As a consequence, there is an increase in the viscosity of the medium due to the release of nucleotides, and the target product is released along with all other intracellular molecules, which increases the diversity of contaminants [121]. The second step is intermediate purification, where the aim is to reduce volume and remove components with properties that are substantially different from those of the product. Typically, processes for intermediate purification are relatively non-selective, however significant increases in product quality and concentration can be accomplished. Unit operations such as solvent extraction, adsorption, precipitation, and ultrafiltration are commonly performed [122]. Finally, for the last step called polishing, the goal is to separate the product from impurities with properties close to those of the product or the unwanted forms of biomolecule of interest that is formed due to the misfolding during previous steps of the downstream processing. Chromatography is commonly used to achieve the desired purity level of biopharmaceuticals, in order to achieve the specifications established by the regulatory agencies [119, 123]. Every technique offers a balance between resolution, capacity, speed and recovery [124]. Figure 6 shows the bioseparation steps that may be involved in a biopharmaceutical product recovery process.

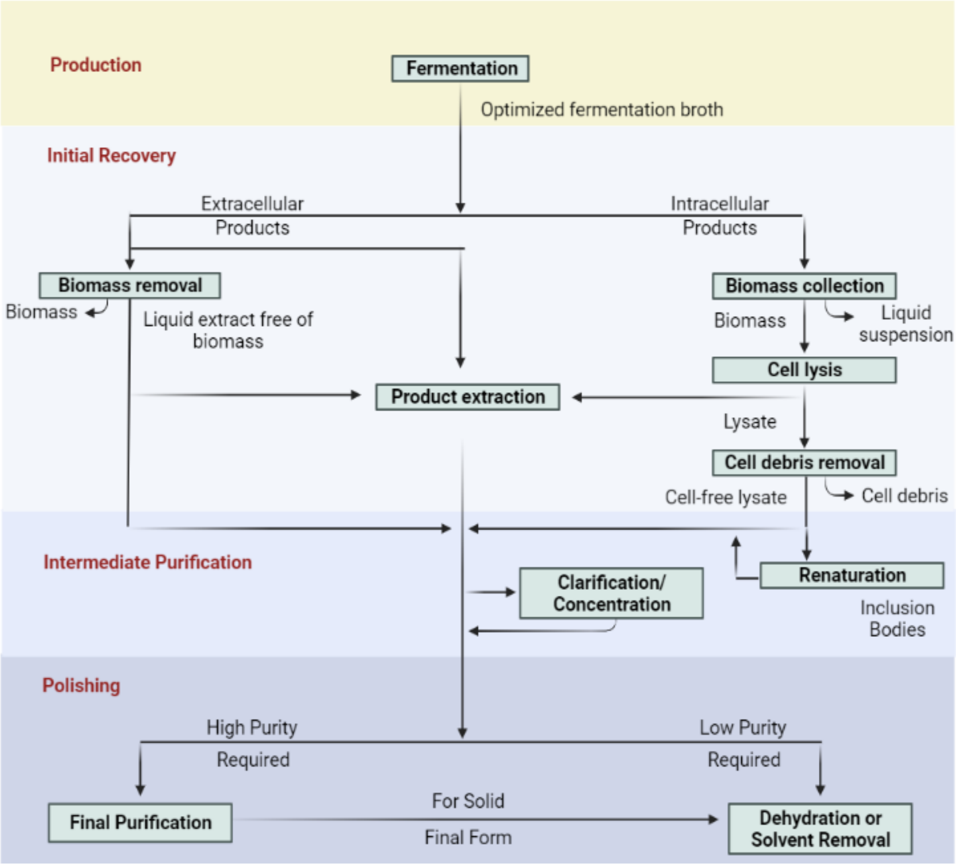

Figure 6- Generalized block diagram of downstream processing (Adapted from [128]).

1.4- Capture and Intermediate Purification

Multiple steps of capture and purification are adopted to separate the target product from pools of contaminants after cell separation (for extracellular product) and disruption processes (for intracellular product). These steps normally contribute substantially to the total production cost [125]. The liquid medium resulting from the cell disruption operation is called a homogenate or cell lysate. This lysate is quite complex and is where the biopharmaceutical product of interest is diluted. Therefore, the main objective of the intermediate purification step is to concentrate as much as possible and purify the product, since this lysate also contains host contaminants, such as genomic DNA (gDNA), RNA and proteins [126, 127]. These contaminants must therefore be progressively eliminated so that the final solution ends up with the biopharmaceutical product [128].

The complex extract entering the intermediate purification step can be processed by various techniques such as precipitation, membrane separation, liquid-liquid extraction, and adsorption. The choice of technique is usually dictated by the nature of the product, not disregarding the aim of minimal loss of product activity [119].

1.4.1- Precipitation

This method allows the separation of biological products from a complex lysate [119]. Precipitation is applied in downstream processing of several fermentation products such as citric acid and antibiotics, and may be used to remove unwanted contaminants such as pigments, calcium, proteins, and nucleic acids from process streams. Typically, addition of precipitants, such as salts (e.g., ammonium sulfate for protein precipitation), solvents (e.g., precipitating polysaccharides and nucleic acids with ethanol), and polymers (e.g., precipitating proteins with PEG), and changes in the pH, ionic strength, or temperature of the solution, are used to reduce the solubility of the product, causing precipitation. The precipitated solids are then recovered by filtration, microfiltration, or centrifugation [122]. Ideally, the objective is to simultaneously concentrate and purify the product, although precipitation is more efficient as a concentration step. Precipitation is, thus, typically used early in the isolation and purification of a biological product, reducing the volume to be processed. It is a relatively inexpensive method, easy to scale up, and can be carried out with simple equipment at a continuous operation mode. However, it can present high costs, and may require further purification steps [119, 122].

1.4.2- Membrane Separation

In order to produce molecules, emulsions, and particles, membrane techniques are increasingly being used in reaction, clarification, and recovery schemes. The selectivity, high surface-area-per-unit-volume, and capability of membrane systems to regulate the degree of contact and/or mixing between two phases are all advantages. They operate at very low temperatures and pressures, do not include phase changes or require chemical additives, and are particularly well adapted to processing biological molecules. This reduces the amount of denaturation, deactivation, and/or degradation of biological products [129].

The membrane acts as a selective barrier separating two phases and limiting the transport of different compounds. Its composition can be homogeneous or heterogeneous, its structure can be symmetric or asymmetric, it can be solid or liquid, and its charge can be neutral, positive, or negative. An influent stream that flows tangential to the membrane is often divided into two effluent streams called the permeate and the retentate in a membrane-based separation. The fraction of the fluid that permeates the membrane is referred to as the permeate, while the portion that is rejected is referred to as the retentate. The semipermeable membrane serves as a selective barrier during the separation, keeping out biomolecules and particles larger than the pore size while allowing smaller molecules to pass through the pores [119]. The main disadvantages associated with this process result from the robustness and reliability of the membranes used. For example, membranes are susceptible to fouling, have limited resistance to cleaning chemicals, solvents, and wide pH ranges, and can be damaged by fluctuations in operating pressure [122].

1.4.3- Liquid-liquid extraction (LLE)

The most well-known liquid extraction process relies on the product's preferential solubility in an additional organic phase that is immiscible with the aqueous phase. The appropriateness of the solvent has a significant impact on the efficiency of solvent extraction, which is assessed in terms of a distribution coefficient that indicates the concentrations of the solute in the various phases. A high distribution coefficient suggests good separation and preferred solubility in the solvent [130]. This is a traditional technique widely used in the chemical industry because of its simplicity, low cost, low separation time, and easy scale-up. However, its use in the biotechnology area faces some concerns, namely due to the impact of organic solvents on the structure and biological activity of various biologics. In addition, the most commonly used organic solvents pose very significant environmental risks, often exhibiting high toxicity (ranging from irritation to acute and chronic toxicity), volatility, flammability, and persistence in the environment. Thus, considering the environmental concerns, and especially the negative effect on biopharmaceuticals, this strategy becomes inappropriate for the recovery of biopharmaceuticals due to the negative impact of organic solvents on structural integrity and biological activity [131]. In order to overcome the major concerns of using volatile organic solvents, another type of liquid-liquid extraction that does not require organic solvents to form immiscible phases became more popular among biotechnologists. This approach is known as aqueous two-phase systems (ATPS) and has emerged as an ideal solution for the concentration and separation of biological products, mainly due to the immiscible phase nature. Additionally, its popularity is also due to its cheaper and more sustainable characteristics, which can reduce production costs and environmental impacts [132].

1.4.4- Adsorption

Separation of complex low-concentration systems still presents a great impact on the industrial structure and economy [133]. The low concentration of the target molecule and a large number of similar components will lead to low separation efficiency, high cost, complicated steps and other problems. In 2016, a commentary published in Nature listed 7 technologies that urgently need to be developed in the field of products separation. Among them, 3 technologies are widely used in the separation and extraction of target molecules from complex solutions of low concentration [134]. For this reason, efficient, accurate and controllable separation of target molecules in complex solutions of low concentration and large volume is a target topic of research in the field of separation science [133].

Adsorption, often confused with chromatography, is a very common way of separating biomolecules. It consists of contacting the solution containing the biomolecule of interest with adsorbent particles, which will bind the target molecule through van der Waals, electrostatic, hydrophobic, or specific interactions such as antibody-antigen or protein-heparin interactions. The adsorbent is a solid particulate material, and although it can be in contact with solutions in stirred containers, it is more common and efficient to place it in a packed column and move only the solutions. The operation consists of adsorption, or binding (passing the sample through the column, with the solute binding to the adsorbent) and then changing the mobile phase to conditions favorable for desorption, or release of the solute, which is more concentrated and has fewer contaminants. Additionally, intermediate washing steps can be used [135]. Currently, there are 2 types of adsorption processes with very good efficiency percentages: adsorption in batch systems and column adsorption.

In the batch system, adsorption takes place between the two liquid–solid phases, where the solid phase moves continuously along with the liquid phase. The main advantages of this process are: (1) the adsorbent and adsorbate are constantly mixed and the solution volume is constant, (2) it is an easy and economical method and is used in many studies, and (3) enables predicting the performance of adsorbent before application in larger scale, and (4) provides critical information about the efficacy of particular adsorbate-adsorbent system. The disadvantage of this technique is that in industry it is not recommended to work with small amounts of adsorbent material [136]. Among the column adsorption processes, adsorption on a fixed bed has some important advantages: (1) the process is continuous because the adsorbate is continuously in contact with the adsorbent, (2) it is simple and has low costs, (3) it can be used on an industrial scale.

However, in column adsorption, the contact time is not long as in batch adsorption and therefore equilibrium is not reached for certain adsorptions [137]. Adsorption of the molecules to the adsorbent surface can occur in 2 ways which are "physical adsorption," also called "physisorption," and "chemical adsorption," also called "chemisorption" [138]. This depends on the interactions between the molecules and the surface. In physical adsorption, the weaker forces such as electrostatic interactions and van der Waals forces are involved. The strong chemical bonds such as covalent bonds are formed between the surface and the adsorbed molecules in chemical adsorption. Chemical adsorption is slower than physical adsorption and usually a monomolecular layer (monolayer) is formed on the adsorbent surface while physical adsorption usually involves the formation of thick multilayer on the surface [139]. Table 8 shows the differences between physical adsorption and chemical adsorption [138].

Table 8- Comparison Between Physical Adsorption and Chemical Adsorption (Adapted from [138]).

Physical Adsorption	Chemical Adsorption
Electrostatic interactions and van der Waals forces are involved	Covalent bonds are formed between the surface and the adsorbed molecules
Fast	Slow
Reversible	Irreversible
Not very specific	Specific
Multilayers are formed	Monolayers are formed
Activation energy is not required	Activation energy is required
It usually occurs at low temperature and decreases with increasing temperature	High temperature is needed

Ideal adsorbent materials have a high surface area per unit volume, what can be achieved if the solid contains a network of fine internal pores that provide an extremely large internal surface area [122]. In adsorption studies, one must know the influence of key operating variables throughout the process in order to achieve high recovery rates and economic yield [140].

1.4.4.1- Solid-phase extraction (SPE)

Solid phase extraction (SPE) based on LLE procedure is a technique that can separate and enrich the target analytes from complex matrices successfully [141]. In 1971, Broich and co-workers used the technique to extract drugs from urine samples of drug-abusing persons, for the first time [142]. The equipment was considered a revolution of sample pretreatment techniques, as it could integrate separation and concentration, and had the advantages of high extraction efficiency, good selectivity, wide application range, briefness and ease of automation. SPE enables the separation and purification of the sample, based on the liquid chromatographic separation principle of selective adsorption and selective elution [143]. Over the years, SPE has undergone steady growth driven by the need for analysis to find sample preparation procedures that are simple and relatively inexpensive, that provide good recovery of the molecule of interest and adequate selectivity, that reduce the use of organic solvents, and that can be automated when the need arose [143]. In accordance to the green chemistry, the SPE method complies with the principles of decreasing the amount of solvents used in purification and preparation of samples [144]. It has various purposes of use in purification [145], trace enrichment [146], desalting [147] and class fractionation [148]. The principle of SPE is similar to that of LLE, involving a partitioning of solutes between two phases. However, instead of two immiscible liquid phases, as in LLE, SPE involves partitioning between a liquid (sample matrix) and a solid (sorbent) phase. This technique consists of 4 main steps that include conditioning, sample loading, washing, and analyte elution (Figure 7) [143].

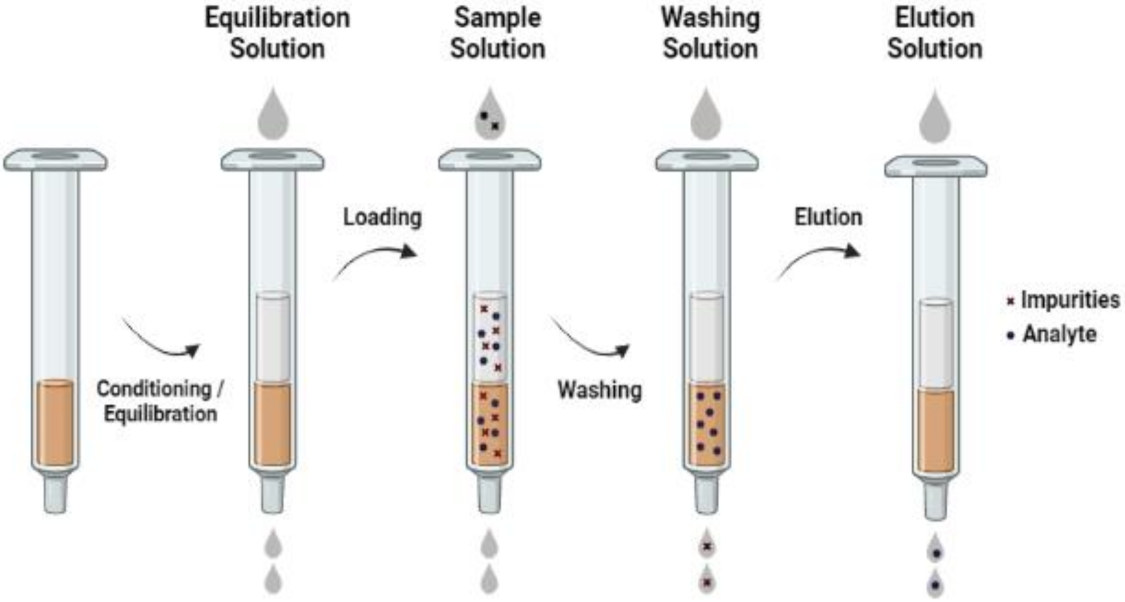

Figure 7- SPE operation steps (Adapted from [150]).

Although both methods (SPE and LLE) have a high recovery rate, high selectivity and robustness, and low time requirements, there are some differences that mostly benefit the SPE method, as illustrated in Table 9 [143].

Table 9- Main differences between LLE and SPE (Adapted from [143]).

Differences	**Liquid-liquid extraction (LLE)**	**Solid phase extraction (SPE)**
Separation result	Two immiscible liquid phases	Involve partition between a liquid which is sample matrix or solvent and solid phase as sorbent
Price	Cheaper	Expensive cartridge
Rate of separation	Slower	Faster
Handling technique	Too labour intensive	Easier to automate and less manual effort
Solvents	High purity solvents required	Low purity solvents still can give best separation
Selectivity	Limited	High range of immiscible solvents available
“Art of extraction”	More gentle extraction and give high recovery	Easily oxidized during drying
Repeatability	Low	High

There are many variations of the SPE method due to the extraction process, the shape and size of the adsorbent bed, and the type of adsorbent material. Over the past few years, several modifications of SPE were discovered, most being based on miniaturization and automation of various stages of the SPE. Particularly noteworthy are the following: dynamic solid-phase extraction (SPDE), microextraction by packed sorbent (MEPS), matrix solid-phase dispersion (MSPD), stir-bar sorptive extraction (SBSE), solid-phase microextraction (SPME), and dispersive solid-phase extraction (d-SPE) [149]. In particular, d-SPE has gained popularity since 2003, when Anastassiades and co-workers reported it as an effective cleaning procedure for extracting pesticides. In this very accessible method, the solid sorbent is applied directly to the volume of a liquid sample solution without the need for prior sample preparation, and the entire procedure relies entirely on processes such as agitation and centrifugation or through an external magnet when using magnetic particles. This simple approach ensures a high contact surface between the sorbent and the sample, allowing the extraction equilibrium to be reached quickly. The resulting method is fast and proven effective, and considering the very low amounts of sorbent and solvent required, can be seen as a more environmentally friendly method than standard solid phase extraction [150].

1.4.5- Carbon materials as adsorbents

Carbon nanomaterials have fascinated the scientific community since their discovery. The high surface atom fractions that lead to a high surface-to-volume ratio of carbon-based nanomaterials are one of the most important characteristics of these materials when compared to micro- and large-sized materials. For this reason, a high surface area of carbon-based nanomaterials leads to a high adsorption capacity for different organic, inorganic, and bioactive species. In addition, these materials also provide easy functionalization and reusability, enhanced electronic properties such as high conductivity, fast response to physical events, and chemical reactions [151]. Considering these unique properties, interaction with organic compounds is possible through non-covalent forces including electrostatic forces, hydrogen bonding, van der Waals forces, π-π stacking, and hydrophobic interactions (Figure 8) [152, 153].

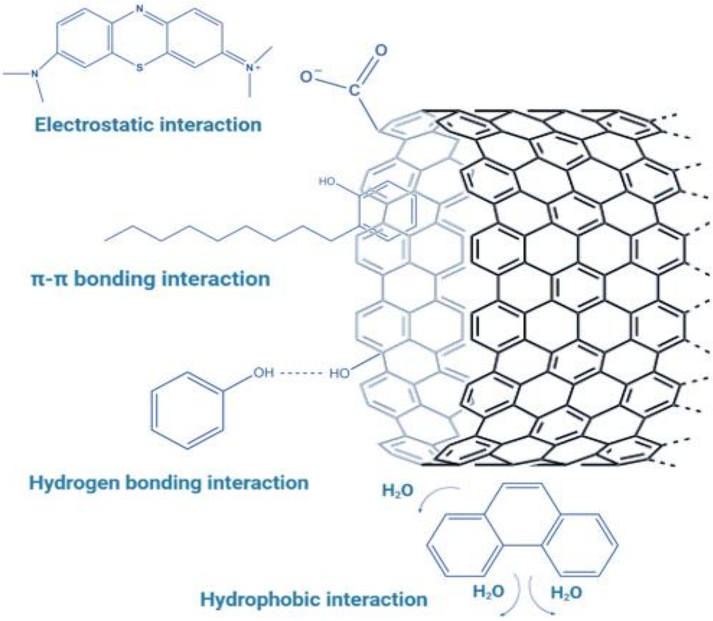

Figure 8- Adsorption mechanisms of organic compounds onto carbon materials (Adapted from 153).

Due to these properties, carbon-based nanomaterials have gained remarkable recognition in various fields of analytical chemistry, such as sample preparation methods, separation techniques, and qualitative and quantitative analysis [154]. Fullerenes, CNTs, carbon nanofibers, graphene, graphene oxide (GO) and their functionalized forms have been used preferentially as adsorbents in many SPE methods, constituting the most researched and studied materials of the 21st century. The extremely high surface area of these materials ensures the adsorption of target analytes using only a few milligrams or tens of milligrams of adsorbent compared to other common adsorbents such as alumina, silica and certain synthetic resins [151, 155]. In particular, the separation and purification of different molecules from complex biological samples represents a particularly important step during the separation and analysis of the entire system [156]. Numerous potential interferents and low concentrations of the target molecules make extraction, concentration, and purification procedures necessary and often involve multi-step operations. Therefore, the development of new, simpler, more efficient, sensitive, and selective techniques is increasingly necessary. Within this context, the improvement of existing techniques using new extraction materials has gained considerable prominence as one of the main trends in this area [157].

1.4.5.1- CNTs as adsorbents

In the family of adsorbents, CNTs are used for separation and enrichment of dyes, heavy metals, proteins, nucleic acids, and other complex samples. This adsorptive capacity is mainly due to their remarkable structure, large surface area, and high mechanical strength. In addition, carbon nanotubes grafted with different functional groups will improve its excellent adsorption properties [158].

The selectivity of the CNTs adsorbent is similar to the other carbon-based materials whilst adsorption capacity of CNTs is significantly higher. This allows the use of a small amount of material, which is very important for economic reasons. In addition, CNTs are an excellent solid sorbent for use in d-SPE. However, more research is still needed in this field as this approach is not yet widely investigated [159]. In all cases, the development of these SPE-CNTs undergoes a series of steps until it is optimized. Diverse factors affect the previous stages, like the type and quantity of CNTs used, the influence of pH, sample volume, buffer type, and concentration of the binding and elution solutions, among others [160]. The properties of CNTs can improve the separation and pre-purification performance of traditional phases, while modified CNTs are applied to improve the selectivity for target analytes. Recently, 3 types of CNTs can be distinguished according to their use in SPE: as-grown, oxidized and functionalized CNTs. Information about these 3 types of CNTs is described in Table 10 [161, 162].

Table 10- Characteristics of the different types of CNTs used as SPE adsorbents (Adapted from [164, 165]).

Type of CNTs	Description	Characteristics
as-grown CNT	Obtained after synthesis and purification. Consist of one or more perfect graphene layers rolled up as one or several cylinders.	Have nonpolar bonds and high length to diameter ratio. Are insoluble in most organic solvents and aqueous solutions. Tendency to aggregation that makes it difficult to use in SPE.
Oxidized CNT	Obtained by oxidation of CNTs which introduces hydroxyl, carbonyl and carboxyl groups in the nanotube surface.	Good solubility and dispersion in aqueous solutions. High polarity, hydrophilicity and ion-exchange capacity of CNTs
Functionalized CNT	Functionalization made by binding a series of functional groups to the CNT sidewalls by means of different chemical reactions or physical interactions.	Improved solubility and selectivity.
	Chemical functionalization Formation of covalent bonds between the functional groups and the carbon atoms of the CNTs that can occur directly on the CNT sidewalls or through the carboxylic groups and defects generated by previous oxidation of the CNTs. Amidation, esterification, thiolation, and silanization reactions cause the formation of a wide diversity of functionalized CNTs with interesting analytical applications.	Chemical defect functionalization is the most preferred approach when compared to the sidewall option. All types of functionalization attach useful groups onto the CNT surface with a corresponding improvement in selectivity.
	Physical functionalization Involves non-covalent bonds. Polymer wrapping is a typical physical case in which the interaction between CNT and polymer is based on van der Waals and π-π stacking forces between nanotube and functional molecule. Functionally modified CNTs may be either prepared by adsorption of different ionic and non-ionic surfactants. Another way is the use of surfactants to prevent the formation of aggregates and facilitate their dispersion in polar solvents commonly used.	Increased dispersion in polar solvents commonly used.

In short, the first type of CNTs is obtained by a synthesis process. The second type of CNTs is obtained by oxidation of new ones and the third type is mainly obtained by modification of oxidized CNTs. From the first to the third type, there is also a significant increase in the material selectivity [161].

1.5- RNA as a biopharmaceutical

The use of nucleic acids for therapeutic applications has become an approach of potential interest, with plasmid DNA being the focus of numerous studies. However, recent technological improvements have presented serious opportunities for the employment of RNA-based approaches [163]. Since its discovery in 1961, the study of the RNA molecule has gone through different stages [164]. For a long time, the RNA molecule was only known to play an intermediary role in the flow of information from genes to functional molecules in living cells and was therefore less studied compared to proteins and DNA. However, the discovery of new classes of RNA has proven the importance of this molecule, mainly in biotic evolution and inheritance, but also in gene regulation, which has highlighted its therapeutic potential as a biopharmaceutical [127]. The first clinical approval of a therapeutic RNA occurred in 1998 with the FDA approval of Vitravene for the treatment of retinitis caused by cytomegalovirus. Since then, 16 additional approvals have followed with the most recent approval in 2021 of the Spikevax and Comirnaty vaccines against the SARS-CoV-2 virus (COVID-19 disease) [165]. In particular, the rapid and efficient global response to the pandemic COVID-19 has greatly increased the potential of RNA-derived therapeutics, demonstrating their versatility as an indispensable and exciting technology in preventing and combating disease. [166]. The development of RNA-based therapies has largely focused on 2 different approaches: messenger RNA (mRNA), where mRNAs encoding certain proteins cause their transient expression in the cytoplasm to replace defective proteins or present antigens for vaccination, or RNA interference (RNAi), where short oligonucleotides recognize and hybridize with complementary sequences in endogenous RNA transcripts, altering their processing [167]. The great therapeutic potential of RNA has been assessed in recent studies for the treatment of cancer and neurodegenerative diseases involving the application of mRNA, transfer RNA (tRNA) and RNAi [168]. The notable advances in understanding the biological roles of RNAs have been crucial in moving the biopharmaceutical industry to focus on them as biotherapeutic tools [127]. However, understanding the biological role of RNAs or their use as biotherapeutic agents mandates a widespread need for optimization of production and purification processes for this biomolecule, particularly in developing new bioseparation methods that are selective, efficient, and more cost-effective while ensuring pure, intact RNA with adequate integrity, stability, and biological activity [169].

1.6- Challenges in RNA isolation and purification

The capture and purification processes of biomolecules are crucial when thinking about a biotechnological process because they are the starting point for the downstream phase and, consequently, for the development of biopharmaceutical products [170]. In particular, the processes used for the RNA molecule present several differences compared to those used for DNA and proteins [171]. RNA is an unstable molecule that has a very short half-life time, once extracted from the cell or tissues. The chemistry of RNA requires special care and precautions for its isolation because the presence of RNA degrading enzymes (RNases) both in biological samples and in the laboratory environment can easily degrade it, thus compromising its integrity and biological activity [127]. In addition, maximizing RNA recovery yield is another major challenge as it is intended to end up with a final RNA sample free of undesirable contaminants and impurities that arise throughout the biotechnological process [127]. Many methods have been developed in an attempt to circumvent the various challenges of RNA purification and achieve the goal of good quality RNA. Strong denaturants have always been used in RNA isolation. As an example, the RNA isolation method based on the use of a mixture of phenol and chloroform is considered the standard method [127, 170]. For this reason, simpler and environmentally safer methods for obtaining RNA samples are needed.

The use of carbon-based adsorbents then emerges as a highly promising method to overcome these obstacles, as these materials emerge as excellent candidates to capture various molecules with different characteristics [152]. In particular, CNTs have gained well-deserved popularity in this field due essentially to their excellent adsorptive capabilities, emerging as a promising option worthy of further study for the capture of nucleic acids, particularly RNA. Taking advantage of the differences in hydrophobicity between RNA and DNA, the latter being considered as an impurity when biotechnological processes are involved, a competition for the active sites available on carbon materials for adsorption is possible, as RNA is a single-stranded molecule, while DNA is a double-stranded molecule. As such, the possibility exists to exploit the interactions between the exposed bases, allowing a selective method of separation between nucleic acids, contributing to an undeniable progress for experiments on RNA pre-purification [127, 157].

CHAPTER 2

Objectives

The RNA molecule has recently gained increased importance from the point of view of its therapeutic potential. Examples of this are the recent investigations that led to the development of mRNA-based vaccines against COVID-19. This interest compels a need for new methods and strategies for the recovery and purification of this biomolecule that must be efficient and reliable, while avoiding the use of certain reagents, thus making the process greener and more cost-effective. Solid-phase extraction using carbon-based materials, especially CNTs, has emerged as a promising alternative for RNA capture and recovery, since the unique adsorption properties of these materials allow their conjugation with different biomolecules, namely DNA, RNA, and proteins, making these materials an advantageous option for RNA separation from complex cell extracts. Thus, the main objective of this study is to investigate the applicability of a simple and efficient method for the capture and pre-purification of RNA from *E. coli* lysates, exploiting the adsorptive properties of different carbon materials. This requires achieving selectivity between different nucleic acid species, allowing their separation based on their distinct properties. Thus, the structural differences between RNA and DNA will be explored, more specifically the exposure of RNA bases that, in theory, will show more affinity with the surface of carbon materials, allowing the development of a method that effectively intends to improve the purification of different RNA-based biopharmaceuticals.

To achieve a simple and efficient method for RNA isolation capable of being integrated and applied in biotechnological processes, a series of tasks were outlined:

1. Evaluate the maximum RNA adsorption capacity of MWCNTs and study different regeneration strategies for MWCNTs.
2. Investigate different conditions for RNA adsorption and desorption from new carbon-based materials (differing in structure and surface modifications).
3. Develop an effective and reliable strategy to desorb RNA from carbon materials.
4. Verify the potential for reuse of carbon materials in order to establish a relationship with the circular economy.
5. Study the affinity and selectivity of carbon materials towards RNA and pDNA.
6. Evaluate the performance of carbon materials in RNA capture and recovery from a cell lysate sample.
7. Control the reduction of impurities in the recovered RNA sample after capture with the carbon materials.
8. Confirm the integrity and stability of the RNA after recovery.

CHAPTER 3

Materials and Methods

3.1- Materials

To perform the solid phase dispersive extraction method (d-SPE) for RNA capture and recovery, different carbon-based materials were studied (provided by Dr. Maria José Sampaio, from the Faculty of Engineering of the University of Porto). Table 11 presents a brief description of these materials and their main characteristics.

Table 11- General carbon-based materials characteristics.

MWCNTs	Purchased from NTP Shenzhen Nanotechnologies Co., Ltd. (Shenzhen, China) (purity > 97%; diameter < 10 nm; length > 5 µm; specific surface area = 250~500 m^2/g).
Purified CNTs	Pristine CNT sample was purchased from Nanocyl Belgium (purity > 95%; diameter = 5–50 nm) and were purified with 50 vol.% sulfuric acid (99.9 wt.% H_2SO_4, Sigma–Aldrich, 120 °C, 3 hours).
N-doped purified CNTs	N-doped CNTs were synthesized by catalytic-CVD in a fluidized bed reactor using ethylene as carbon source and acetonitrile/N_2 as carbon/nitrogen source, as described elsewhere [172].
Carbon fibers	Large-diameter carbon nanofibers (Pyrograph III; diameter = 60–150 nm) were supplied by Applied Sciences.
Graphene	Few layer graphene was synthesized by CVD, as described elsewhere [173].
Fullerene (C_{60})	The fullerene (C_{60}) sample was purchased from Sigma–Aldrich and used as received.
CNTs (ARKEMA)	Graphistrength® CNT (purity > 90%; diameter = 5–50 nm) were supplied by Arkema, France.
CNTs (NANOCYL)	CNT sample (purity > 95%) were supplied by Nanocyl (NC3100), Belgium.
Graphite-like carbon nitride (GCN-T)	Obtained by thermal polymerization of dicyandiamide (99%, Sigma-Aldrich) in a two-step thermal treatment to obtain an exfoliated material (GCN-T) leading to an increase in the specific surface area from 10 to 117 m^2/g, for the bulk and exfoliated material, respectively [174, 175].

N-doped CNTs, carbon fibers, graphene, CNTs (ARKEMA) and CNTs (NANOCYL) were subjected to surface oxidation processing. Samples were oxidized with nitric acid (65 wt.% HNO_3, Sigma–Aldrich) at 120 °C for 3 hours under reflux. After cooling, the suspensions were washed with distilled water and dried at 130 °C for 12 hours.

The different adsorption and desorption/regeneration experiments performed in this work required the use of several reagents, namely ammonium sulfate ($(NH_4)_2SO_4$), Tween-20 ($C_{58}H_{114}O_{26}$), sodium hydroxide (NaOH), sodium chloride (NaCl) commercialized by Panreac (Barcelona, Spain), Triton X-100 ($C_{16}H_{26}O_2$) from Thermo Fisher Scientific Inc. (Waltham, USA) and tris(hydroxymethyl)aminomethane (Tris) from Merck (Darmstadt, Germany). All solutions were prepared with ultrapure deionized water, purified with Millipore's Milli-Q system (Billerica, MA, USA). For *E. coli* DH5 growth, "Luria-Bertani" (LB) agar medium from Pronalab (Mérida, Mexico), yeast extract and tryptone from Biokar (Beauvais, France), glycerol from Himedia (Einhausen, Germany), potassium hydrogen phosphate (K_2HPO_4) from Panreac (Barcelona, Spain), potassium dihydrogen phosphate (KH_2PO_4) from Sigma-Aldrich (St. Louis, Missouri, USA) and the antibiotic kanamycin from Thermo Fisher Scientific Inc. (Waltham, EUA) have been used.

For nucleic acids extraction, the reagents used were guanidine thiocyanate, N-Lauroylsarcosine sodium salt, sodium citrate and isoamyl alcohol from Sigma-Aldrich (St. Louis, Missouri, USA), isopropanol from Thermo Fisher Scientific Inc. (Waltham, USA), β-mercaptoethanol from Merck (Whitehouse Station, USA). All mentioned solutions were prepared with 0.05% diethyl pyrocarbonate treated water (DEPC) from Fluka, Sigma-Aldrich (St. Louis, Missouri, USA). For plasmid DNA extraction, the NZYMaxiprep kit from NZYTech Genes and Enzymes (Lisbon, Portugal) was used. For the lysate preparation by alkaline cell lysis, solution A composed of Tris from Merck (Darmstadt, Germany) and EDTA from Sigma-Aldrich (St. Louis, Missouri, USA); solution B composed of NaOH and SDS from Panreac (Barcelona, Spain); and solution C with potassium acetate from Panreac (Barcelona, Spain) were previously prepared. To verify the integrity and purity of the nucleic acids in the electrophoresis, 1% agarose gel electrophoresis was used with GRS Agarose LE and Green Safe from Grisp (Porto, Portugal).

Dye Reagent Concentrate and bovine serum albumin (BSA) from Bio-Rad (California, USA) were used for protein quantification.

3.2- Methods

3.2.1- Bacterial growth conditions and nucleic acids production

RNA and pDNA production were performed by culture of *E. coli* DH5α previously transformed with the plasmid pBHSR1-RM containing the sequence of human pre-miRNA29b. First, *E. coli* was grown on a plate with solid "Luria-Broth Agar" (LB-Agar) medium with 50 µg/mL kanamycin and its growth occurred overnight at 37 ˚C. After growth on the solid medium, pre-fermentation was performed by transferring few colonies to an Erlenmeyer containing 125 mL of "Terrific Broth" medium (TB) (12 g/L Tryptone, 24 g/L yeast extract, 4 mL/L glycerol, 0.017 M KH_2PO_4, 0.072 M K_2HPO_4), supplemented with 50 µg/mL of kanamycin, and using a medium/oxygen ratio of 1:4. Bacterial growth was carried out at 37 ˚C on an Aralab Agitorb 200 orbital shaker (Albarraque, Portugal) at 250 rpm, and then stopped at the end of the log phase after reaching an optical density (OD) at 600 nm of almost 2.6.

After this step, a specific volume of this growth medium was transferred to 4 Erlenmeyers with TB medium to initiate the fermentation with an OD of 0.2. This transferred volume was calculated from the equation (2):

$$V_{pre-fermentation}\,\frac{(OD_{fermentation}-V_{fermentation})}{(OD_{pre-fermentation}-OD_{fermentation})} \qquad (2)$$

To measure the OD, a spectrophotometer Pharmacia Biotech Ultraspec 3000 UV/Visible (Cambridge, England) was used. After 8 hours or 16 hours, bacterial growth was suspended if low molecular weight RNA or pDNA were required, respectively. The total volume of fermentation was then divided into 50 mL tubes for posterior collection of cells by centrifugation at 3900 g for 10 minutes, and then stored at -20 ºC until use.

3.2.2- Low molecular weight RNA extraction

RNA extraction was performed using the method of acid guanidinium thiocyanate-phenol-chloroform. First, the pellets previously stored at -20 ˚C were thawed and resuspended in 0.8% NaCl, followed by centrifugation at 6000 g for 10 minutes at 4 ˚C. After that, the supernatant was discarded and the resulting cell pellets were resuspended in 5 mL of solution D, which corresponds to denaturing solution, composed of 4 M guanidinium thiocyanate, 0.5% sodium N-lauroyl sarcosinate, 0.025 M sodium citrate pH 7, and 0.1 M β-mercaptoethanol, and incubated on ice for 10 minutes. The next step consists of adding 0.5 mL of 2 M sodium acetate pH 4 and 5 mL of phenol to the suspensions and homogenizing very carefully at each step. Then, a chloroform/isoamyl alcohol mixture (49:1) was prepared and 1 mL was added to the suspension, followed by vigorous shaking and incubation on ice for 15 minutes. After centrifugation, two aqueous phases are formed, the upper phase being rich in RNA, while the bottom phase is rich in DNA. For this reason, the upper phase should be transferred very carefully to new lysis tubes, to avoid possible contamination with the bottom phase containing DNA. To these new tubes, 5 mL of isopropanol were added to precipitate the RNA and the suspension was centrifuged at 10000 g for 20 minutes at 4 °C. After discarding the supernatant, RNA reprecipitation was performed by dissolving the RNA pellets in 1.5 mL of solution D and then 1.5 mL of isopropanol, followed by centrifugation at 10000 g for 10 minutes at 4 °C. The supernatant was discarded and the resulting pellets were resuspended in 2.5 mL of 75% ethanol in DEPC water to wash the RNA. Next, the samples were incubated at room temperature for 10-15 minutes to dissolve possible residual traces of guanidinium. After that, the suspension was centrifuged at 10000 g for 5 minutes at 4 °C. The supernatant was discarded and the resulting pellets were dried for 5-10 minutes at room temperature. Finally, the RNA pellets were dissolved in 1 mL of DEPC-treated water and incubated at room temperature for 10-15 minutes to ensure complete solubilization. RNA concentration was measured using a Nano Photometer (IMPLEN, United Kingdom) and RNA integrity was verified by agarose gel electrophoresis, then samples were stored at -80 °C until the moment of use.

3.2.3- Plasmid DNA extraction

For pDNA extraction, NZYMaxiprep kit was used, according to the protocol provided by the manufacturer. Thus, bacterial pellets from 100 mL of culture were resuspended in 12 mL of Buffer M1 containing RNase A by vigorous vortexing. After that, to promote cell lysis, 12 mL of Buffer M2 were added and the tubes were carefully inverted and incubated at room temperature for 5 minutes. The lysis step was stopped by adding 12 mL of Buffer M3 and the lysate was carefully homogenized. Then, the tubes were centrifuged for 30 minutes at 20000 *g*, at 4 °C and the supernatant was transferred to new lysis tubes. The tubes were then centrifuged again under the same conditions to ensure that there was no cell debris in the suspension, clarifying the lysate. Meanwhile, the NZYTech column was equilibrated with 6 mL of Buffer MEQ. The supernatants were added to the columns, and the pDNA was retained onto the columns, while contaminants were removed by washing the columns with 32 mL of Buffer MW. Elution of the pure pDNA was promoted directly to new lysis tubes by adding 15 mL of Buffer ME. pDNA was precipitated by adding 10.5 mL of isopropanol, followed by very careful homogenization and incubation on ice for 15 minutes. Then, centrifugation was performed at 15000 *g* for 30 minutes, at 4 ˚C. After this step, the supernatants were discarded and the DNA pellets were washed and resuspended in 5 mL of 70% ethanol. Centrifugation was repeated at 15000 *g* for 15 minutes at 4 ˚C. The ethanol was carefully removed and the DNA pellets were left to dry at room temperature. Finally, the DNA pellets were dissolved in 1 mL of TE Buffer (10 mM Tris-HCl and 1 mM EDTA pH 8.0). The final pDNA samples were quantified using a NanoPhotometer (IMPLEN, UK) and the integrity of the samples was verified by agarose gel electrophoresis, with the samples being stored at -80 ˚C.

3.2.4- Cell lysate extraction

To obtain a complex cell lysate sample composed of pDNA, gDNA, RNA, and proteins, a modified alkaline lysis method was used. Thus, the bacterial pellets were resuspended in 10 mL of solution A composed of 50 mM Tris-HCl, and 10 mM EDTA at pH 8.0, and then the volume was divided into two new lysis tubes by adding 5 mL of solution B (200 mM NaOH and 1% (w/v) SDS), followed by 5 minutes incubation at room temperature to promote cell lysis. To neutralize the samples, 5 mL of solution C (3 M potassium acetate at pH 5.0) was added and incubated on ice for 20 minutes. Next, the tubes were centrifuged twice at 20000 *g* for 30 minutes at 4 ˚C to eliminate major cellular debris, and the supernatant was stored at -80 ˚C until use.

3.2.5- Dispersive solid-phase extraction (d-SPE) of RNA using carbon materials

The RNA capture method of choice for this work was d-SPE, based on a method previously described in another work, where as-grown MWCNTs were used for RNA capture from an *E. coli* cell lysate [176]. In the present work, the d-SPE method was also applied primarily for the capture and recovery of RNA from complex *E. coli* lysates using different carbon-based materials.

For this purpose, an optimization of the experimental parameters was required as an initial screening to determine the most influential parameters affecting the performance of the developed method. These parameters are described in detail in the "Results" section. The process is divided into 3 main steps: equilibrium step, adsorption step, and desorption step. For a better interpretation of the method, a schematic representation of the 3 steps mentioned above is shown in Figure 9.

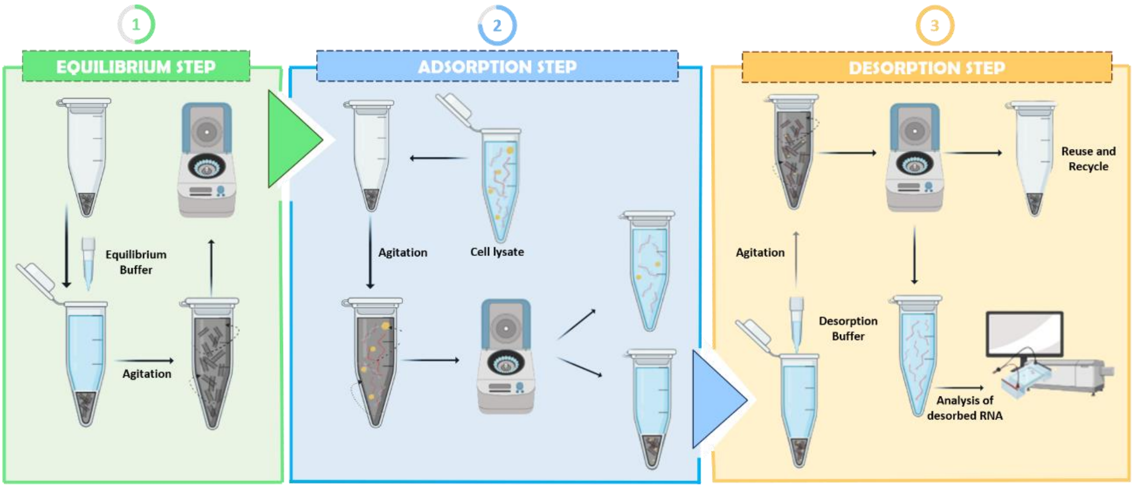

Figure 9- Overview of the applied d-SPE method.

Equilibrium step:

To initiate the experiments, 1 mg of each carbon material under study was equilibrated with an appropriate equilibration buffer. For this, different solutions were tested by adjusting the type and concentration of salt and the pH in order to make a correct choice of the equilibrium buffer to be used. After that, agitation was performed for 20 minutes with subsequent centrifugation at 9000 *g* for 4 minutes to remove the aqueous phase.

Adsorption step:

The sample to be extracted, in this case, RNA, was diluted with the equilibrium buffer used in the previous step and subsequently applied to the carbon material. The mixture was kept agitated for 20 minutes at room temperature to allow adsorption of the RNA to the carbon material. After that, further centrifugation at 9000 *g* for 4 minutes was performed to separate the solid phase from the aqueous phase (supernatant). The recovery of this supernatant is very important because it will allow us to evaluate the behavior and, consequently, the efficiency of the RNA adsorption. Thus, the absorbance of the supernatant was measured using a Nano Photometer (IMPLEN, UK) and an agarose gel electrophoresis was performed.

Desorption step:

An appropriate elution buffer was applied to allow RNA recovery that was adsorbed to the carbon material. Similar to the choice of equilibrium buffer, the elution buffer required initial screening of different solutions varying in salt type and concentration, and pH. This mixture was agitated for 20 minutes and then centrifuged at 9000 *g* for 4 minutes to remove the aqueous phase containing the desorbed RNA. In order to assess the purity and integrity of the RNA, agarose gel electrophoresis and circular dichroism spectrum analysis were performed using Jasco J-815 spectropolarimeter (Jasco, Easton, MD, USA).

In parallel, to ensure complete removal of the elution buffer, 3 washes with deionized water were performed. Finally, the carbon material was oven-dried at 37 ˚C for 24 hours and stored for later use. In order to recycle and reuse the carbon material for new RNA adsorption/desorption cycles, different regeneration approaches were adopted in order to study the most suitable regeneration strategy to be applied.

3.2.6- Regeneration strategies for MWCNTs

In previous works, it was verified that the application of different elution buffers was not efficient in the total elution of the RNA adsorbed to MWCNTs. Thus, different regeneration experiments were performed to study the elimination of the species adsorbed to this material and, consequently, to investigate the variations in adsorption capacity when a new RNA adsorption cycle was performed. All applied regeneration strategies were repeated twice to validate the repeatability of the results.

• Chemical regeneration

For chemical regeneration experiments, the exhausted carbon material (material containing adsorbed RNA) was subjected to a first chemical regeneration step using 5% Tween-20, followed by agitation for 20 minutes at room temperature. After that, a second regeneration step with 1 M NaOH is applied, followed by further agitation for 20 minutes at room temperature. After the 2 regeneration steps, 3 washes with deionized water are carried out and the material is dried in an oven at 37 ˚C until reaching a constant mass.

• Ultrasonic regeneration

For ultrasonic regeneration experiments, the exhausted carbon material was subjected to an ultrasonic water bath using the Ultrasonic Cleaner from lbx instruments (Barcelona, Spain) for 40 minutes at room temperature.

• Thermal regeneration

For thermal regeneration, the exhausted carbon material was heat up at 10 ºC/min in a vertical furnace under nitrogen flow until reaching 400 ºC. This temperature was maintained for 1 hour and then the material was cooled down until room temperature.

3.2.7 Characterization of MWCNTs

For surface characterization of MWCNTs after being subjected to the different regeneration strategies described above, FTIR spectra were traced. For this, measurements were performed with a JASCO FT/IR-6800 spectrometer (JASCO Analytical Instruments) equipped with a MIRacle™ Single Reflection attenuated total reflectance (ATR) ZnSe crystal plate accessory (PIKE Technologies).

3.2.8- Adsorption experiments

For adsorption isotherm studies, solutions with different concentrations of small RNAs (10, 20, 30, 40, and 50 µg/mL RNA) were added to the carbon material and the equilibrium time was fixed at 20 minutes, which was sufficient to adsorb RNAs, according to the preliminary experiments. The determination of the absorbance at 260 nm was performed using a NanoPhotometer (IMPLEN, UK). The blank used in the experiment was the equilibrium buffer. The amount of RNA adsorbed was calculated from the measurement of the absorbance at 260 nm of the supernatants recovered after the adsorption step. Each experiment was performed in triplicate under identical conditions.

The RNA adsorption at equilibrium, qe (mg/g), was calculated by the equation (3):

$$q_e = V \times \frac{C_0 - C_e}{m} \tag{3}$$

where C_0 and Ce are the initial and equilibrium concentrations of RNA (mg/L) in solution, respectively; V is the volume of the solution (L), and m is the weight of the adsorbent (g).

3.2.9- Agarose gel electrophoresis

The content of nucleic acids in the supernatant recovered after the adsorption and desorption steps was evaluated by horizontal gel electrophoresis using a 1% agarose gel stained with 0.012 µL/mL of Green-Safe. Electrophoresis was performed at 120 V for 30 minutes in TAE buffer (40 mM Tris base, 20 mM acetic acid, 1 mM EDTA pH=8). The gels were visualized and analyzed using ultraviolet (UV) light with the Uvitec Cambridge Fire-Reader UV system (UVITEC Cambridge, Cambridge, UK).

3.2.10- Circular Dichroism spectroscopy

Circular Dichroism (CD) experiments were performed to evaluate the stability of the recovered RNA after the d-SPE procedure. CD was performed in the Jasco J-815 spectropolarimeter (Jasco, Easton, MD, USA), using a Pelter-type temperature control system and quartz cell with a 1 mm optical path. The CD spectra were obtained at a constant temperature of 20 ˚C, scanning speed of 50 nm/min, with a response time of 1 second within a wavelength range of 200 to 320 nm. The samples subjected to CD analysis were the pure small RNAs sample (reference) and the RNA samples recovered from carbon materials after performing the described method. All samples were prepared in DEPC-treated water. Three scans were measured per spectrum to improve the signal-to-noise ratio, and the spectra were smoothed using the smooth tool in Origin 2021 software.

3.2.11- Total protein quantification

The Bradford protein assay was used to determine the total protein concentration present in the RNA samples recovered from the carbon materials after 3 consecutive cycles. For this, a calibration curve was designed, using BSA as standard protein, in the linear range of 0.05 to 0.5 mg/mL. Next, the dye reagent was prepared by diluting 1 part dye reagent to 4 parts deionized distilled water, with subsequent filtration to remove possible particulate material. Each standard and sample solution were prepared in a 96-well microplate, in triplicate using 10 µL of sample and 200 µL of dye reagent. Then, the absorbance of the microplate was recorded at 595 nm in an xMarkTM Microplate Absorbance Spectrophotometer (Bio-Rad, USA), and the amount of protein was calculated using the previously designed calibration curve, shown in Figure 10.

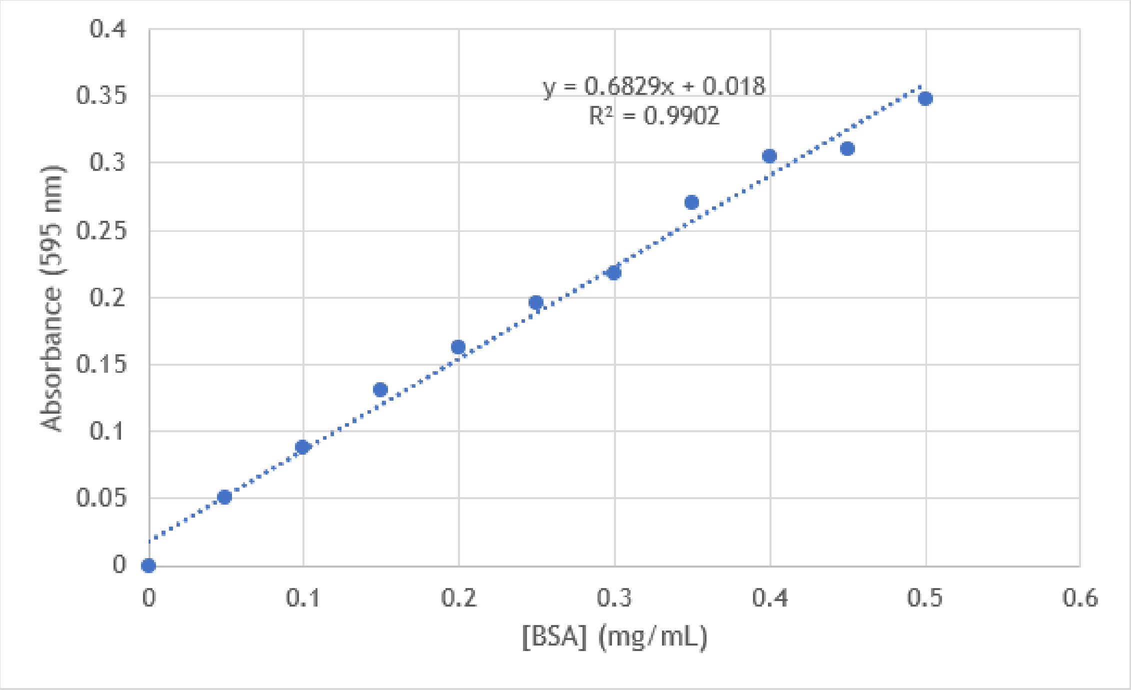

Figure 10- Calibration curve obtained with BSA standards (0.05 – 0.5 mg/mL).

CHAPTER 4

Results and Discussion

4.1- RNA adsorption and regeneration experiments on MWCNTs

4.1.1- Adsorption capacity of MWCNTs

MWCNTs were previously used in the research group to capture RNA from a complex cell lysate [176]. In that study, it was verified that RNA is adsorbed to the MWCNTs' surface mainly through π-π stacking interactions occurring between the aromatic structure of the MWCNTs and the hydrophobic bases of the RNA. However, to best characterize the adsorption performance of these materials, additional experiments were performed. By applying the RNA adsorption conditions that were previously studied and characterized for this material, we proceeded to determine the maximum RNA adsorption capacity. This study allows the assessment of the maximum amount of RNA that MWCNTs can capture since MWCNTs will be saturated at a certain level of RNA adsorption. For this purpose, aliquots containing 1 mg of MWCNTs were prepared and equilibrated with 1.5 M $(NH_4)_2SO_4$ in 10 mM Tris-HCl pH 8, since hydrophobic conditions were considered to be optimal for RNA binding. The equilibration step was followed by 20 minutes of agitation and subsequent centrifugation at 8000 *g* for 2 minutes to recover equilibrated MWCNTs. Then, small RNA samples with different concentrations, ranging from 150 µg/mL to 200 µg/mL, were diluted in equilibration buffer, and added to the MWCNTs, to allow RNA adsorption to the material. From the previous studies it was supposed that the RNA adsorption capacity could be around 175 µg/mL. Thus, the definition of the concentration range between 150 µg/mL to 200 µg/mL was related with this previous knowledge. The non-adsorbed RNA was determined for each assay, and the maximum capacity of RNA adsorbed onto MWCNTs was calculated. The results presented in Figure 11 confirmed that the highest RNA adsorption capacity is approximately 175 mg RNA/g MWCNT, and higher RNA concentrations resulted in a considerable decrease in the RNA adsorption capacity of this material. This decrease may be happening because for the higher concentrations of RNA, some repulsion may occur between the RNA and the material surface associated with the negative charge of the RNA, limiting the adsorption of the material. In addition, accessibility constraints may occur on the MWCNTs as the active sites may no longer be available, reducing the adsorption capacity of the material.

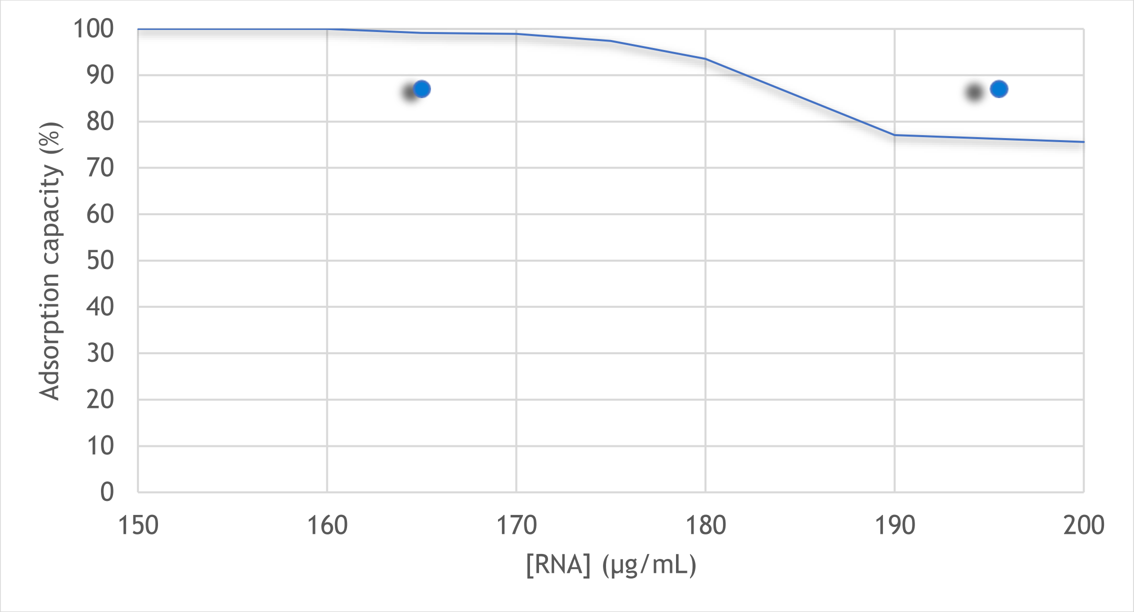

Figure 11- RNA adsorption capacity of MWCNTs.

4.1.2- Sonication of MWCNTs as dispersion strategy

The surface of CNTs is highly hydrophobic and lacks active groups, so their solubility in water and other solvents is extremely low. In addition, the large specific surface area and ratio make it relatively easy for CNTs to form agglomerates due to van der Waals forces, which can restrict the adsorption process. Considering the previous results, it was evaluated the possibility to increase the adsorption capacity of CNTs, as it could be advantageous for the RNA extraction process. Ultrasonic cavitation emerges as a possibility to increase the dispersion of CNTs, increasing the active sites available for RNA adsorption. In the ultrasonic treatment process, the duration of the ultrasonic time can affect the dispersion of the CNTs. Thus, the MWCNTs used in this work were dispersed in equilibrium buffer (1.5 M $(NH_4)_2SO_4$ in 10 mM Tris-HCl, pH 8) by sonication for 40 minutes or 60 minutes. Afterwards, RNA samples with a concentration of 350 µg/mL were added to the MWCNTs, and the stipulated adsorption method was applied. The results of these assays are shown in Figure 12. As it can be seen, there was a slight increase in RNA adsorption capacity when the 40-minute time was used, compared to the original MWCNTs. When 60 minutes of sonication was applied, the RNA adsorption capacity was almost the same as the original MWCNTs. These results are in line with a study by Li and co-workers in 2012, in which the dispersion of CNTs using polyvinylpyrrolidone at different ultrasonic times was investigated. In that study, it was found that the number of dispersed CNTs increased with increasing ultrasonic time when the ultrasonic time was lower than 60 minutes. When the ultrasonic time was longer than 60 minutes, there was a decrease in the average length of the CNTs, indicating that the material's chemical structure may be damaged if the ultrasonic time is too long [177]. However, since the increase in adsorption capacity of MWCNTs by using 40 minutes of sonication was not very significant, this step was not included in the following assays, avoiding also the possible degradation of CNTs.

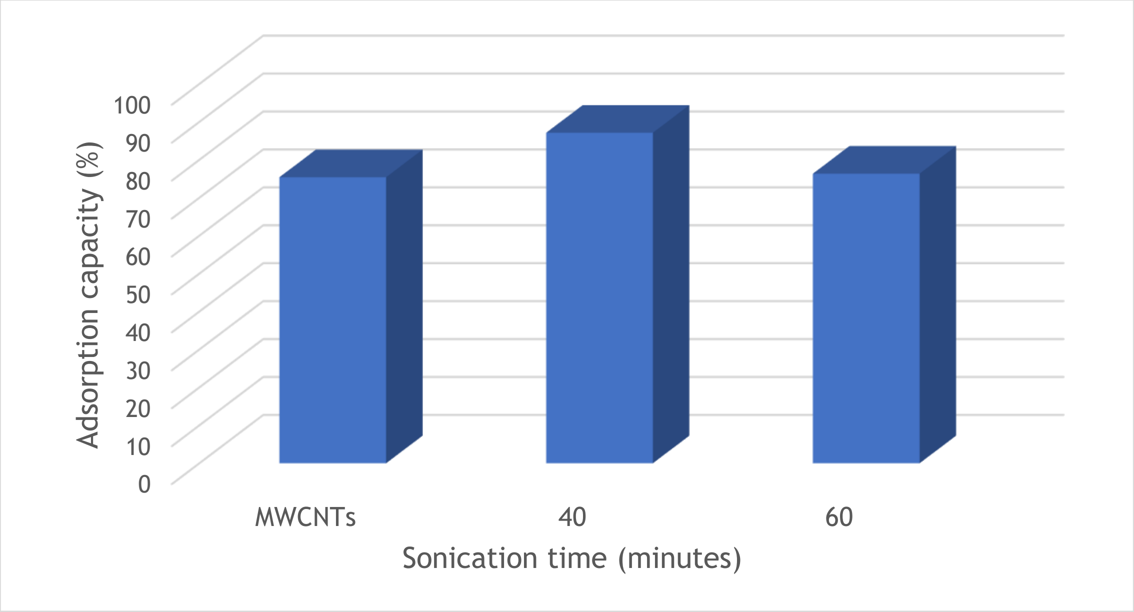

Figure 12- Effect of different sonication times on RNA adsorption capacity of MWCNTs.

4.1.3- Regeneration and reusability of MWCNTs

The adsorbents used in adsorption processes can be used once and discarded or used in several cycles, after regeneration, making the operational method more effective, reducing costs and environmental impact, and thus stimulating the circular economy. In this work, it was studied the possibility to perform the regeneration of the MWCNTs to be reused on RNA capture. For this, a chemical regeneration strategy was first applied, based on 2 steps: a first step where 0.5% Tween-20 is applied followed by a second step where 1 M NaOH is added. For this, the same adsorption method reported earlier was used, and a 1 mL RNA sample with a concentration of 175 ug/mL (corresponding to the maximum RNA adsorption capacity) was applied to the MWCNTs. After that, the chemical regeneration protocol was carried out by adding 1 mL of 0.5% Tween-20 to the exhausted material as the first regeneration step. The selection of Tween-20 for the regeneration is mainly due to its chemical properties. Since surfactants are amphiphilic molecules that have both hydrophobic groups that can anchor to the hydrophobic surface of the MWCNTs and hydrophilic groups that tend toward the aqueous phase, they can be useful on the regeneration process. Tween-20 could be able to compete with RNA for the surface of the MWCNTs [178], eliminating the strongly bound molecules from the carbon material. After agitation for 20 minutes and subsequent centrifugation to remove this buffer, NaOH was applied as the second regeneration step. The use of NaOH as a regeneration buffer is widely used in carbon adsorbents, as it can break down or hydrolyze organic molecules, thus making them less adsorbable [179]. This mixture was then homogenized for 20 minutes, and after centrifugation and removal of the buffer, the absorbance of the aqueous phase was measured. This procedure was repeated 4 times, thus completing 4 cycles of regeneration of MWCNTs, and the RNA adsorption capacities of regenerated and reused MWCNTs are shown in Figure 13. Immediately after the first cycle, a sudden decrease in RNA adsorption capacity can be seen. Additionally, after subsequent regeneration cycles, the RNA adsorption capacity gradually decreased, and in the second cycle, there is already a loss of 50% on the RNA adsorption. This loss of adsorption capacity can be related with 3 important factors: (1) loss of adsorbent material during pipetting and centrifugations required throughout the experimental method; (2) possibility of adsorption of Tween-20 to MWCNTs, resulting from π-π stacking interactions that decreased the active binding sites; and (3) oxidation effect of MWCNTs caused by NaOH that may lead to a reduction in RNA adsorption capacity.

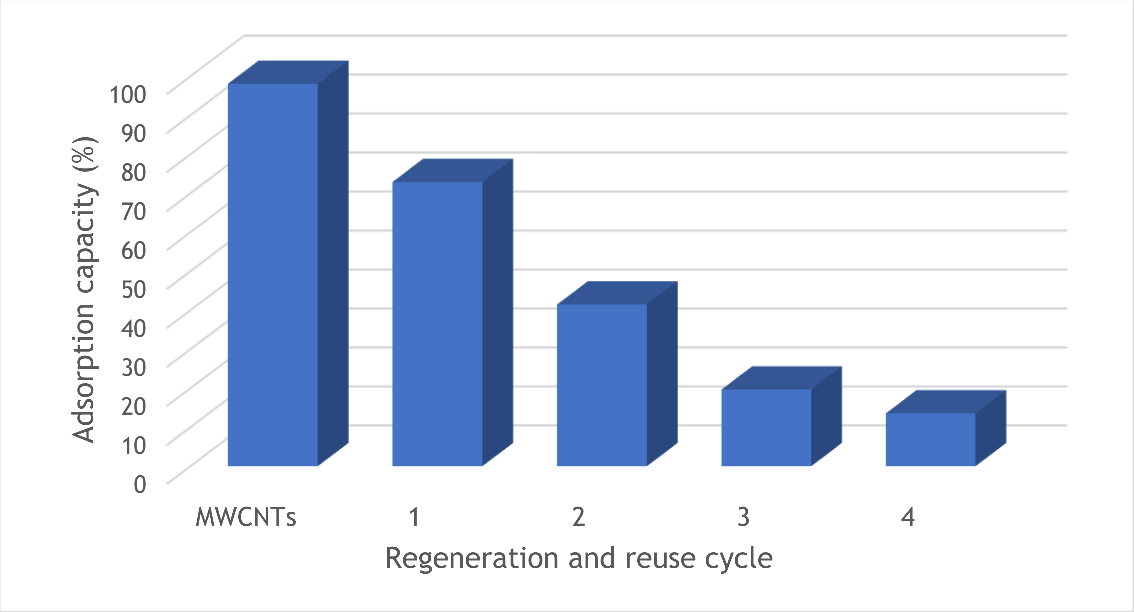

Figure 13- RNA adsorption capacity after 4 cycles of chemical regeneration of MWCNTs.

Previous desorption assays performed with this material demonstrated that either Tris-HCl or different surfactants, such as SDS and Tween-20, were insufficient to promote efficient RNA elution and recovery [176]. This behavior can be explained by the strong interactions occurring between the hydrophobic RNA bases that establish π-π interactions with the surface of the MWCNTs. Although these results allow RNA recovery that was adsorbed onto the MWCNTs, it is important to note that the RNA was subjected to the addition of NaOH, which can quickly lead to its degradation [180]. For this reason, these experiments are referred to as MWCNTs regeneration experiments, rather than desorption experiments.

4.1.4- New regeneration strategies for MWCNTs

In an attempt to obtain better RNA adsorption results after the regeneration of MWCNTs, new approaches were studied, and a comparison was made with the results obtained through chemical regeneration. Thus, strategies such as ultrasonic regeneration, and thermal regeneration were evaluated. The results of RNA adsorption capacity after 1 regeneration cycle using the different strategies mentioned are shown in Figure 14.

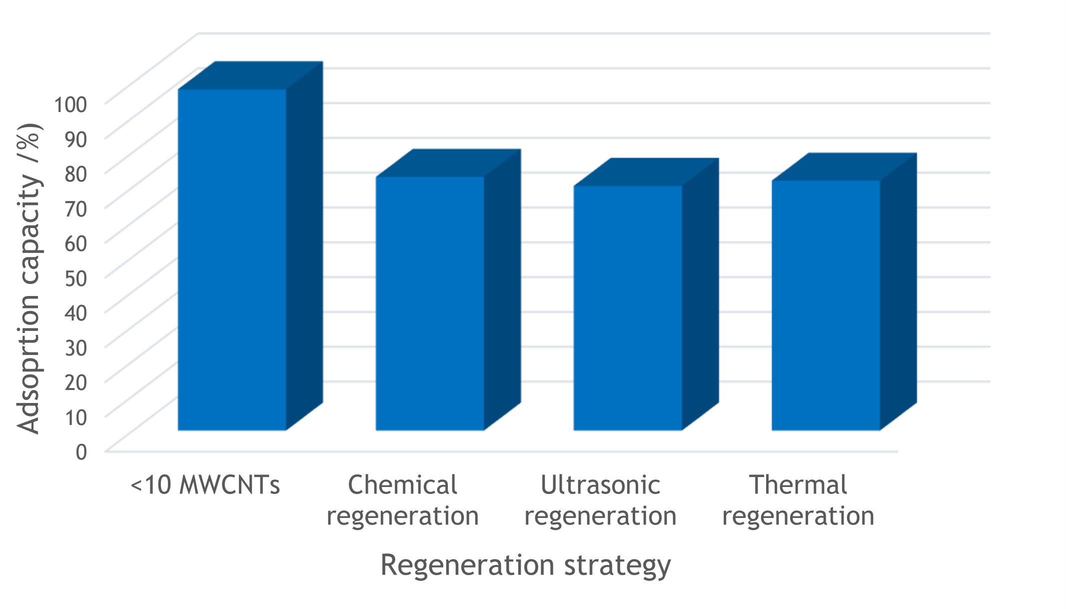

Figure 14- RNA adsorption capacity after 1 cycle of MWCNTs regeneration, using different strategies.

Figure 14 shows that after 1 cycle of regeneration and reuse, the different strategies of MWCNTs regeneration resulted in a reduction on the RNA adsorption capacity when compared with the RNA adsorption capacity of as-grown original MWCNTs (in first use). As explained earlier, ultrasonic treatment can be used as a dispersion method for CNTs, but it can also be used as a regeneration method. Sonication can weaken the interaction between MWCNTs and RNA due to the violent collapse between air bubbles that produce powerful hydromechanical shear forces at the water/solid material interface, thus increasing RNA desorption from the solid adsorbent [181]. Actually, this treatment allowed an RNA adsorption capacity, after the 1st cycle of regeneration/reuse, of about 70%. On the other hand, thermal treatment has also been extensively investigated in the regeneration of CNTs. This approach is conventionally performed in specific ovens where the carbon bed is indirectly heated by conduction and convection, allowing direct decomposition of previously adsorbed organic molecules [182]. Due to the thermal stability of CNTs (stable at a temperature below 500 °C), heating to 400 °C was selected to regenerate the material, and at the end of the 1st cycle, an RNA adsorption capacity of 72% was obtained. These results constitute good adsorption capacity values, as there was only a loss of approximately 30% on the RNA adsorption capacity after the 1st cycle, compared to the original MWCNTs. This loss may be associated with structural and morphological changes in the material after performing each regeneration strategy. Even so, since the thermal regeneration treatment presented practically the same values of RNA adsorption capacity as the chemical treatment, it would be important to continue future research on this strategy, as it can present the advantage of not using chemical reagents as required in chemical regeneration. However, this strategy will only serve as regeneration and not as a desorption strategy, because the use of high temperatures will lead to RNA degradation. To better interpret the adsorption results previously obtained, when using the chemical and thermal regeneration strategies, a FTIR analysis was performed to assess any surface modification, establishing a comparison with a control sample composed of pristine CNTs (Figure 15).

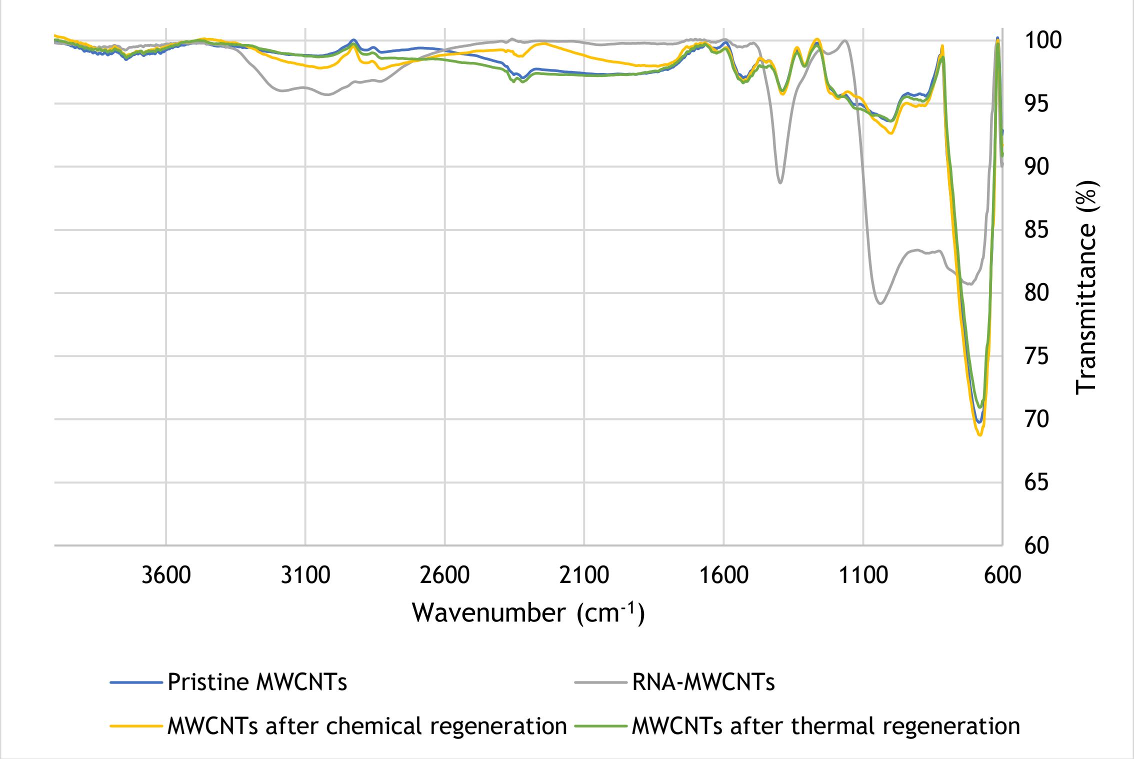

Figure 15- FTIR-ATR spectrum. The blue line represents the primitive MWCNTs, the gray line represents the MWCNTs after adsorption step with RNA, the yellow line represents the MWCNTs after chemical regeneration, and the green line represents the MWCNTs after thermal regeneration.

It can be observed that the strong band at 667 cm^{-1} in the spectrum of neat MWCNTs is typical of C-H bending vibrations in aromatic rings. The bands in the 1600 – 1400 cm^{-1} range are assigned to C=C groups in the aromatic rings. The bands 3100 – 3000 cm^{-1} are typical of =C-H stretching vibrations.

The FTIR-ATR spectrum of the MWCNT sample obtained after RNA adsorption presents a well-defined band at 1400 cm^{-1}, typical of in-plane vibration of the C_2'OH group of the ribose ring. The strong band peaking at c.a. 1085 cm^{-1} is typical from RNA backbone. The absence of the RNA ribose ring vibration band (at 917-916 cm^{-1}) and the significant decrease in the intensity of the bands at 1600 – 1400 cm^{-1} (C=C bonds in the aromatic rings of the CNTs) suggest that π-π interactions are the main driving force for the attachment of RNA at the surface of the CNTs [183] .

By analyzing the FTIR-ATR spectrum referring to the samples of RNA-MWCNTs after chemical and thermal regeneration treatments, it is possible to conclude that the material was able to recover their initial surface properties, since the FTIR-ATR spectra overlap to that of the pristine CNTs, especially the thermal treatment spectrum that allows an almost total superposition with the pristine CNTs spectrum. This result suggests that further investigations about the thermal regeneration approach are definitely needed because the 30% decrease in RNA adsorption capacity after 1 regeneration cycle described above is apparently due to changes occurring on the material surface that the FTIR technique was not sensitive enough to detect, but may also be related to other factors. One of the factors that may be occurring is the loss of material mass after heat treatment which subsequently limits adsorption. Thus, it would be interesting to study the adsorption behavior of CNTs over several cycles of thermal regeneration in order to establish a comparison with chemical regeneration, allowing to understand if this approach would be able to maintain higher percentages of RNA adsorption capacity over 3 or 4 cycles.

4.2- RNA adsorption and desorption experiments using new carbon-based materials

4.2.1- Screening of RNA adsorption and desorption conditions

To address the problem of significant loss of RNA adsorption capacity over several cycles, and simultaneously outline a simple and efficient RNA desorption strategy applying more environmentally friendly techniques and conditions, other CNTs with different surface functionalities were studied. More specifically, nitrogen-containing CNTs (N-doped CNTs) and N-doped CNTs oxidized with HNO_3, were studied regarding RNA adsorption and desorption efficiency, and compared with the MWCNTs. In addition, for a more complete evaluation, other carbon materials were also studied, namely carbon fibers, carbon fibers oxidized with HNO_3, graphene, graphene oxidized with HNO_3, fullerene, and exfoliated carbon nitride. Several screening assays were performed to find the most favorable conditions for RNA adsorption and desorption. First, hydrophobic and electrostatic interactions were promoted between all carbon-based materials and RNA to understand which interactions prevailed in RNA adsorption. For this purpose, the experimental method previously used for the MWCNTs <10, was also applied for the adsorption and desorption of RNA from these alternative materials. Therefore, for the experiments where hydrophobic interactions were to be established, aliquots containing 1 mg of each carbon material were prepared and equilibrated with 1 mL of 1.5 M $(NH_4)_2SO_4$ in 10 mM Tris-HCl, pH 8. On the other hand, when the objective was to establish electrostatic interactions, the equilibrium buffer used was 1 mL of 10 mM Tris-HCl, pH 8. Similarly, for the previously described assays for MWCNTs, a model sample of low molecular weight RNA (50 μg/mL) was prepared and diluted in the respective equilibration buffer, depending on the requirement for hydrophobic or electrostatic interactions.

Through the analysis of Figure 16, it is possible to observe that when promoting electrostatic interactions, a considerably low RNA adsorption was achieved for all carbon materials and there was an inability to elute the adsorbed RNA. This phenomenon occurs for materials without surface functionalization due to their surface inertia; therefore, electrostatic interactions are practically null. On the other hand, treatment with HNO_3 acidifies the surface of the materials due to the incorporation of a large number of oxygen-containing groups, especially carboxylic groups (COOH). Several studies in the literature have shown that the carboxylic groups generated during the oxidation of various carbon-based materials caused an increase in surface negative charge. As an example, in 2013, a study by Hamilton, Jr. and co-workers proceeded to oxidize the surface of MWCNTs with HNO_3 and measured the zeta potential of as-grown MWCNTs and the oxidized MWCNTs, and the values obtained were -9.76 mV and -13.8 mV, respectively [8]. The reason was that the COOH fraction can be dissociated into negatively charged COO^- due to the low isoelectric point, leading to a more negative surface charge [184]. This evidence may be the cause behind the results obtained for the non-existent electrostatic interactions due to electrostatic repulsion between the negatively charged surface of the oxidized carbon-based materials and the negatively charged RNA.

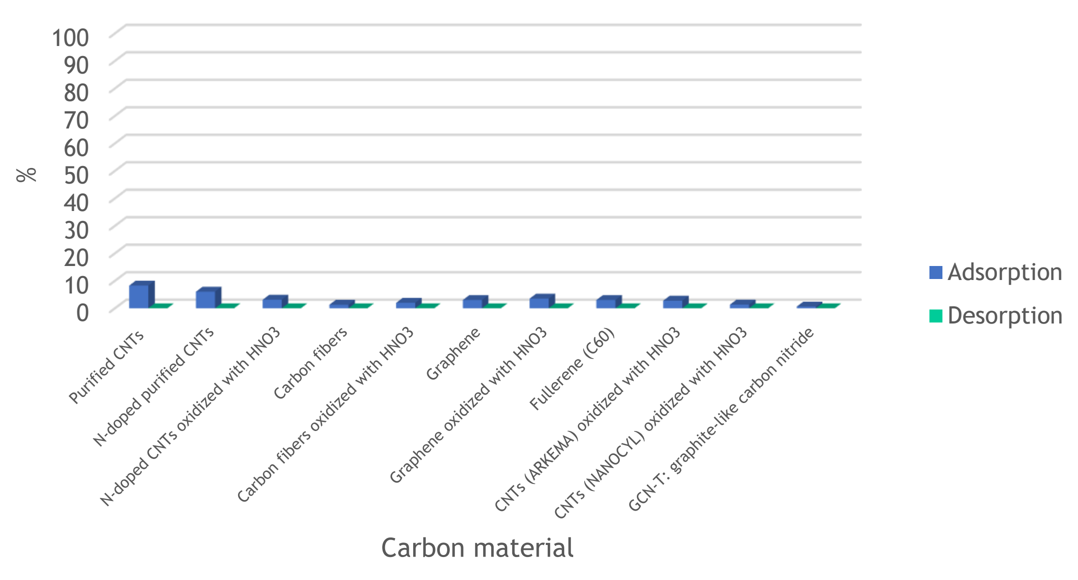

Figure 16- RNA adsorption and desorption capacity from different carbon-based materials when electrostatic interactions are promoted.

On the other hand, as shown in Figure 17, higher percentages of RNA adsorption were found, when establishing hydrophobic interactions. As expected, the purified CNTs enabled an RNA adsorption percentage of 100%, corroborating the results obtained with MWCNTs. Comparing the carbon materials, without any surface modification, such as carbon fibers, graphene, and fullerene, it was observed that purified CNTs were able to adsorb a higher amount of RNA. In parallel, the RNA adsorption capacity of carbon materials was highly influenced by the surface chemistry of these materials. As mentioned throughout this work, the surfaces of CNTs are highly hydrophobic, demonstrating strong adsorption of RNA via π-π and hydrophobic interactions. Doping carbon nanotubes with nitrogen leads to a change in the polarity and wettability of the material. Thus, there is a reduction in RNA adsorption, since the introduction of hydrophilic moieties implies a reduction of hydrophobic regions, thus compromising RNA capture. As can be seen, there was a reduction of approximately 20% in the RNA adsorption capacity of the N-doped CNTs oxidized with HNO_3 in comparison with the purified CNTs. Furthermore, it is expected that compared to undoped CNTs, doped CNTs exhibit more polarized graphitic surfaces, as the presence of nitrogen can significantly affect the π electron distribution on the surfaces of the materials. In 2014, a study by Arenal and co-workers demonstrated that the additional nitrogen electron became relatively localized and disrupted local conjugation, reducing local π contributions, which could help understand the percentage of RNA adsorption by N-doped CNTs oxidized with HNO_3 as the π-π interactions between the material and RNA could have been affected [185]. However, the effects of nitrogen doping on the adsorption affinities of CNTs are not yet well understood [186], and therefore, no conclusion can be made about the doping effects on RNA adsorption. In addition, the presence of the oxygen-containing functional groups generated by HNO_3 treatment may also alter the accessibility and affinity of RNA molecules to the surface of CNTs, contributing to the low RNA adsorption capacity of N-doped CNTs oxidized with HNO_3 (35%). Also, CNTs (ARKEMA) oxidized with HNO_3 and CNTs (NANOCYL) oxidized with HNO_3 exhibited lower RNA adsorption capacities (70% and 23%, respectively) when compared to MWCNTs (100%) and purified CNTs (100%). This may be a consequence of 2 factors: first, the acidic oxygen groups present on the surface may remove electrons from the π electron system, leading to weaker interactions between the π electrons present in the aromatic rings of RNA nitrogen bases and the π electrons of those present on the surface of CNTs, thus reducing RNA capture; and second, it may occur a blocking of the internal cavities of these materials due to possible water clusters formed around the functional groups, which may associate within the pores of CNTs, preventing RNA adsorption to a large portion of the active surface [187]. Of note, in 2017, a study conducted by Sun and co-workers showed that RNA bases are also capable of establishing hydrogen bonds with oxygen-containing functional groups present in carbon nanotubes, so this type of interaction cannot be discarded as it may be present among the carbon materials studied here that have oxidative treatment [188].

A very curious result was the RNA adsorption percentages of carbon fibers and carbon fibers oxidized with HNO_3. Contrary to the other materials in which the surface oxidation process limited the RNA adsorption (CNTs oxidized with HNO_3 and graphene oxidized with HNO_3), in this case carbon fibers oxidized with HNO_3 presented a higher RNA adsorption capacity (46%) when compared to carbon fibers without any surface modification (29%). Overall, the atomic structure of carbon fibers consists of sp^2 bonded carbon atoms (graphene layers) arranged perpendicular or at an angle to the fiber axis [189]. Therefore, RNA is expected to adsorb to the fiber surface mainly through the mechanisms described above: π-π interactions and hydrophobic interactions. However, considering Table 11, the diameter of the fibers (60-150 nm) is quite larger than the diameter reported for Purified CNTs and CNTs (ARKEMA) (5-50 nm), which may have a direct negative impact on the RNA adsorption of this material because a larger diameter results in a decreased surface area, which consequently can lead to a lower RNA adsorption percentage. Furthermore, it was also expected that the generation of oxygen-containing functional groups on the surface of the carbon fibers would result in a decrease in the percentage of RNA adsorption. This did not occur and may be explained by the effect of nitric acid on the porosity of the material. The pores present in carbon fibers are believed to be poorly developed, causing the carbon layers to expose little surface area and pore volume [190]. In 2003, a study published by Pamula and co-workers demonstrated that oxidative HNO_3 treatment of carbon fibers resulted not only in an increase in oxygen-containing functional groups on the surface of the material, but also an increase in the microporosity of the fibers [191]. According to the International Union of Pure and Applied Chemistry (IUPAC), the classification of pores for their size can be based on adsorption properties [192]. Since micropores are characterized by their width of less than 2 nm [192] and DNA is composed of 2 main chains with a width of 2 nm, it is possible that RNA can enter this microstructure since its size is smaller than DNA. Therefore, this may be one of the possible reasons for the increased RNA adsorption percentage for HNO_3 oxidized carbon fibers. However, it is important to mention that, so far, there are no reports in the literature about the adsorption of nucleic acids to carbon fibers, so more specific studies are needed on this subject, mainly complemented with techniques to characterize in detail the treated and untreated surface of this material.

Regarding RNA desorption and recovery, in general, no significant percentages were obtained, except for the N-doped CNTs oxidized with HNO_3 and carbon fibers oxidized with HNO_3, which presented good RNA desorption percentages compared to the adsorption level. These results suggest that these materials are very promising and, for this reason, they have proceeded to the remaining assays.

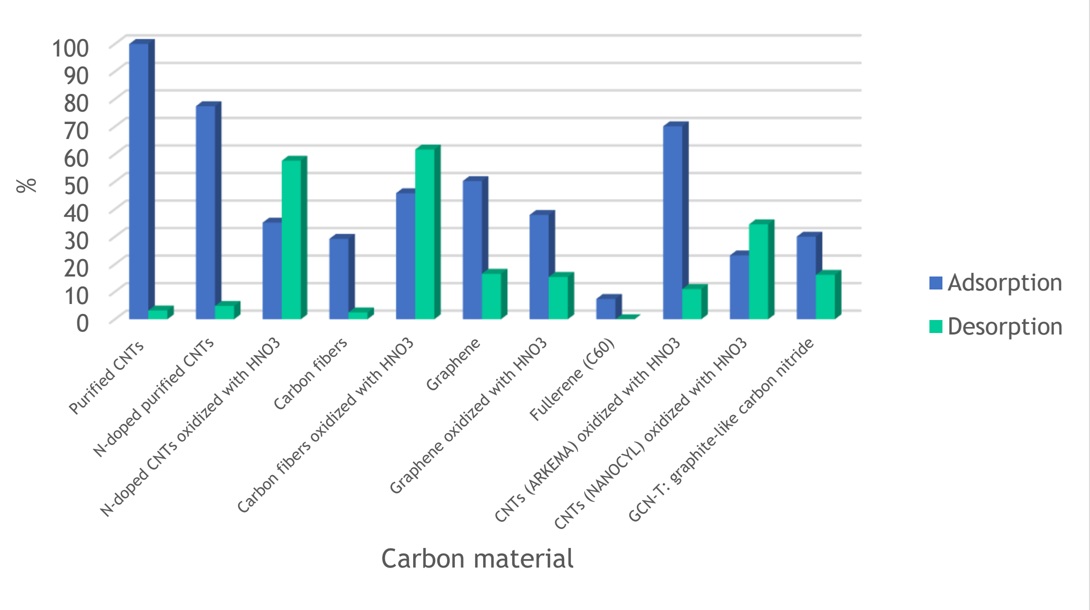

Figure 17- RNA adsorption and desorption capacity of different carbon-based materials when hydrophobic interactions are promoted.

4.2.2- Effect of ionic strength on RNA adsorption

After hydrophobic interactions were chosen as ideal interactions to promote RNA adsorption to the studied carbon materials, we investigated the effect of ionic strength on RNA capture by N-doped CNTs oxidized with HNO_3 and carbon fibers oxidized with HNO_3. Since separation based on hydrophobic interactions is usually accomplished by adsorbing the hydrophobic molecule using a mobile phase with high ionic strength, the concentration of $(NH_4)_2SO_4$ in equilibrium/binding buffer was increased to 2 M $(NH_4)_2SO_4$ in 10 mM Tris-HCl pH 8 and 2.5 M $(NH_4)_2SO_4$ in 10 mM Tris-HCl pH 8 for further comparison with the previously used binding buffer, of 1.5 M $(NH_4)_2SO_4$ in 10 mM Tris-HCl pH 8. The results presented in Figure 18 showed that, in general, increasing the concentration of $(NH_4)_2SO_4$ led to an increase in RNA adsorption capacity for both tested materials, as it was expected. Particularly, increasing the concentration of $(NH_4)_2SO_4$ to 2 M resulted in the best percentages of RNA adsorption: 42% for N-doped CNTs oxidized with HNO_3 and 55% for carbon fibers oxidized with HNO_3. Considering this, the concentration of 2M of ammonium sulfate in the binding buffer was established for further studies.

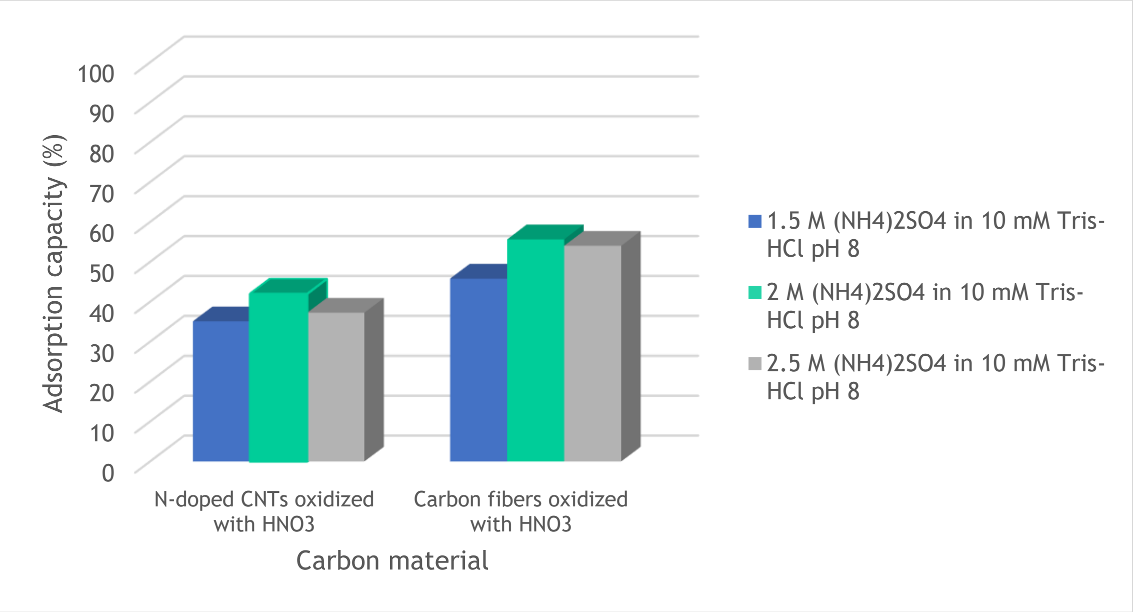

Figure 18- RNA adsorption capacity of N-doped CNTs oxidized with HNO_3 and carbon fibers oxidized with HNO_3 by increasing the ionic strength in the binding buffer.

4.2.3- RNA adsorption Isotherms

The study of adsorption isotherms is very important because it indicates how the molecules are distributed between the liquid phase and the solid phase when the adsorption process reaches the equilibrium state, allowing us to infer how the solutes interact with the adsorbents. In that study, the initial RNA concentration (10-50 µg/mL) was varied to study the adsorption isotherms, keeping constant the solution volume (1 mL), the amount of adsorbent (1 mg), and the contact time between the adsorbent and the adsorbate (20 minutes). According to Giles and co-workers [193], the Langmuir isotherm is one of the best known and occurs in most cases of adsorption. According to this model, when the monolayer coverage of the molecules on the adsorbent surface is completed without interaction between the adsorbed molecules, this will be the maximum adsorption capacity. The Langmuir equation (equation 4) in non-linearized form is represented by:

$$q_e = \frac{Kl \times q_{max} \times C_e}{1 + Kl \times C_e} \tag{4}$$

where *qe* (mg/g) and *Ce* (mg/L) are the amount of RNA adsorbed at equilibrium and RNA concentration at equilibrium (mg/L), respectively. Q_{max} (mg/g) is the RNA maximum adsorption capacity, and *Kl* is the adsorption equilibrium constant (L/mg) that is related to the free energy of adsorption. Figure 19 depicts the adsorption isotherm of RNA on N-doped CNTs oxidized with HNO_3 and on carbon fibers oxidized with HNO_3. The experimental data are represented as symbols and the Langmuir model as solid lines. The Langmuir parameters, as determined through the fitting, are presented in Table 12.

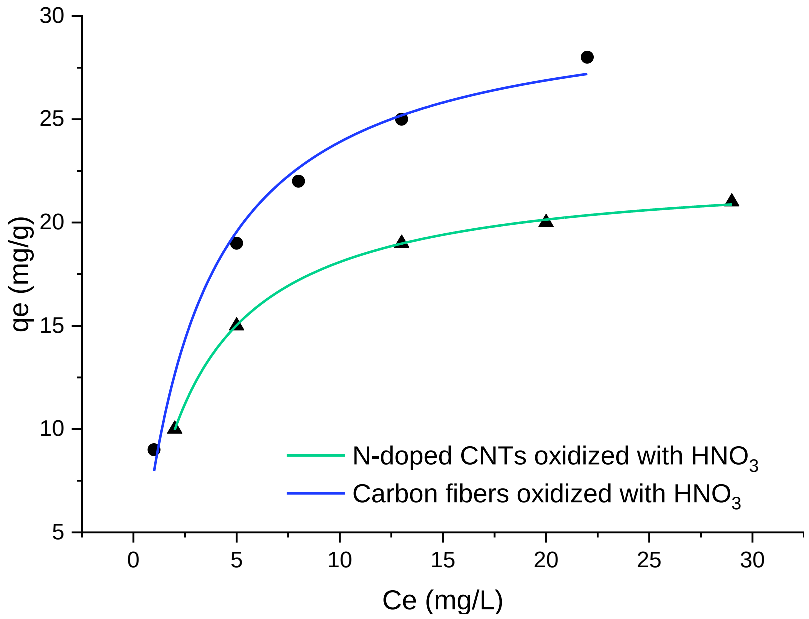

Figure 19- RNA adsorption isotherms. The green curve is representative of N-doped CNTs with HNO_3 and the blue curve represents carbon fibers oxidized with HNO_3.

Table 12- Langmuir parameters obtained by fitting the data in Figure 19.

Carbon material	***R^2***	***Qmax* (mg/g)**	***Kl* (L/mg)**
N-doped CNTs oxidized with HNO_3	0,9995	22,7	0,3907
Carbon fibers oxidized with HNO_3	0,9884	30,8	0,3501

Considering Table 12, when comparing the determination coefficients (R^2), it can be concluded that this model proved to be quite adequate to describe the RNA adsorption processes onto these materials, with an R^2 of 0.99954 for the N-doped CNTs oxidized with HNO_3 and an R^2 of 0.98455 for the carbon fibers oxidized with HNO_3 (values very close to 1). When analyzing the isotherms of both materials (Figure 19), they are characterized by a large increase in the amount of RNA adsorbed at low concentrations, decreasing around an equilibrium concentration, and followed by a tendency to form a plateau when the concentration is higher. This behavior is because there is greater adsorption for a lower concentration of RNA due to the presence of more available sites on the adsorbent than the amount of RNA available in the solution. However, at higher concentrations, the amount of RNA is relatively higher than the available sites for adsorption, leading to a saturation state. N-doped CNTs oxidized with HNO_3 showed a Q_{max} of 22.7 mg/g, while carbon fibers oxidized with HNO_3 showed a superior Q_{max} value, of 30.7 mg/g (Table 12). Comparing these values of maximum RNA adsorption capacity with the value obtained for MWCNTs (175 mg/g), it is confirmed that the presence of oxygen-containing functional groups on the surface of the carbon-based materials has a great impact on RNA adsorption performance. Actually, the adsorption capacity can be lower, but an advantage can be found, as the recovery of adsorbed RNA can be facilitated on these oxidized materials.

4.2.4- RNA desorption

It has already been proven that exploring hydrophobic interactions are the optimal conditions for adsorption and desorption of RNA from N-doped CNTs oxidized with HNO_3 and carbon fibers oxidized with HNO_3. The use of 10 mM Tris-HCl pH 8 buffer was relatively effective in recovering RNA from the materials. However, for a more complete characterization of the potential for RNA recovery from these materials, other elution buffers were tested, by changing the buffer and the pH. These experiments involved the use of 10 mM Tris-HCl pH 9, 100 mM Acetate buffer pH 5, 0.01% Tween-20, and 0.2% Triton X-100 (Figure 20 and Figure 21). Except for the use of the 100 mM Acetate buffer pH 5, there was an increase in the percentage of RNA desorption for both materials relative to the percentage obtained with the 10 mM Tris-HCl buffer pH 8. Compared to MWCNTs, it is evident that the material's surface functionalization was fundamental to enabling RNA desorption. This can be explained on the basis of the increased dispersion of the materials that may have led to faster removal of RNA during desorption and the fact that the presence of the oxygen-containing functional groups leads to weaker interactions between the materials and RNA, providing RNA desorption. For both materials, the best percentage of RNA desorption was obtained when using the 0.2% Triton X-100 buffer, with 95.2% and 85.8% of RNA recovery for N-doped CNTs oxidized with $HNO_{3,}$ and carbon fibers oxidized with HNO_3, respectively. However, since the percentages of RNA desorption with 10 mM Tris-HCl pH 9 (81% for N-doped CNTs oxidized with HNO_3 and 72.5% for carbon fibers oxidized with HNO_3) were not very different from the percentages obtained using Triton X-100, this was the selected desorption condition. This strategy was defined as the optimal strategy for RNA desorption from these materials, as there was no risk of compromising RNA integrity when resorting to the use of surfactants, in addition to not influencing the RNA adsorption capacity when reusing these materials in new cycles due to the binding capacity of surfactants to carbon materials.

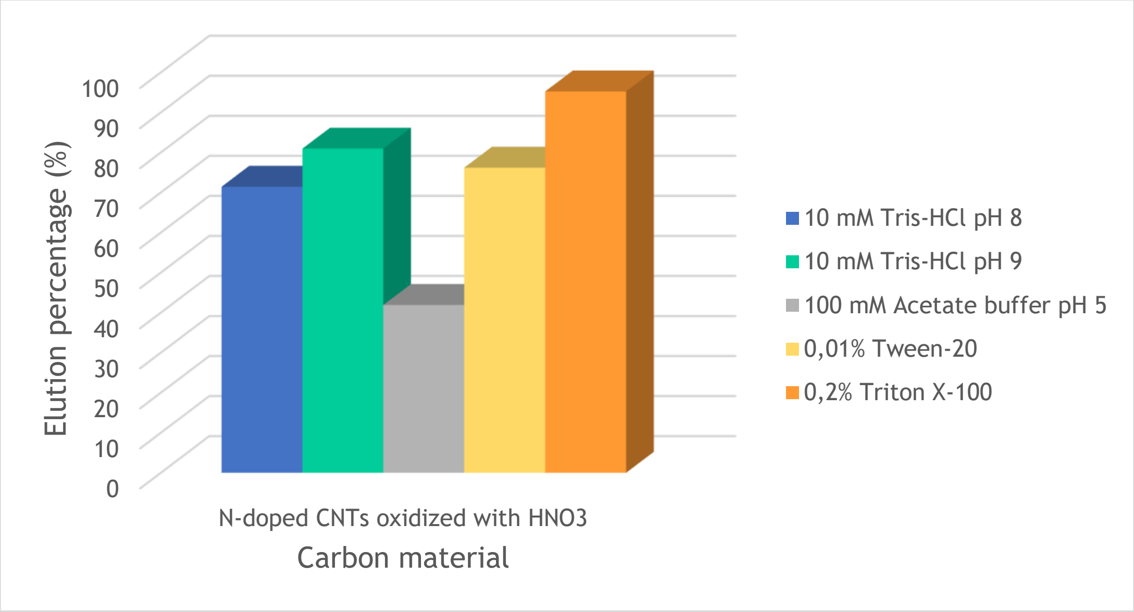

Figure 20- RNA elution of N-doped CNTs oxidized with HNO_3 with different buffers.

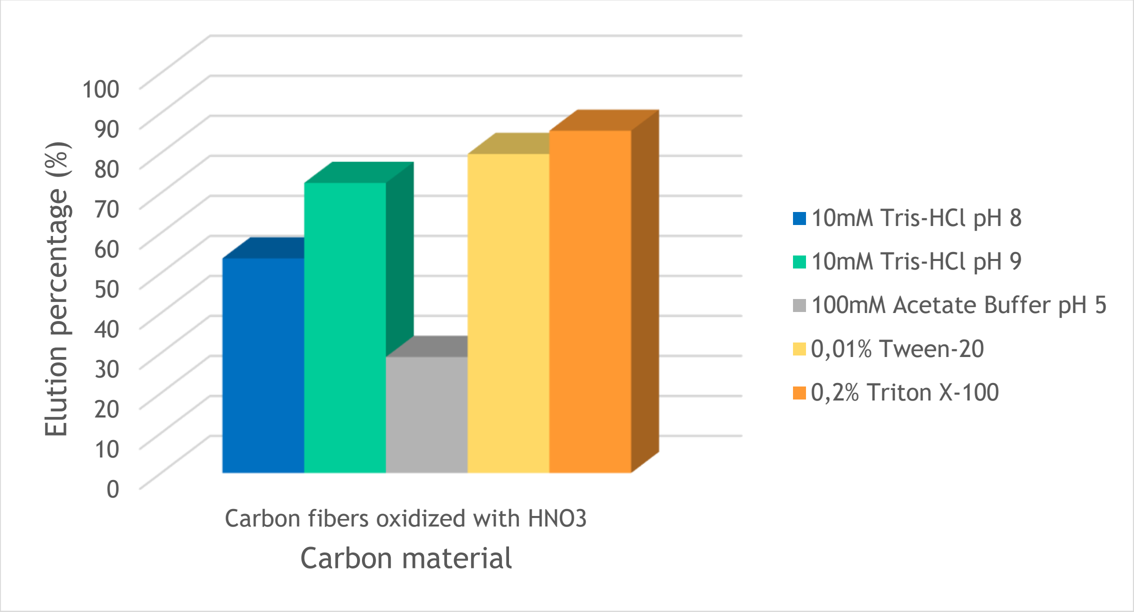

Figure 21- RNA elution of carbon fibers oxidized with HNO_3 with different buffers.

4.2.5- Reuse of materials

Similar to the regeneration and reuse experiments performed for MWCNTs, reuse experiments were also performed for N-doped CNTs oxidized with HNO_3 and carbon fibers oxidized with HNO_3. Since almost complete RNA desorption capacity was confirmed when the appropriate elution buffer (10 mM Tris-HCl pH 9) was applied, it was expected that after a new RNA capture cycle, the RNA adsorption capacity of the materials would be maintained or not change significantly. Thus, the application of this RNA desorption buffer was applied not only as a desorption strategy but also as a regeneration strategy for the materials under study. Therefore, for both materials, the RNA capture method previously used was applied, and after the application of the desorption buffer for RNA recovery, a step of washing with deionized water was applied to subsequently repeat the adsorption/desorption experiments, over 4 cycles. The results of these assays for the 2 materials are shown in Figures 22 and 23. Looking at Figure 22, it can be concluded that over 4 cycles there was a slight loss of RNA adsorption capacity by the N-doped CNTs oxidized with HNO_3. Comparing the RNA adsorption capacity of the original CNTs with the RNA adsorption capacity at the end of the 4th cycle, there was a loss of approximately 10%, which is considered an excellent result. On the other hand, considering Figure 23, after the 1st cycle, the RNA adsorption capacity by the carbon fibers oxidized with HNO_3 remained practically the same. Only after the 2nd cycle, there was some loss of RNA adsorption capacity, with almost a 30% loss of adsorption capacity at the end of the 4th cycle. Thus, it is concluded that despite some loss of capacity to capture RNA, both materials showed a good capacity to be reused, making this process more efficient and environmentally friendly, focusing on carbon materials that showed very promising results.

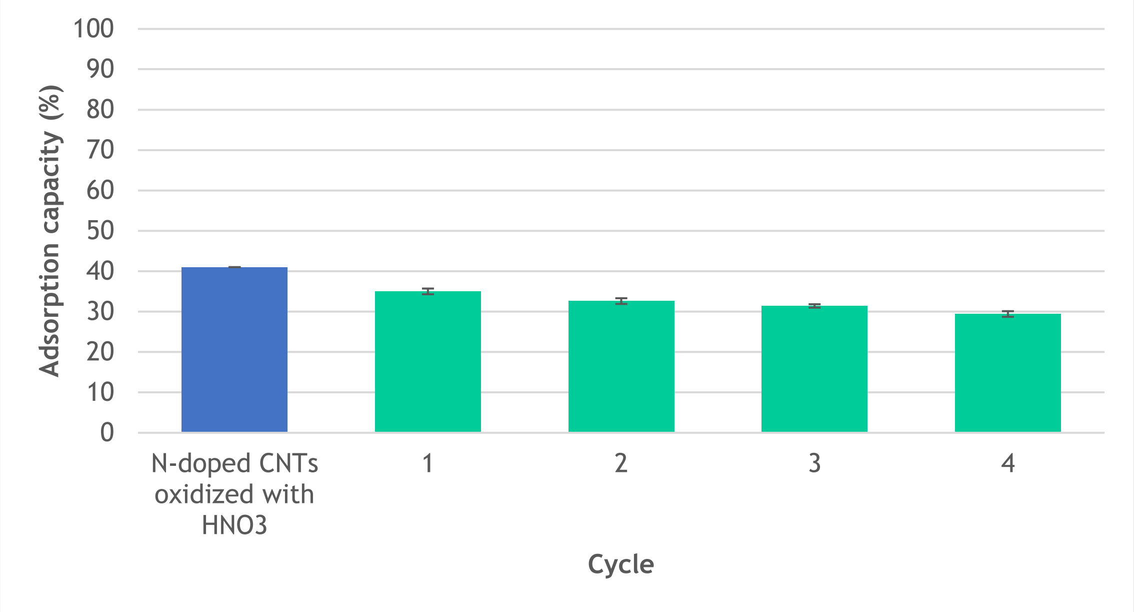

Figure 22- RNA adsorption capacity of N-doped CNTs oxidized with HNO$_3$ when employing RNA elution buffer (10 mM Tris-HCl pH 9) followed by new adsorption assays, over 4 cycles. Values were calculated with the data obtained from two independent measurements (mean ± SD, n = 2).

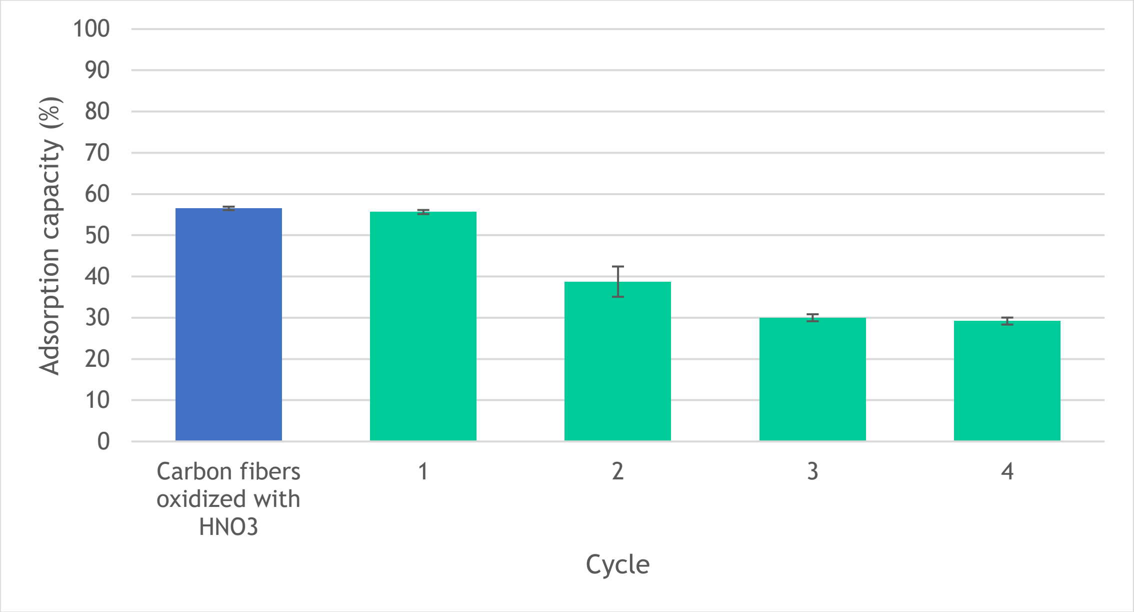

Figure 23- RNA adsorption capacity of carbon fibers oxidized with HNO$_3$ when employing RNA elution buffer (10 mM Tris-HCl pH 9) followed by new adsorption assays, over 4 cycles. Values were calculated with the data obtained from two independent measurements (mean ± SD, n = 2).

To make a comparison with the chemical regeneration strategy performed for the MWCNTs, the N-doped CNTs oxidized with HNO$_3$ and the carbon fibers oxidized with HNO$_3$ were also subjected to the chemical regeneration protocol using 0.5% Tween-20 and 1 M NaOH with a final washing step with deionized water. The results of RNA adsorption capacity using this regeneration strategy for both materials are presented in Figures 24 and 25. Interestingly, Figure 24 for the N-doped CNTs oxidized with HNO$_3$

shows that in the 1st cycle, there was an increase of approximately 23% in the RNA adsorption capacity compared with the original CNTs, and then a decrease over the last cycles. This phenomenon may be based on the functionalization of the CNTs themselves. It has been reported in the literature that the HNO_3 oxidation strategy of CNTs produces oxidative carbonaceous fragments, identified as polycyclic aromatic molecules with oxidized edges, which adsorb to the surface of CNTs through π-π stacking, and it is a difficult task to remove them even with a thorough washing with water [194]. The possible effect of these fragments on the adsorption capacity of CNTs is not yet fully known. Still, a study done in 2020 by Amaral and collaborators aimed to evaluate the impact of the presence of those fragments on the adsorption capacity of oxidized MWCNTs. They concluded that the fragments led to blockage of the interstitial channels and the outer surface of the CNTs, and could negatively affect the adsorption capacity of the material [195]. One of the procedures used to remove the fragments is to solubilize them by prolonged digestion in a NaOH solution followed by separation of fragments by filtration, centrifugation, or ultracentrifugation. Amaral and co-workers concluded that this strategy led to potential adsorption sites becoming free. Thus, it is very likely that after the addition of 1 M NaOH to N-doped CNTs oxidized with HNO_3, followed by agitation for 20 minutes and subsequent separation of the fragments by centrifugation, there was an increase in active sites on the surface of the material for RNA adsorption and thus there was a considerable increase in adsorption capacity in the 1st cycle, followed by a progressive decrease in the remaining cycles.

It was also already reported that the exposure of carbon fibers oxidized with HNO_3 to NaOH removes surface layers of partially oxidized graphitic fragments that arise due to the oxidative process on the surface of the carbon fibers [196]. However, according to Figure 25 and contrary to what was observed for CNTs, this removal did not lead to an increase in the RNA adsorption capacity, but to a progressive decrease over the several adsorption cycles, which may lead to the belief that the oxidative role of NaOH may have prevailed before the removal of the generated fragments. However, more detailed studies are necessary to understand what kind of modifications occur on the material's surface upon exposure to NaOH.

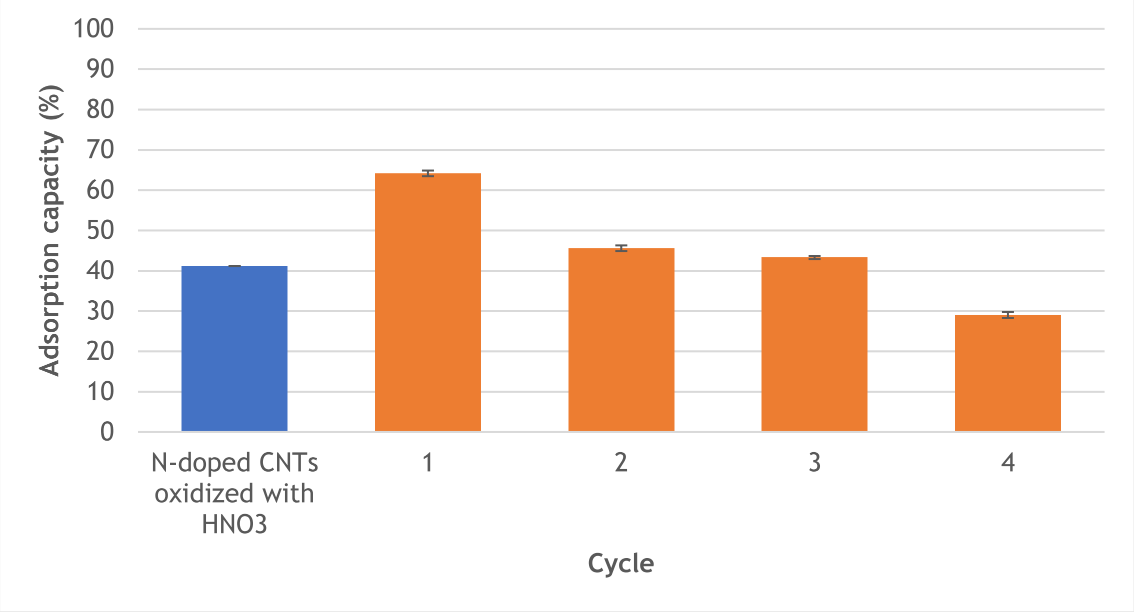

Figure 24- RNA adsorption capacity of N-doped CNTs oxidized with HNO_3 when employing the chemical regeneration strategy (0.5% Tween-20 + 1M NaOH) followed by new adsorption assays, over 4 cycles. Values were calculated with the data obtained from two independent measurements (mean ± SD, n = 2).

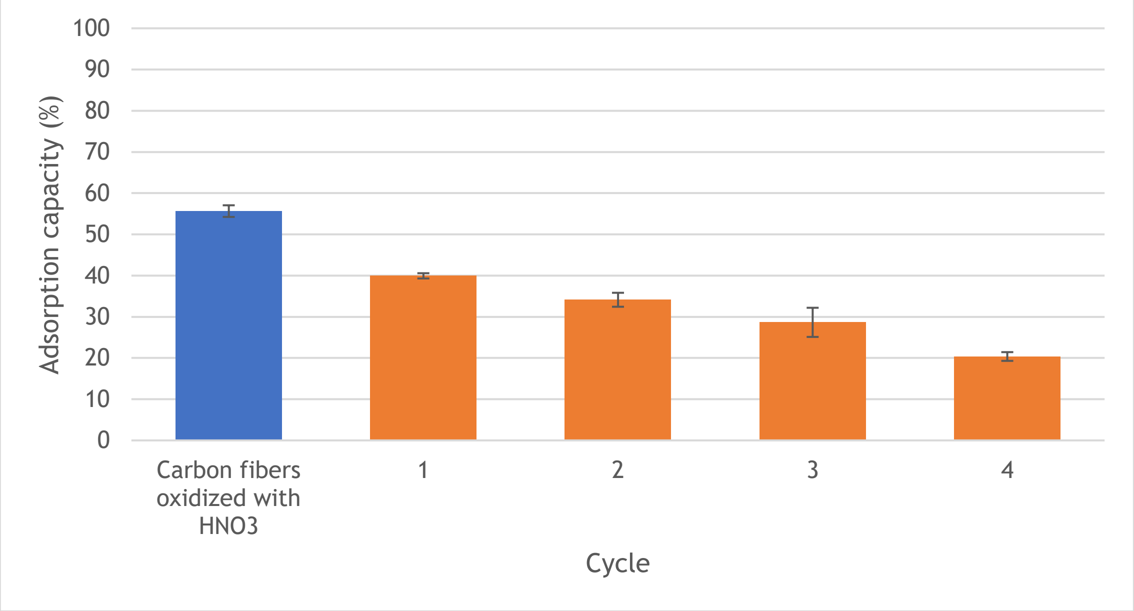

Figure 25- RNA adsorption capacity of carbon fibers oxidized with HNO_3 when employing the chemical regeneration strategy (0.5% Tween-20 + 1M NaOH) followed by new adsorption assays over 4 cycles. Values were calculated with the data obtained from two independent measurements (mean ± SD, n = 2).

4.2.6- Selectivity between RNA and pDNA

To evaluate the ability to separate RNA from other impurities, selectivity assays between RNA and pDNA were performed to understand the influence that the presence of pDNA may have on RNA capture. For these experiments, 3 different ratios of RNA and pDNA were used: 1:1 (RNA/pDNA), 1:2 (RNA/pDNA), and 2:1 (RNA/pDNA). For this and considering the maximum RNA adsorption capacities of materials, mixtures were prepared with the following final concentrations: 20 µg/mL + 20 µg/mL (RNA/pDNA), 30 µg/mL + 30 µg/mL (RNA/pDNA), 20 µg/mL + 40 µg/mL (RNA/pDNA) and 20 µg/mL + 10 µg/mL (RNA/pDNA) and the results are present in Figures 26 and 27.

Considering the representative agarose gel electrophoresis of the N-doped CNTs oxidized with HNO_3 (Figure 26), it was possible to observe that for all tested ratios, part of the RNA is adsorbed while apparently most of the DNA remains in solution. This happens because DNA is characterized by a compact structure with limited spatial availability of nitrogenous bases, contrary to RNA which presents the nitrogenous bases much more exposed, enabling a higher interaction with the CNTs [197]. When analyzing the bands corresponding to the desorbed fraction, it was clear that the bands corresponding to the RNA were quite visible, while the DNA bands were practically insignificant. Even when a higher concentration of DNA is present in the sample (40 µg/mL), the band corresponding to the RNA in the non-bound sample was almost inexistent, inferring that there was selectivity of the N-doped oxidized with HNO_3, as, although they did not totally capture the RNA, they contributed considerably to greater clarification of pDNA in the non-bound sample, considering all the ratios of RNA/DNA tested. In Figure 27, which represents the agarose gel electrophoresis for the carbon fibers oxidized with HNO_3, it was possible to observe a very similar behavior to the N-doped CNTs oxidized with HNO_3. It should only be noted that for all the tested RNA and DNA proportions, there was a higher RNA adsorption by the fibers relatively to the CNTs, corroborating the results obtained for the maximum RNA adsorption capacity. However, the bands representing the DNA in the non-bound samples were fainter than for the CNTs, even when considering the sample with the lowest concentration of DNA (10 µg/mL), thus evidencing a weak point compared with CNTs.

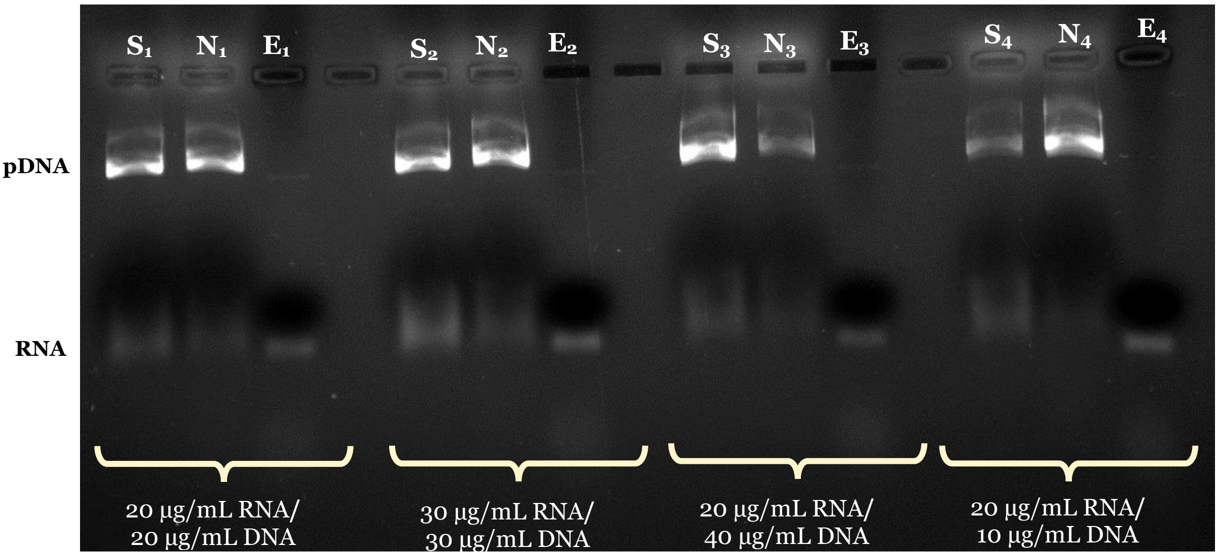

Figure 26- Agarose gel electrophoresis of RNA and DNA mixtures before and after capture with N-doped CNTs oxidized with HNO_3, using 4 different ratios. S-Initial sample; N-Sample after adsorption, comprising all solutes not adsorbed to N-doped CNTs oxidized with HNO_3; E-Sample after desorption, comprising all solutes eluted from N-doped CNTs oxidized with HNO_3.

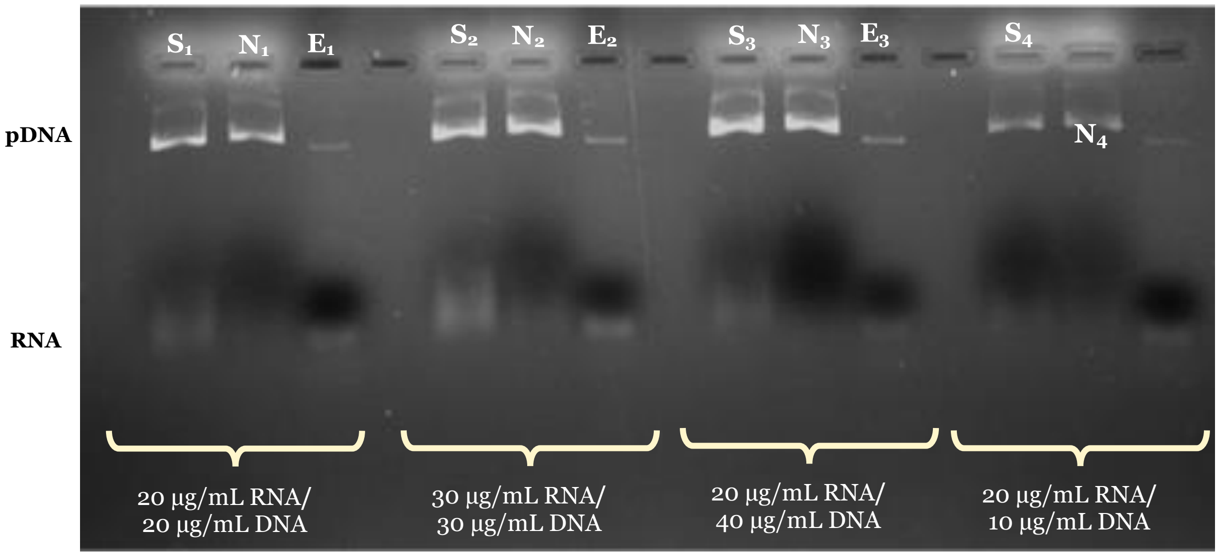

Figure 27- Agarose gel electrophoresis of RNA and DNA mixtures before and after capture with carbon fibers oxidized with HNO_3 using 4 different ratios. S-Initial sample; N-Sample after adsorption, comprising all solutes not adsorbed to carbon fibers oxidized with HNO_3; E-Sample after desorption, comprising all solutes eluted from N-doped CNTs oxidized with HNO_3.

4.2.7- RNA adsorption from a lysate sample

To evaluate the performance of the materials in RNA capture and recovery from a complex sample, and investigate the selectivity between RNA and other contaminating biomolecules, an *E. coli* lysate sample was then used. In this case, both materials were used over 3 consecutive cycles, i.e., the initial sample used in the 1st cycle corresponded to the complex lysate sample, and then the supernatant resulting from the 1st cycle was applied in a 2nd cycle, and the sample resulting from the 2nd cycle was applied in a 3rd cycle. The supernatants corresponding to each cycle were collected, as well as the desorbed RNA fractions. The results were analyzed by absorbance measurements and agarose gel electrophoresis, as shown in Figure 28.

By analyzing the agarose gel electrophoresis of the N-doped CNTs oxidized with HNO_3 (Figure 28 A), it can be seen that compared to the initial lysate sample (Figure 28 A S_1), there was a decrease in the intensity of the RNA band after each cycle. More importantly, by analyzing the desorbed RNA bands (Figure 28 A D1, D2, D3), it is evident the recovery of RNA after the 3 cycles without the presence of contaminating DNA. This result was quite good because immediately after the 1st cycle, it was possible to recover RNA without the presence of DNA (Figure A 28 D1), confirming the selectivity of the material and an apparently total clarification of the recovered RNA, which is a remarkable advance for the pre-purification of this biomolecule. On the other hand, observing the agarose gel electrophoresis of the carbon fibers oxidized with HNO_3 (Figure 29 B), it is possible to observe that, similarly to the CNTs, there was a decrease in the intensity of the RNA band after each cycle compared to the initial lysate sample. When analyzing the desorbed RNA band after the 1st cycle (Figure 29 B D1), it was possible to recover a considerable amount of RNA but also eluted some DNA. However, when analyzing the following cycles (Figure 29 B D2, D3), there continued to be RNA recovery, while the DNA band decreased in intensity, apparently remaining in minimal amounts. Thus, compared to CNTs, the fibers required more than 1 cycle for the recovery of RNA free of large amounts of DNA, evidencing lower selectivity. Nevertheless, using the method described for these carbon materials, it was possible to capture and recover RNA from a complex lysate sample without the need to use the large amounts of toxic solvents normally applied in commonly used RNA isolation techniques that have changed little in recent years. In addition, the method used in this work is neither time-consuming nor highly operator-dependent. All these issues contribute to the fact that this method allows the isolation of biologically active and chemically stable RNA.

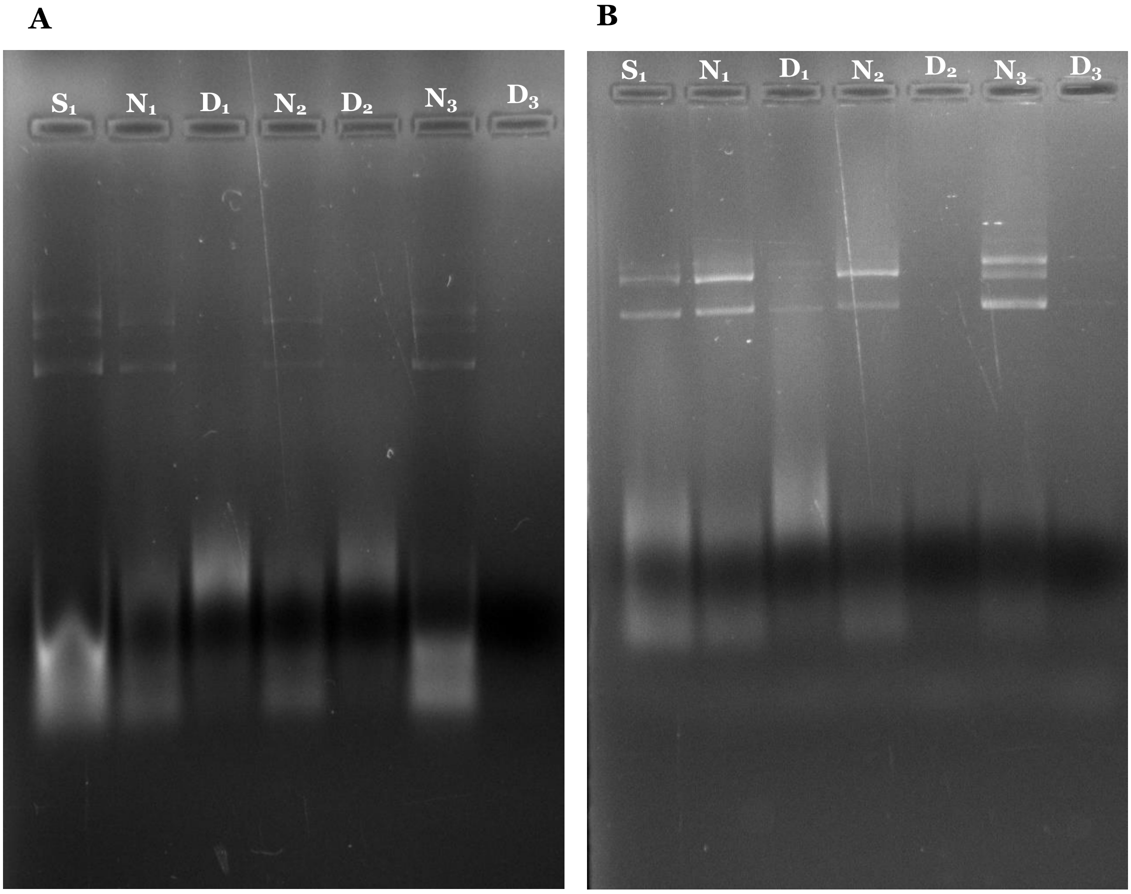

Figure 28- Agarose gel electrophoresis of E. coli lysate before and after capture method for 3 consecutive cycles. A: N-doped CNTs oxidized with HNO_3; B: carbon fibers oxidized with HNO_3. S1- Initial E. coli lysate samples for the 1st adsorption cycle; N1-Samples after the 1st adsorption cycle, comprising all non-adsorbed solutes; E1-Samples after the 1st desorption cycle, comprising all desorbed solutes; N2-Samples after the 2nd consecutive cycle, comprising all non-adsorbed solutes; E2- Samples after the 2nd desorption cycle, comprising all desorbed solutes; N3- Samples after the 3rd consecutive cycle, comprising all non-adsorbed solutes; E3- Samples after the 3rd desorption cycle, comprising all desorbed solutes.

4.2.8- Contaminating proteins quantification

The main components of the *E. coli* host that constitute impurities related to the RNA isolation process are proteins, gDNA, and endotoxins. In particular, it is known that *E. coli* comprises about 4300 protein-coding genes and that, according to FDA recommendations, the maximum level of protein in a biopharmaceutical product for it to have therapeutic application should preferably be less than 1% (weight of impurity/weight of plasmid) [198]. For these reasons, the removal of these biomolecules is very important to prevent possible immunogenic responses upon administration of biopharmaceuticals. In this regard, protein quantification experiments were performed using the Bradford protein assay on the complex *E. coli* lysate sample and the samples recovered from the previous experiment of the 3 consecutive cycles. The results are shown in Table 13. Analyzing the results obtained for the N-doped CNTs oxidized with HNO_3, they suggest that there is full protein capture as early as the 1st cycle. In fact, a study by Burch and co-workers demonstrated the remarkable ability of N-doped MWCNTs oxidized with H_2SO_4 and HNO_3 to capture metalloproteins. The observations from this study suggested that this capture was mainly due to the hydrophilic nature of the amino acid side chains present on the outer surface of the proteins that enabled interaction with the hydrophilic domains present on the oxidized surface of the material. Additionally, the formation of hydrogen bonds between these chains and the carboxyl moieties on the surface of the MWCNTs could facilitate the stable adsorption of the proteins. In addition, doping the MWCNTs with nitrogen improved the capture of the metalloproteins as the presence of nitrogen enhanced the hydrophilicity of the material, further facilitating the interaction with the proteins [199]. This study then proposes an explanation for the full capture of the proteins present in the lysate sample by the N-dopes CNTs oxidized with HNO_3. A very promising result is also the fact that in the desorbed RNA sample, no protein is present, thus showing a 100% protein reduction of the desorbed sample compared to the initial lysate sample. This phenomenon may also have an explanation based on the study cited above, because the metalloproteins remained adsorbed to the MWCNTs despite the application of steps such as washing and centrifugation, indicating strong interactions between the proteins and the material. This suggest that the desorption step is effective on RNA recovery, but proteins remain boun, what is very important to guarantee the clarification of the RNA sample.

Regarding the carbon fibers oxidized with HNO_3, the results obtained indicate that in the 1st adsorption cycle there was a significant protein capture, corresponding to a 63% protein reduction in comparison with the initial lysate sample. Although there are no studies in the literature that elucidate the interaction between proteins and carbon fibers, this interaction is likely based on the same interactions that occurred for the N-doped CNTs oxidized with HNO_3, since carbon fibers present the same surface chemistry. Still, the carbon fibers showed a lower capacity to capture proteins. On the other hand, there was also no presence of proteins in the sample desorbed after the 1st cycle, demonstrating once again the strong interactions occurring between the surface of the material and the proteins. It can also be seen that at the end of the 2nd cycle, it was possible to capture all the proteins that were present in the lysate sample, and again, no proteins were detected in the desorbed fraction. These results proved to be very auspicious as it was possible to recover RNA samples without the presence of a protein that corresponds to one of the main impurities in a complex lysate sample, concluding that both materials maintained their performance in reducing protein levels throughout all the trials. However, these results are only preliminary results, so future research on this topic is needed.

Table 13- Amount of proteins present in the complex E. coli lysate sample and in the samples recovered from the capture method, using 3 consecutive cycles, for N-doped CNTs oxidized with HNO_3. Values were calculated with the data obtained from one independent measurement (n = 1).

Samples	[Protein] (µg/mL)
Crude *E. coli* lysate	105
Sample not adsorbed after 1st cycle	n.d
Sample desorbed after 1st cycle	n.d
Sample not adsorbed after 2nd cycle	n.d
Sample desorbed after 2nd cycle	n.d
Sample not adsorbed after 3rd cycle	n.d
Sample desorbed after 3rd cycle	n.d

n.d: not detected.

Table 14- Amount of protein of the complex E. coli lysate sample and the samples recovered from the extraction method steps over 3 consecutive cycles for carbon fibers oxidized with HNO_3. Values were calculated with the data obtained from one independent measurement (n = 1).

Samples	[Protein] (µg/mL)
Crude *E. coli* lysate	101
Sample not adsorbed after 1st cycle	38
Sample desorbed after 1st cycle	n.d
Sample not adsorbed after 2nd cycle	n.d
Sample desorbed after 2nd cycle	n.d
Sample not adsorbed after 3rd cycle	n.d
Sample desorbed after 3rd cycle	n.d

n.d: not detected.

4.2.9- RNA integrity after the capture and recovery from carbon materials

To evaluate the integrity and stability of the RNA recovered from the capture method with N-doped CNTs oxidized with HNO_3 and carbon fibers oxidized with HNO_3, circular dichroism (CD) analysis was performed. For comparison purposes, a control sample of low molecular weight RNA was used and compared with the spectra of the RNA recovered from both materials after performing the proposed method (Figure 29 and 30). Analyzing Figure 29, it can be seen that both spectra have similar profiles, with a negative band at 215 nm and a positive band at 265 nm, which are the characteristic bands of a typical RNA spectrum. The same behavior is seen in Figure 30 where there are no significant differences in the characteristic RNA bands. These results indicate that there were no relevant alterations in the structure and conformation of the RNA during the process of clarification with carbon materials. Therefore, the RNA capture method applied in this work, using the tested materials does not compromise the integrity of the RNA, allowing it to maintain its native conformation.

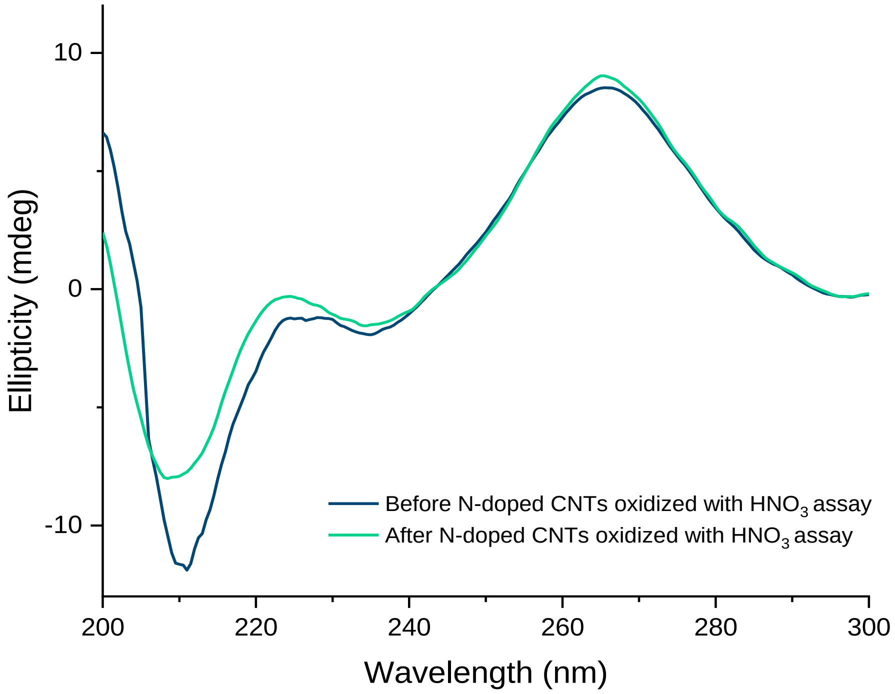

Figure 29- CD spectra from 200 to 320 nm, of RNA before and after capture assay with N-doped CNTs oxidized with HNO_3. Dark blue line represents control RNA before the capture procedure and the green blue line represents RNA after desorption procedure.

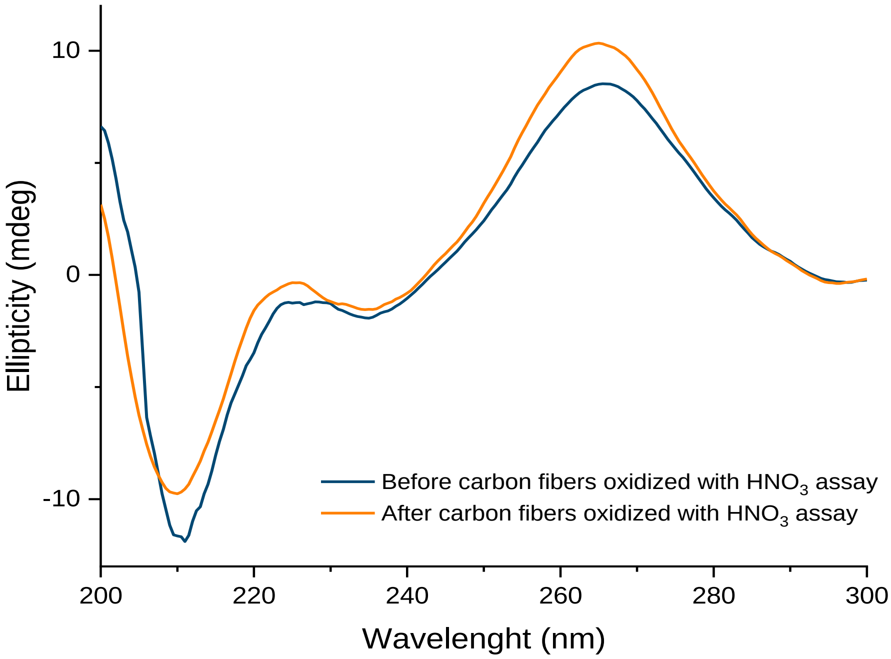

Figure 30- CD spectra from 200 to 320 nm, of RNA before and after capture assay with carbon fibers oxidized with HNO_3. Dark blue line represents control RNA before the capture procedure and orange line represents RNA after desorption procedure.

CHAPTER 5

Conclusions and Future Perspectives

In recent years, the discovery and understanding of the RNA diverse functions has increased drastically, providing several avenues to explore this biomolecule as a therapeutic agent. The unquestionable success of mRNA vaccines for the treatment of COVID-19 has opened horizons and shown the versatility of RNA-based therapies. The demand for RNA for the treatment of various diseases and, more recently, for vaccine development has increased exponentially. Thus, a widespread need arises to optimize the purification processes of this biomolecule to obtain RNA with full integrity, highly pure, and biologically active. To address this challenge, different carbon materials differing in dimensionality, shape, and surface modifications were explored as a promising alternative for RNA capture and recovery from a complex matrix sample. Thus, parameters commonly found in other RNA extraction methods, such as time-consuming and complex procedures, use of organic solvents that can compromise product integrity and have a negative environmental impact, and low efficiency can be overcome by applying a fast, efficient, reliable and cost-effective method that takes advantage of the notable adsorptive capabilities of carbon materials for RNA capture. This method can be seen as a pre-purification step, and can be integrated into a biotechnological process to reduce impurities such as DNA and proteins.

First, experiments were performed with MWCNTs to evaluate the maximum RNA adsorption capacity of this material and its reusability for new adsorption cycles through different regeneration approaches (chemical, ultrasonic and thermal) with subsequent characterization of the material surface, using FTIR technique. The results obtained suggested that the maximum RNA adsorption capacity was approximately 175 mg/g and that the chemical regeneration strategy was the most efficient because, after new RNA adsorption cycle, the highest percentage of RNA adsorption (73%) was obtained. In addition, the surface characterization results demonstrated that the MWCNTs could restore their surface properties after chemical and thermal regeneration. Next, new carbon materials with different structures and surface modifications were tested. To evaluate their behavior, screening experiments of RNA adsorption and desorption were initially outlined. In general, these experiments were important to understand the impact of the oxidative treatment of materials on the RNA adsorption and desorption capacities, because despite limiting adsorption, it contributes significantly to RNA desorption, being a crucial result for the success of this work. Thus, N-doped CNTs oxidized with HNO_3 and carbon fibers oxidized with HNO_3 were the most promising carbon materials, exhibiting RNA adsorption percentages of 42% and 55%, respectively, and RNA desorption percentages of 81% and 72%, respectively. Subsequent experiments with these materials proved their ability to maintain RNA adsorption capacity over multiple cycles. Furthermore, when brought into contact with complex samples, the N-doped CNTs oxidized with HNO_3 proved to be able to capture RNA with greater selectivity compared to carbon fibers. However, both materials were able to recover RNA without the presence of DNA over 3 cycles. Both materials under study were also able to fully capture the amount of protein present in the lysate sample, without compromising RNA desorption in the final recovery step. More importantly, it only required 1 extraction cycle for the N-doped CNTs to capture all proteins. Finally, circular dichroism experiments confirmed the integrity and stability of the RNA recovered from both materials.

Altogether, this work shows the applicability of a simple, rapid, and environmentally friendly method for efficient capture and pre-purification of RNA from bacterial lysates by exploiting the notable potential of carbon materials. This work may contribute positively to future investigations based on RNA extraction methods using carbon nanotubes and other carbon-based materials. Thus, in the future it would be very interesting to evaluate the ability of the studied carbon materials to reduce other types of impurities that may be present in complex lysate samples, namely gDNA and endotoxins, inferring whether the materials are able to establish a more efficient and complete RNA pre-purification. Another approach that may be explored in the future is to evaluate the cytotoxicity profile of the tested materials in cell lines, to ensure the safety of the RNA for use as a biopharmaceutical product. In this regard, although the materials of this study have proven to be efficient in RNA capture, it would be interesting to evaluate other types of surface functionalization that are more targeted and specific for RNA, conjugating the carbon material/RNA complex as a possible delivery system.

CHAPTER 6

References

1. Singh, S.K., P.P. Kulkarni, and D. Dash, *Biomedical Applications of Carbon-Based Nanomaterials*. Bio-Nanotechnology: A Revolution in Food, Biomedical and Health Sciences, 2013: p. 443-463.
2. Zaytseva, O. and G. Neumann, *Carbon nanomaterials: production, impact on plant development, agricultural and environmental applications*. Chemical and Biological Technologies in Agriculture, 2016. **3**(1): p. 1-26.
3. Inagaki, M. and L.R. Radovic, *Nanocarbons*. Carbon (New York, NY), 2002. **40**(12): p. 2279-2282.
4. Joris, F., et al., *Assessing nanoparticle toxicity in cell-based assays: influence of cell culture parameters and optimized models for bridging the in vitro–in vivo gap*. Chemical Society Reviews, 2013. **42**(21): p. 8339-8359.
5. *"What is Nanotechnology? | nano.gov."*. [cited 2021 Dec 10]; Available from: https://www.nano.gov/nanotech-101/what/definition.
6. Madannejad, R., et al., *Toxicity of carbon-based nanomaterials: Reviewing recent reports in medical and biological systems*. Chemico-biological interactions, 2019. **307**: p. 206-222.
7. Chow, E.K.-H., M. Gu, and J. Xu, *Carbon nanomaterials: fundamental concepts, biological interactions, and clinical applications*, in *Nanoparticles for Biomedical Applications*. 2020, Elsevier. p. 223-242.
8. Soukiassian, P.G. and M.R. Rao, *Carbon-based nanoscience and nanotechnology: where are we, where are we heading?* Journal of Physics D: Applied Physics, 2010. **43**(37): p. 370301.
9. Kroto, H.W., et al., *C60: Buckminsterfullerene*. nature, 1985. **318**(6042): p. 162-163.
10. Iijima, S., *Helical microtubules of graphitic carbon*. nature, 1991. **354**(6348): p. 56-58.
11. Novoselov, K.S., et al., *Electric field effect in atomically thin carbon films*. science, 2004. **306**(5696): p. 666-669.
12. Hong, G., et al., *Carbon nanomaterials for biological imaging and nanomedicinal therapy*. Chemical reviews, 2015. **115**(19): p. 10816-10906.
13. Raccichini, R., et al., *The role of graphene for electrochemical energy storage*. Nature materials, 2015. **14**(3): p. 271-279.
14. Díez-Pascual, A.M., *Carbon-Based Nanomaterials*. 2021, MDPI. p. 7726.
15. Riley, P.R. and R.J. Narayan, *Recent advances in carbon nanomaterials for biomedical applications: A review*. Current Opinion in Biomedical Engineering, 2021. **17**: p. 100262.

16. d’Amora, M. and S. Giordani, *Carbon nanomaterials for nanomedicine*, in *Smart nanoparticles for biomedicine*. 2018, Elsevier. p. 103-113.

17. Konios, D., et al., *Dispersion behaviour of graphene oxide and reduced graphene oxide*. Journal of colloid and interface science, 2014. **430**: p. 108-112.

18. Liu, W. and G. Speranza, *Functionalization of carbon nanomaterials for biomedical applications*. C, 2019. **5**(4): p. 72.

19. Kumar, A., *Natural Materials—Interesting Candidates for Carbon Nanomaterials*. Physchem, 2021. **1**(1): p. 4-25.

20. Rajakumar, G., et al., *Current use of carbon-based materials for biomedical applications—A prospective and review*. Processes, 2020. **8**(3): p. 355.

21. Huang, X., et al., *A sensitive H2O2 biosensor based on carbon nanotubes/tetrathiafulvalene and its application in detecting NADH*. Analytical biochemistry, 2020. **589**: p. 113493.

22. Thanihaichelvan, M., et al., *Selective and electronic detection of COVID-19 (Coronavirus) using carbon nanotube field effect transistor-based biosensor: A proof-of-concept study*. Materials Today: Proceedings, 2021.

23. Ojeda, I., et al., *Grafted-double walled carbon nanotubes as electrochemical platforms for immobilization of antibodies using a metallic-complex chelating polymer: Application to the determination of adiponectin cytokine in serum*. Biosensors and Bioelectronics, 2015. **74**: p. 24-29.

24. Wells, C., et al., *Engineering of Mesoporous Silica Coated Carbon-Based Materials Optimized for an Ultrahigh Doxorubicin Payload and a Drug Release Activated by pH, T, and NIR-light*. Advanced Functional Materials, 2018. **28**(17): p. 1706996.

25. Mirmusavi, M.H., et al., *Evaluation of physical, mechanical and biological properties of poly 3-hydroxybutyrate-chitosan-multiwalled carbon nanotube/silk nano-micro composite scaffold for cartilage tissue engineering applications*. International journal of biological macromolecules, 2019. **132**: p. 822-835.

26. Ravanbakhsh, H., et al., *Carbon nanotube composite hydrogels for vocal fold tissue engineering: biocompatibility, rheology, and porosity*. Materials Science and Engineering: C, 2019. **103**: p. 109861.

27. Li, H., et al., *Construction and nanoscale detection of interfacial charge transfer of elegant Z-scheme WO3/Au/In2S3 nanowire arrays*. Nano letters, 2016. **16**(9): p. 5547-5552.

28. Yamaguchi, T., S. Bandow, and S. Iijima, *Synthesis of carbon nanohorn particles by simple pulsed arc discharge ignited between pre-heated carbon rods.* Chemical physics letters, 2004. **389**(1-3): p. 181-185.
29. Manawi, Y.M., et al., *A review of carbon nanomaterials' synthesis via the chemical vapor deposition (CVD) method.* Materials, 2018. **11**(5): p. 822.
30. Barros, E.B., et al., *Review on the symmetry-related properties of carbon nanotubes.* Physics reports, 2006. **431**(6): p. 261-302.
31. Abbas, A., et al., *Heavy metal removal from aqueous solution by advanced carbon nanotubes: critical review of adsorption applications.* Separation and Purification Technology, 2016. **157**: p. 141-161.
32. Jha, R., et al., *Smart carbon nanotubes for drug delivery system: A comprehensive study.* Journal of Drug Delivery Science and Technology, 2020. **58**: p. 101811.
33. Klumpp, C., et al., *Functionalized carbon nanotubes as emerging nanovectors for the delivery of therapeutics.* Biochimica et Biophysica Acta (BBA)-Biomembranes, 2006. **1758**(3): p. 404-412.
34. Gupta, N., S.M. Gupta, and S. Sharma, *Carbon nanotubes: Synthesis, properties and engineering applications.* Carbon Letters, 2019. **29**(5): p. 419-447.
35. Dresselhaus, M., G. Dresselhaus, and R. Saito, *Physics of carbon nanotubes.* Carbon, 1995. **33**(7): p. 883-891.
36. Kim, G., et al., *Carbon nanotube (CNT) incorporated cementitious composites for functional construction materials: The state of the art.* Composite Structures, 2019. **227**: p. 111244.
37. Zaporotskova, I.V., et al., *Carbon nanotubes: Sensor properties. A review.* Modern Electronic Materials, 2016. **2**(4): p. 95-105.
38. Nessim, G.D., *Properties, synthesis, and growth mechanisms of carbon nanotubes with special focus on thermal chemical vapor deposition.* Nanoscale, 2010. **2**(8): p. 1306-1323.
39. Samadishadlou, M., et al., *Magnetic carbon nanotubes: preparation, physical properties, and applications in biomedicine.* Artificial cells, nanomedicine, and biotechnology, 2018. **46**(7): p. 1314-1330.
40. Arici, E. and S. Karazhanov, *Carbon nanotubes for organic/inorganic hybrid solar cells.* Materials Science in Semiconductor Processing, 2016. **41**: p. 137-149.
41. Fleming, N. *Should we give up on the dream of space elevators?* [cited 2021 19]; Available from: http://www.bbc.com/.

42. Rasmussen, A.J. and M. Ebbesen, *Characteristics, properties and ethical issues of carbon nanotubes in biomedical applications.* Nanoethics, 2014. **8**(1): p. 29-48.

43. Konsta-Gdoutos, M.S., Z.S. Metaxa, and S.P. Shah, *Highly dispersed carbon nanotube reinforced cement based materials.* Cement and Concrete Research, 2010. **40**(7): p. 1052-1059.

44. Salvetat, J.-P., et al., *Mechanical properties of carbon nanotubes.* Applied Physics A, 1999. **69**(3): p. 255-260.

45. Yu, M.-F., et al., *Tensile loading of ropes of single wall carbon nanotubes and their mechanical properties.* Physical review letters, 2000. **84**(24): p. 5552.

46. Lan, Y., Y. Wang, and Z. Ren, *Physics and applications of aligned carbon nanotubes.* Advances in Physics, 2011. **60**(4): p. 553-678.

47. Han, Z. and A. Fina, *Thermal conductivity of carbon nanotubes and their polymer nanocomposites: A review.* Progress in polymer science, 2011. **36**(7): p. 914-944.

48. Lekawa-Raus, A., et al., *Electrical properties of carbon nanotube based fibers and their future use in electrical wiring.* Advanced Functional Materials, 2014. **24**(24): p. 3661-3682.

49. Ibrahim, K.S., *Carbon nanotubes-properties and applications: a review.* Carbon letters, 2013. **14**(3): p. 131-144.

50. Rastogi, V., et al., *Carbon nanotubes: an emerging drug carrier for targeting cancer cells.* Journal of drug delivery, 2014. **2014**.

51. Guo, X., J. Wang, and H. Zhang, *Mechanical properties of single-walled carbon nanotubes based on higher order Cauchy–Born rule.* International Journal of Solids and Structures, 2006. **43**(5): p. 1276-1290.

52. Chakraborty, A.K., et al., *Chemical vapor deposition growth of carbon nanotubes on Si substrates using Fe catalyst: What happens at the nanotube/Fe/Si interface.* Journal of applied physics, 2006. **100**(8): p. 084321.

53. Yang, D., et al., *Thermal and electrical transport in multi-walled carbon nanotubes.* Physics Letters A, 2004. **329**(3): p. 207-213.

54. Dürkop, T., B. Kim, and M. Fuhrer, *Properties and applications of high-mobility semiconducting nanotubes.* Journal of Physics: Condensed Matter, 2004. **16**(18): p. R553.

55. Melechko, A.V., et al., *Vertically aligned carbon nanofibers and related structures: Controlled synthesis and directed assembly.* Journal of applied physics, 2005. **97**(4): p. 3.

56. Kamil, A.M., et al., *Preparation, characterization, and photocatalytic applications of MWCNTs/TiO2 composite.* International Journal of Photoenergy, 2014. **2014**.

57. Ma, P.-C., et al., *Dispersion and functionalization of carbon nanotubes for polymer-based nanocomposites: A review.* Composites Part A: Applied Science and Manufacturing, 2010. **41**(10): p. 1345-1367.

58. Herrera-Herrera, A.V., et al., *Carbon nanotubes applications in separation science: a review.* Analytica Chimica Acta, 2012. **734**: p. 1-30.

59. Thess, A., et al., *Crystalline ropes of metallic carbon nanotubes.* science, 1996. **273**(5274): p. 483-487.

60. Kumar, S., et al., *Carbon nanotubes: a novel material for multifaceted applications in human healthcare.* Chemical society reviews, 2017. **46**(1): p. 158-196.

61. Singh, I., et al., *Carbon nanotubes: synthesis, properties and pharmaceutical applications.* Fullerenes, Nanotubes and Carbon Nanostructures, 2009. **17**(4): p. 361-377.

62. Kingston, C.T. and B. Simard, *Fabrication of carbon nanotubes.* Analytical letters, 2003. **36**(15): p. 3119-3145.

63. Moret, Y. and P. Schmid-Hempel, *Immune defence in bumble-bee offspring.* Nature, 2001. **414**(6863): p. 506-506.

64. Li, H., et al., *Direct synthesis of high purity single-walled carbon nanotube fibers by arc discharge.* The Journal of Physical Chemistry B, 2004. **108**(15): p. 4573-4575.

65. Collins, P.G., M.S. Arnold, and P. Avouris, *Engineering carbon nanotubes and nanotube circuits using electrical breakdown.* science, 2001. **292**(5517): p. 706-709.

66. Rafique, M.M.A. and J. Iqbal, *Production of carbon nanotubes by different routes-a review.* Journal of encapsulation and adsorption sciences, 2011. **1**(02): p. 29.

67. Balasubramanian, K. and M. Burghard, *Chemically functionalized carbon nanotubes.* small, 2005. **1**(2): p. 180-192.

68. Maio, A., et al., *Statistical Study of the Influence of CNTs Purification and Plasma Functionalization on the Properties of Polycarbonate-CNTs Nanocomposites.* Plasma Processes and Polymers, 2014. **11**(7): p. 664-677.

69. Caccamo, M.T., G. Mavilia, and S. Magazù, *Thermal investigations on carbon nanotubes by spectroscopic techniques.* Applied Sciences, 2020. **10**(22): p. 8159.

70. Mehra, N.K. and N. Jain, *Development, characterization and cancer targeting potential of surface engineered carbon nanotubes.* Journal of Drug Targeting, 2013. **21**(8): p. 745-758.

71. Zhu, W., et al., *Multi-walled carbon nanotube-based systems for improving the controlled release of insoluble drug dipyridamole.* Experimental and Therapeutic Medicine, 2019. **17**(6): p. 4610-4616.

72. Ünlü, A., et al., *Cytotoxicity of doxrubicin loaded single-walled carbon nanotubes.* Molecular biology reports, 2018. **45**(4): p. 523-531.

73. Aqel, A., et al., *Carbon nanotubes, science and technology part (I) structure, synthesis and characterisation.* Arabian Journal of Chemistry, 2012. **5**(1): p. 1-23.

74. Hou, P.-X., C. Liu, and H.-M. Cheng, *Purification of carbon nanotubes.* carbon, 2008. **46**(15): p. 2003-2025.

75. Rathinavel, S., K. Priyadharshini, and D. Panda, *A review on carbon nanotube: An overview of synthesis, properties, functionalization, characterization, and the application.* Materials Science and Engineering: B, 2021. **268**: p. 115095.

76. Bandow, S., et al., *Purification and magnetic properties of carbon nanotubes.* APPLIED PHYSICS A MATERIALS SCIENCE AND PROCESSING, 1998. **67**: p. 23-28.

77. Lavagna, L., et al., *Functionalization as a way to enhance dispersion of carbon nanotubes in matrices: A review.* Materials Today Chemistry, 2021. **20**: p. 100477.

78. Al-Hamadani, Y.A., et al., *Stabilization and dispersion of carbon nanomaterials in aqueous solutions: A review.* Separation and Purification Technology, 2015. **156**: p. 861-874.

79. Norizan, M.N., et al., *Carbon nanotubes: Functionalisation and their application in chemical sensors.* RSC Advances, 2020. **10**(71): p. 43704-43732.

80. Foldvari, M. and M. Bagonluri, *Carbon nanotubes as functional excipients for nanomedicines: I. Pharmaceutical properties.* Nanomedicine: Nanotechnology, Biology and Medicine, 2008. **4**(3): p. 173-182.

81. Sahoo, N.G., et al., *Polymer nanocomposites based on functionalized carbon nanotubes.* Progress in polymer science, 2010. **35**(7): p. 837-867.

82. Georgakilas, V., et al., *Organic functionalization of carbon nanotubes.* Journal of the American chemical society, 2002. **124**(5): p. 760-761.

83. Sajid, M.I., et al., *Carbon nanotubes from synthesis to in vivo biomedical applications.* International journal of pharmaceutics, 2016. **501**(1-2): p. 278-299.

84. Onyancha, R.B., et al., *A systematic review on the detection and monitoring of toxic gases using carbon nanotube-based biosensors.* Sensing and Bio-Sensing Research, 2021. **34**: p. 100463.

85. Dyke, C.A. and J.M. Tour, *Covalent functionalization of single-walled carbon nanotubes for materials applications.* The Journal of Physical Chemistry A, 2004. **108**(51): p. 11151-11159.

86. Zhou, Y., Y. Fang, and R.P. Ramasamy, *Non-covalent functionalization of carbon nanotubes for electrochemical biosensor development.* Sensors, 2019. **19**(2): p. 392.

87. Polo-Luque, M., B. Simonet, and M. Valcárcel, *Functionalization and dispersion of carbon nanotubes in ionic liquids.* TrAC Trends in Analytical Chemistry, 2013. **47**: p. 99-110.

88. Kiran, A.R., G.K. Kumari, and P.T. Krishnamurthy, *Carbon nanotubes in drug delivery: Focus on anticancer therapies.* Journal of Drug Delivery Science and Technology, 2020. **59**: p. 101892.

89. Zhang, X., L. Meng, and Q. Lu, *Cell behaviors on polysaccharide-wrapped single-wall carbon nanotubes: a quantitative study of the surface properties of biomimetic nanofibrous scaffolds.* Acs Nano, 2009. **3**(10): p. 3200-3206.

90. Ko, J.W., et al., *Multi-order dynamic range DNA sensor using a gold decorated SWCNT random network.* Acs Nano, 2011. **5**(6): p. 4365-4372.

91. Siu, K.S., et al., *Non-covalently functionalized single-walled carbon nanotube for topical siRNA delivery into melanoma.* Biomaterials, 2014. **35**(10): p. 3435-3442.

92. Chen, R.J., et al., *Noncovalent sidewall functionalization of single-walled carbon nanotubes for protein immobilization.* Journal of the American Chemical Society, 2001. **123**(16): p. 3838-3839.

93. Zhao, X. and J.K. Johnson, *Simulation of adsorption of DNA on carbon nanotubes.* Journal of the American Chemical Society, 2007. **129**(34): p. 10438-10445.

94. Amenta, V. and K. Aschberger, *Carbon nanotubes: potential medical applications and safety concerns.* Wiley Interdisciplinary Reviews: Nanomedicine and Nanobiotechnology, 2015. **7**(3): p. 371-386.

95. Mendes, R.G., et al., *Carbon nanostructures as multi-functional drug delivery platforms.* Journal of Materials Chemistry B, 2013. **1**(4): p. 401-428.

96. Ema, M., M. Gamo, and K. Honda, *A review of toxicity studies of single-walled carbon nanotubes in laboratory animals.* Regulatory Toxicology and Pharmacology, 2016. **74**: p. 42-63.

97. Firme III, C.P. and P.R. Bandaru, *Toxicity issues in the application of carbon nanotubes to biological systems.* Nanomedicine: Nanotechnology, Biology and Medicine, 2010. **6**(2): p. 245-256.
98. Soto, K., K. Garza, and L. Murr, *Cytotoxic effects of aggregated nanomaterials.* Acta Biomaterialia, 2007. **3**(3): p. 351-358.
99. Liang, X., M. Zeng, and C. Qi, *One-step synthesis of carbon functionalized with sulfonic acid groups using hydrothermal carbonization.* Carbon, 2010. **48**(6): p. 1844-1848.
100. Zare, H., et al., *Carbon nanotubes: Smart drug/gene delivery carriers.* International journal of nanomedicine, 2021. **16**: p. 1681.
101. Yan, Y., et al., *Stacking of doxorubicin on folic acid-targeted multiwalled carbon nanotubes for in vivo chemotherapy of tumors.* Drug delivery, 2018. **25**(1): p. 1607-1616.
102. Gutiérrez-Praena, D., et al., *Influence of carboxylic acid functionalization on the cytotoxic effects induced by single wall carbon nanotubes on human endothelial cells (HUVEC).* Toxicology in Vitro, 2011. **25**(8): p. 1883-1888.
103. Alshehri, R., et al., *Carbon nanotubes in biomedical applications: factors, mechanisms, and remedies of toxicity: miniperspective.* Journal of medicinal chemistry, 2016. **59**(18): p. 8149-8167.
104. Madani, S.Y., et al., *Functionalization of single-walled carbon nanotubes and their binding to cancer cells.* International Journal of Nanomedicine, 2012. **7**: p. 905.
105. Wang, X. and Z. Liu, *Carbon nanotubes in biology and medicine: An overview.* Chinese Science Bulletin, 2012. **57**(2): p. 167-180.
106. Walsh, G., *Biopharmaceutical benchmarks 2018.* Nature biotechnology, 2018. **36**(12): p. 1136-1145.
107. Jozala, A.F., et al., *Biopharmaceuticals from microorganisms: from production to purification.* brazilian journal of microbiology, 2016. **47**: p. 51-63.
108. C Silva, A., et al., *Delivery systems for biopharmaceuticals. Part I: Nanoparticles and microparticles.* Current pharmaceutical biotechnology, 2015. **16**(11): p. 940-954.
109. Wright, S., *Recombinant DNA technology and its social transformation, 1972-1982.* Osiris, 1986. **2**: p. 303-360.
110. Santos-Neto, J.F., et al., *Technological advancements in monoclonal antibodies.* The Scientific World Journal, 2021. **2021**.
111. Walsh, G., *Biopharmaceutical benchmarks 2010.* Nature biotechnology, 2010. **28**(9): p. 917-924.

112. Mitragotri, S., P.A. Burke, and R. Langer, *Overcoming the challenges in administering biopharmaceuticals: formulation and delivery strategies.* Nature reviews Drug discovery, 2014. **13**(9): p. 655-672.

113. Harloff-Helleberg, S., L.H. Nielsen, and H.M. Nielsen, *Animal models for evaluation of oral delivery of biopharmaceuticals.* Journal of Controlled Release, 2017. **268**: p. 57-71.

114. Allmendinger, A., *Opportunities in an Evolving Pharmaceutical Development Landscape: Product Differentiation of Biopharmaceutical Drug Products.* Pharmaceutical Research, 2021. **38**(5): p. 739-757.

115. Rasmussen, A.S.B., et al., *Definition, categorization, and environmental risk assessment of biopharmaceuticals.* Science of The Total Environment, 2021. **789**: p. 147884.

116. Ho, R.J., *Biotechnology and biopharmaceuticals: transforming proteins and genes into drugs*. 2013: John Wiley & Sons.

117. Benyahia, B., et al., *Biopharmaceutical development, production, and quality*, in *New and Future Developments in Microbial Biotechnology and Bioengineering*. 2020, Elsevier. p. 69-89.

118. Tripathi, N.K. and A. Shrivastava, *Recent developments in bioprocessing of recombinant proteins: expression hosts and process development.* Frontiers in bioengineering and biotechnology, 2019. **7**: p. 420.

119. Aires-Barros, M. and A. Azevedo, *Fundamentals of biological separation processes*, in *Current Developments in Biotechnology and Bioengineering*. 2017, Elsevier. p. 187-237.

120. Moo-Young, M., *Comprehensive biotechnology*. 2019: Elsevier.

121. Singh, A., et al., *Protein recovery from inclusion bodies of Escherichia coli using mild solubilization process.* Microbial cell factories, 2015. **14**(1): p. 1-10.

122. Doran, P.M., *Bioprocess engineering principles*. 1995: Elsevier.

123. Mehta, A., *Downstream processing for biopharmaceuticals recovery*, in *Pharmaceuticals from Microbes*. 2019, Springer. p. 163-190.

124. Poole, C.F., *Handbook of Methods and Instrumentation in Separation Science: Volume 1.* Vol. 1. 2009: Academic Press.

125. Lee, S.Y., K.W. Chew, and P.L. Show, *Cell separation and disruption, product recovery, and purification*, in *Essentials in fermentation technology*. 2019, Springer. p. 237-271.

126. Kilikian, B.V. and A. Pessoa Jr, *Purificação de produtos biotecnológicos.* Biotecnologia Industrial. Engenharia Bioquímica, 2001. **2**: p. 1.

127. Martins, R., J. Queiroz, and F. Sousa, *Ribonucleic acid purification.* Journal of Chromatography A, 2014. **1355**: p. 1-14.

128. Prazeres, D.M.F., *Plasmid biopharmaceuticals: basics, applications, and manufacturing*. 2011: John Wiley & Sons.

129. Charcosset, C., *Membrane processes in biotechnology: an overview.* Biotechnology advances, 2006. **24**(5): p. 482-492.

130. Clarke, K.G., *Bioprocess engineering: an introductory engineering and life science approach*. 2013: Elsevier.

131. dos Santos, N.V., et al., *Liquid–liquid extraction of biopharmaceuticals from fermented broth: trends and future prospects.* Journal of Chemical Technology & Biotechnology, 2018. **93**(7): p. 1845-1863.

132. Freire, M.G., et al., *Aqueous biphasic systems: a boost brought about by using ionic liquids.* Chemical Society Reviews, 2012. **41**(14): p. 4966-4995.

133. Zhang, C., et al., *Development trend and prospect of solid phase extraction technology.* 中国化学工程学报, 2022. **42**(2): p. 245-255.

134. Sholl, D.S. and R.P. Lively, *Seven chemical separations to change the world.* Nature, 2016. **532**(7600): p. 435-437.

135. de Carvalho, J., et al., *Approaches for the Isolation and Purification of Fermentation Products*, in *Current Developments in Biotechnology and Bioengineering*. 2017, Elsevier. p. 783-805.

136. Sazali, N., Z. Harun, and N. Sazali, *A review on batch and column adsorption of various adsorbent towards the removal of heavy metal.* Journal of Advanced Research in Fluid Mechanics and Thermal Sciences, 2020. **67**(2): p. 66-88.

137. Negrea, A., et al., *Estimation on fixed-bed column parameters of breakthrough behaviors for gold recovery by adsorption onto modified/functionalized amberlite xad7.* International Journal of Environmental Research and Public Health, 2020. **17**(18): p. 6868.

138. Kecili, R. and C.M. Hussain, *Mechanism of adsorption on nanomaterials*, in *Nanomaterials in Chromatography*. 2018, Elsevier. p. 89-115.

139. Dąbrowski, A., *Adsorption—from theory to practice.* Advances in colloid and interface science, 2001. **93**(1-3): p. 135-224.

140. Soto, M.L., et al., *Recovery, concentration and purification of phenolic compounds by adsorption: A review.* Journal of Food Engineering, 2011. **105**(1): p. 1-27.

141. Zhao, X., et al., *Preconcentration procedures for the determination of chromium using atomic spectrometric techniques: A review.* Open Chemistry, 2012. **10**(4): p. 927-937.

142. Broich, J., et al., *Liquid—Solid extraction of lyophilized biological material for forensic analysis: I. Application to urine samples for detection of drugs of abuse.* Journal of Chromatography A, 1971. **63**: p. 309-312.

143. Abd-Talib, N., S.H. Mohd-Setapar, and A.K. Khamis, *The benefits and limitations of methods development in solid phase extraction: Mini review.* Jurnal Teknologi, 2014. **69**(4).

144. Armenta, S., S. Garrigues, and M. de la Guardia, *Green analytical chemistry.* TrAC Trends in Analytical Chemistry, 2008. **27**(6): p. 497-511.

145. Hu, G., J.S. Lee, and D. Li, *A microfluidic fluorous solid-phase extraction chip for purification of amino acids.* Journal of colloid and interface science, 2006. **301**(2): p. 697-702.

146. Bagheri, H., A. Mohammadi, and A. Salemi, *On-line trace enrichment of phenolic compounds from water using a pyrrole-based polymer as the solid-phase extraction sorbent coupled with high-performance liquid chromatography.* Analytica chimica acta, 2004. **513**(2): p. 445-449.

147. Gilar, M., A. Belenky, and B.H. Wang, *High-throughput biopolymer desalting by solid-phase extraction prior to mass spectrometric analysis.* Journal of Chromatography A, 2001. **921**(1): p. 3-13.

148. Mulugeta, M., et al., *Fractionation analysis of oxyanion-forming metals and metalloids in leachates of cement-based materials using ion exchange solid phase extraction.* Talanta, 2009. **78**(3): p. 736-742.

149. Wierucka, M. and M. Biziuk, *Application of magnetic nanoparticles for magnetic solid-phase extraction in preparing biological, environmental and food samples.* TrAC Trends in Analytical Chemistry, 2014. **59**: p. 50-58.

150. Ścigalski, P. and P. Kosobucki, *Recent materials developed for dispersive solid phase extraction.* Molecules, 2020. **25**(21): p. 4869.

151. Yilmaz, E. and M. Soylak, *Functionalized nanomaterials for sample preparation methods*, in *Handbook of Nanomaterials in analytical chemistry*. 2020, Elsevier. p. 375-413.

152. Guo, P.-F., et al., *Nanostructures serve as adsorbents for the selective separation/enrichment of proteins.* TrAC Trends in Analytical Chemistry, 2019. **120**: p. 115650.

153. Song, B., et al., *Carbon nanotube-based environmental technologies: the adopted properties, primary mechanisms, and challenges.* Reviews in Environmental Science and Bio/Technology, 2018. **17**(3): p. 571-590.

154. Wang, X., et al., *Nanomaterials as sorbents to remove heavy metal ions in wastewater treatment*. J. Environ. Anal. Toxicol, 2012. **2**(7): p. 154-158.

155. Herrero-Latorre, C., et al., *Graphene and carbon nanotubes as solid phase extraction sorbents for the speciation of chromium: A review*. Analytica chimica acta, 2018. **1002**: p. 1-17.

156. Li, Z., et al., *Recent development and application of solid phase extraction materials*. Rev. Adv. Mater. Sci, 2017. **48**: p. 87-111.

157. Zhang, B.-T., et al., *Application of carbon-based nanomaterials in sample preparation: A review*. Analytica chimica acta, 2013. **784**: p. 1-17.

158. Li, Y., et al. *Carbon nanotubes-the promising adsorbent in wastewater treatment*. in *Journal of Physics: Conference Series*. 2007. IOP Publishing.

159. Jakubus, A., et al., *The possibility to use multi-walled carbon nanotubes as a sorbent for dispersive solid phase extraction of selected pharmaceuticals and their metabolites: effect of extraction condition*. Microchemical Journal, 2019. **146**: p. 1113-1125.

160. Corazza, M.Z., et al., *Avaliação de nanotubos de carbono funcionalizados visando o desenvolvimento de métodos de pré-concentração de íons metálicos e determinação por técnicas espectrométricas e eletroanalíticas*. Química Nova, 2020. **43**: p. 1086-1103.

161. Latorre, C.H., et al., *Carbon nanotubes as solid-phase extraction sorbents prior to atomic spectrometric determination of metal species: A review*. Analytica chimica acta, 2012. **749**: p. 16-35.

162. Hussain, C.M. and S. Mitra, *Micropreconcentration units based on carbon nanotubes (CNT)*. Analytical and bioanalytical chemistry, 2011. **399**(1): p. 75-89.

163. Lundstrom, K., *Latest development on RNA-based drugs and vaccines*. Future science OA, 2018. **4**(5): p. FSO300.

164. Brenner, S., F. Jacob, and M. Meselson, *An unstable intermediate carrying information from genes to ribosomes for protein synthesis*. Nature, 1961. **190**(4776): p. 576-581.

165. Curreri, A., et al., *RNA therapeutics in the clinic*. Bioengineering & Translational Medicine, 2022: p. e10374.

166. Andreadakis, Z., et al., *The COVID-19 vaccine development landscape*. Nat Rev Drug Discov, 2020. **19**(5): p. 305-306.

167. Damase, T.R., et al., *The limitless future of RNA therapeutics*. Frontiers in Bioengineering and Biotechnology, 2021: p. 161.

168. Jones, B. and A. Schreiber, *mRNA as a therapeutic target in lung disease*. Drug Design Reviews-Online (Discontinued), 2005. **2**(5): p. 361-372.

169. Pedro, A.Q., et al., *Cholinium-based Good's buffers ionic liquids as remarkable stabilizers and recyclable preservation media for recombinant small RNAs.* ACS sustainable chemistry & engineering, 2018. **6**(12): p. 16645-16656.

170. Tan, S.C. and B.C. Yiap, *DNA, RNA, and protein extraction: the past and the present.* Journal of Biomedicine and Biotechnology, 2009. **2009**.

171. Lehman, N., *RNA in evolution.* Wiley Interdisciplinary Reviews: RNA, 2010. **1**(2): p. 202-213.

172. Serp, P., M. Corrias, and P. Kalck, *Carbon nanotubes and nanofibers in catalysis.* Applied Catalysis A: General, 2003. **253**(2): p. 337-358.

173. Sampaio, M.J., et al., *Synergistic effect between carbon nanomaterials and ZnO for photocatalytic water decontamination.* Journal of Catalysis, 2015. **331**: p. 172-180.

174. Moreira, N.F., et al., *Metal-free g-C3N4 photocatalysis of organic micropollutants in urban wastewater under visible light.* Applied Catalysis B: Environmental, 2019. **248**: p. 184-192.

175. Lima, M.J., et al., *Graphitic carbon nitride modified by thermal, chemical and mechanical processes as metal-free photocatalyst for the selective synthesis of benzaldehyde from benzyl alcohol.* Journal of Catalysis, 2017. **353**: p. 44-53.

176. Ferreira, P.F.L., *Rapid and selective capture of nucleic acids using carbon nanotubes.* 2021.

177. Azhari, F. and N. Banthia, *Cement-based sensors with carbon fibers and carbon nanotubes for piezoresistive sensing.* Cement and Concrete Composites, 2012. **34**(7): p. 866-873.

178. Yu, H., et al., *Optimizing sonication parameters for dispersion of single-walled carbon nanotubes.* Chemical Physics, 2012. **408**: p. 11-16.

179. Doepke, A., et al., *Analysis of the electrochemical oxidation of multiwalled carbon nanotube tower electrodes in sodium hydroxide.* Electroanalysis, 2012. **24**(7): p. 1501-1508.

180. Halprin, K.M., et al., *A combined alkali extraction—ethidium bromide technique for the measurement of DNA in small pieces of tissue.* Journal of Investigative Dermatology, 1979. **73**(5): p. 359-363.

181. Ania, C., et al., *Effect of microwave and conventional regeneration on the microporous and mesoporous network and on the adsorptive capacity of activated carbons.* Microporous and Mesoporous Materials, 2005. **85**(1-2): p. 7-15.

182. Wang, Y., et al., *Comparison of chemical, ultrasonic and thermal regeneration of carbon nanotubes for acetaminophen, ibuprofen, and triclosan adsorption.* RSC advances, 2017. **7**(83): p. 52719-52728.

183. Banyay, M., M. Sarkar, and A. Gräslund, *A library of IR bands of nucleic acids in solution.* Biophysical chemistry, 2003. **104**(2): p. 477-488.

184. Hamilton Jr, R.F., et al., *Purification and sidewall functionalization of multiwalled carbon nanotubes and resulting bioactivity in two macrophage models.* Inhalation toxicology, 2013. **25**(4): p. 199-210.

185. Arenal, R., et al., *Atomic configuration of nitrogen-doped single-walled carbon nanotubes.* Nano letters, 2014. **14**(10): p. 5509-5516.

186. Wang, L., et al., *Enhanced adsorption of aromatic chemicals on boron and nitrogen co-doped single-walled carbon nanotubes.* Environmental Science: Nano, 2017. **4**(3): p. 558-564.

187. Rajendran, D., et al., *Role of Solvent Polarity on Dispersion Quality and Stability of Functionalized Carbon Nanotubes.* Journal of Composites Science, 2022. **6**(1): p. 26.

188. Sun, W., J. Zhao, and Z. Du, *Density-functional-theory-based study of interaction of DNA/RNA nucleobases with hydroxyl-and carboxyl-functionalized armchair (6, 6) CNT.* Computational and Theoretical Chemistry, 2017. **1102**: p. 60-68.

189. Huang, X., *Fabrication and properties of carbon fibers.* Materials, 2009. **2**(4): p. 2369-2403.

190. Pittman Jr, C., et al., *Surface area and pore size distribution of microporous carbon fibers prepared by electrochemical oxidation.* Carbon, 1999. **37**(1): p. 85-96.

191. Pamula, E. and P.G. Rouxhet, *Bulk and surface chemical functionalities of type III PAN-based carbon fibres.* Carbon, 2003. **41**(10): p. 1905-1915.

192. Ferreira, O.P., et al., *Ecomateriais: desenvolvimento e aplicação de materiais porosos funcionais para proteção ambiental.* Química Nova, 2007. **30**: p. 464-467.

193. Giles, C., et al., *786. Studies in adsorption. Part XI. A system of classification of solution adsorption isotherms, and its use in diagnosis of adsorption mechanisms and in measurement of specific surface areas of solids.* Journal of the Chemical Society (Resumed), 1960: p. 3973-3993.

194. Martins, E.M.d.N., et al., *Synthesis, Purification and Functionalization of Carbon Nanotubes for Biotechnological Applications*, in *Bioengineering Applications of Carbon Nanostructures.* 2016, Springer. p. 139-163.

195. Amaral, T.K., et al., *The effect of debris on the adsorption and electron-transfer capacity at the interface of oxidized carbon nanotubes.* Chemical Engineering Journal, 2020. **388**: p. 124379.
196. Wu, Z., C.U. Pittman Jr, and S.D. Gardner, *Nitric acid oxidation of carbon fibers and the effects of subsequent treatment in refluxing aqueous NaOH.* Carbon, 1995. **33**(5): p. 597-605.
197. Shakhmaeva, I.I., et al., *Binding and purification of plasmid DNA using multi-layered carbon nanotubes.* Journal of biotechnology, 2011. **152**(3): p. 102-107.
198. Food, U. and D. Administration, *Guidance for industry: considerations for plasmid DNA vaccines for preventive infectious disease indications.* US Food and Drug Administration, Rockville, MD, 2007.
199. Burch, H.J., et al., *Doping of carbon nanotubes with nitrogen improves protein coverage whilst retaining correct conformation.* Nanotechnology, 2008. **19**(38): p. 384001.